

AD-A258 811



AFTT/GA/ENY/92D-14

①

SOLVING NONLINEAR COMPOSITE  
MATERIAL PROBLEMS  
USING THE AUTOMATED STRUCTURAL  
OPTIMIZATION SYSTEM (ASTROS)

THESIS

Robert (Bob) Bolha, Captain, USAF

AFTT/GA/ENY/92D-14

DTIC  
ELECTE  
JAN 06 1993  
S B D

Approved for public release; distribution unlimited

0122 000  
93-00128  
191 192

93 1 04 014

AFIT/GA/ENY/92D-14

SOLVING NONLINEAR  
COMPOSITE MATERIAL  
PROBLEMS USING THE  
AUTOMATED STRUCTURAL  
OPTIMIZATION SYSTEM (ASTROS)

THESIS

Presented to the Faculty of the School of Engineering  
of the Air Force Institute of Technology  
Air University  
In Partial Fulfillment of the  
Requirements for the Degree of  
Master of Science in Aeronautical Engineering

Robert (Bob) Bolha  
Captain, USAF  
AFIT/GA/ENY/92D-15

December 1992

Approved for public release; distribution unlimited

# REPORT DOCUMENTATION PAGE

Form Approved  
OMB No. 0704-0188

Public reporting burden for this collection of information is estimated to average 1 hour per response, including the time for reviewing instructions, searching existing data sources, gathering and maintaining the data needed, and completing and reviewing the collection of information. Send comments regarding this burden estimate or any other aspect of this collection of information, including suggestions for reducing this burden, to Washington Headquarters Services, Directorate for Information Operations and Reports, 1215 Jefferson Davis Highway, Suite 1204, Arlington, VA 22202-4302, and to the Office of Management and Budget, Paperwork Reduction Project (0704-0188), Washington, DC 20503.

1. AGENCY USE ONLY (Leave blank)		2. REPORT DATE December 1992	3. REPORT TYPE AND DATES COVERED Master's Thesis	
4. TITLE AND SUBTITLE SOLVING NONLINEAR COMPOSITE MATERIAL PROBLEMS USING THE AUTOMATED STRUCTURAL OPTIMIZATION SYSTEM (ASTROS)			5. FUNDING NUMBERS	
6. AUTHOR(S) Robert Bolha, Captain, USAF				
7. PERFORMING ORGANIZATION NAME(S) AND ADDRESS(ES) Air Force Institute of Technology, WPAFB OH 45433-6583			8. PERFORMING ORGANIZATION REPORT NUMBER AFIT/GA/ENY/92D-14	
9. SPONSORING / MONITORING AGENCY NAME(S) AND ADDRESS(ES) WL/FIBR, WPAFB OH			10. SPONSORING / MONITORING AGENCY REPORT NUMBER	
11. SUPPLEMENTARY NOTES				
12a. DISTRIBUTION / AVAILABILITY STATEMENT Approved for public release; distribution unlimited			12b. DISTRIBUTION CODE	
13. ABSTRACT (Maximum 200 words) Most advanced composite materials have nonlinear stress versus strain curves--grossly so in the laminas shear direction. If linear approximations are used, overly conservative design will result. This thesis expands the usefulness of the Automated Structural Optimization System (ASTROS) finite element (FE) program by incorporating a newly developed capability to include material nonlinearities. By dividing a FE problem into several intervals, and incorporating the changing nature of the nonlinear material properties within each element, a good approximation of the laminate's actual stresses and strains can be obtained without the undue experimentation involved in testing every individual configuration. Each material property is updated in terms of tension and compression as appropriate. Updating the material properties is possible in the material axes through comparison to cubic spline curves made from experimental data. The resulting piecewise linear analysis accurately captures the nonlinear nature of the changing properties. This research considered plane stress flat plates with and without holes. Graphite/Polyetheretherketone is an advanced composite material that has good high temperature strength properties and nonlinear material properties.				
14. SUBJECT TERMS Nonlinear Materials, Composite Materials, Finite Elements, Graphite/Polyetheretherketone, Gr/PEEK			15. NUMBER OF PAGES 88	
			16. PRICE CODE	
17. SECURITY CLASSIFICATION OF REPORT Unclassified	18. SECURITY CLASSIFICATION OF THIS PAGE Unclassified	19. SECURITY CLASSIFICATION OF ABSTRACT Unclassified	20. LIMITATION OF ABSTRACT UL	

## Acknowledgments

The thesis process is more than this report. This report can mention how much others have helped, but it can't give much depth to what that help meant. I couldn't have done this research on my own. Although I was accountable for it, I was learning and began understanding as the process developed. It's impossible to estimate how much each person's contribution became this report, and even more impossible to convey sufficient thanks.

Each day, Mrs. Vicky (Victoria) Tischler was available to help and guide me. She shared her computer resources with me, and I must publicly confess, I was a hog!

Thank you, Vicky!

Dr. Palazotto has had the biggest impact on my Master's program. Not only has he been an excellent teacher of engineering, but his encouragement, caring and understanding will not be forgotten. His door is open to students—he answers our dumb questions until we understand, and without ever putting us down. This is such a rare quality! If I were ever compared to Dr. Palazotto, I would consider it a very high compliment!

I don't think anyone knows their areas of expertise better than Dr. Venkayya and Dr. Sandhu. They have been eager to teach me and have had to remind me that we learn the most when things don't happen as we expect!

It truly has been a pleasure working on this project. Not that the research wasn't frustrating, but this has been an enjoyable and memorable experience because of the people I was able to work with. I would be amiss if I didn't thank Captain Ben Wham for his help—in answering questions and in helping me run models to compare with mine on Dr. Sandhu's program.

Outside of the Air Force, there has been personal support. Thanks Claire, you are such a wonderful friend and I am eager and fortunate to be your husband.

Most of all, my good friend Jesus has been the factor that sustains this struggling engineer. I might not flatter Him with my abilities, but I hope I live a life that pleases Him as my way of saying thanks to Him.

DTIC QUALITY INSPECTED 6

ii

<input checked="checked" type="checkbox"/>	
<input type="checkbox"/>	
<input type="checkbox"/>	
Bob Bolha /	
Availability Codes	
Dist	Avail and/or Special
A-1	

# Table of Contents

Acknowledgments .....	ii
Abstract .....	i
Table of Contents .....	iii
List of Figures .....	v
List of Tables .....	vi
Abstract .....	vii
I. Introduction .....	1
Motivation.....	1
Purpose .....	1
Background and Overview.....	3
II. Theory .....	5
Nonlinearity .....	5
Plane Stress Elasticity .....	5
Mechanics of Composite Materials .....	7
Lamina Behavior. ....	7
Laminate Behavior. ....	10
Finite Element Modeling (FEM) .....	10
Strain-Displacement Relations. ....	10
Stress-Deformation Relations. ....	11
Stress-Strain Relations. ....	12
Element Formulation. ....	13
ASTROS.....	16
Cubic Spline.....	20
Summary.....	22
III. Results and Discussion .....	25
Finite Element Model Verification .....	25
Mesh Size. ....	25
Constant Stress Versus Constant Displacement Increments. ....	25
Nonlinear Program Verification .....	31
Iteration Size Study .....	38
Linear Versus Nonlinear Analysis.....	41

The (0) Laminate. ....	41
The (90) Laminate. ....	49
The ( $\pm 45$ ) <sub>s</sub> Laminate. ....	49
Conclusion .....	57
Appendix A .....	58
Appendix B .....	62
Appendix C .....	69
Bibliography .....	76
Vita .....	79

## List of Figures

Figure 1. Elements of Design .....	2
Figure 2. Flat Plate .....	6
Figure 3. Lamina with Unidirectional Fibers (15).....	7
Figure 4. Principal Material Axes Oriented at Angle $\theta$ with Reference Coordinate Axes .....	9
Figure 5. Displacement and Distortion of Differential Lengths $dx$ and $dy$ .....	11
Figure 6. Stresses and Body Forces .....	12
Figure 7. Structural Elements .....	14
Figure 8. QUAD 4 Element .....	15
Figure 9. Impact of Design Decisions on Total Product Life Cycle Cost.....	17
Figure 10. Concept, Design, Review, and Retrofit Costs .....	18
Figure 11. Time to Market .....	18
Figure 12. ASTROS' Engineering Disciplines .....	19
Figure 13. ASTROS' Structural Analyses .....	20
Figure 14. The ASTROS System Architecture (14) .....	21
Figure 15. Plate without Hole.....	26
Figure 16. 36 Element Model.....	27
Figure 17. 66 Element Model.....	28
Figure 18. 72 Element Model.....	29
Figure 19. (0) Rectangular Plate without Hole in Transverse Compression.....	30
Figure 20. (0) Rectangular Plate without Hole in Shear .....	31
Figure 21. (0) Rectangular Plate without Hole in Longitudinal Tensile Stress .....	32
Figure 22. (0) Rectangular Plate without Hole Comparison .....	32
Figure 23. Program Verification—Element 1 in Transverse Compression .....	33
Figure 24. Program Verification—Element 6 in Longitudinal Tension .....	34
Figure 25. Program Verification—Element 13 in Shear .....	34
Figure 26. Program Verification—Element 21 in Longitudinal Tension .....	35
Figure 27. Program Verification—Element 62 in Longitudinal Tension .....	35
Figure 28. Program Verification—Nonlinear Displacement Plot.....	36
Figure 29. Program Verification—Linear Displacement Plot.....	37
Figure 30. Effect of Increment Size—Element 1 .....	38
Figure 31. Effect of Increment Size—Element 6.....	39

Figure 32. Effect of Increment Size—Element 13 .....	39
Figure 33. Effect of Increment Size—Element 21 .....	40
Figure 34. Effect of Increment Size—Element 62 .....	40
Figure 35. (0) Element 1 in Transverse Compression .....	42
Figure 36. (0) Element 6 in Longitudinal Tension .....	42
Figure 37. (0) Element 13 in Shear .....	43
Figure 38. (0) Element 38 in Longitudinal Tension .....	43
Figure 39. (0) Element 65 in Longitudinal Tension .....	44
Figure 40. (0) Element 1 in Transverse Compression—Constant Applied Stress .....	44
Figure 41. (0) Element 6 in Longitudinal Tension—Constant Applied Stress .....	45
Figure 42. (0) Element 13 in Shear—Constant Applied Stress .....	45
Figure 43. (0) Element 38 in Longitudinal Tension—Constant Applied Stress .....	46
Figure 44. (0) Element 65 in Longitudinal Tension—Constant Applied Stress .....	46
Figure 45. (0) Element 1 in Transverse Compression—Comparison .....	47
Figure 46. (0) Element 6 in Longitudinal Tension—Comparison .....	47
Figure 47. (0) Element 13 in Shear—Comparison .....	48
Figure 48. (0) Element 38 in Longitudinal Tension—Comparison .....	48
Figure 49. (0) Element 65 in Longitudinal Tension—Comparison .....	49
Figure 50. Constant Applied Stress Displacement Plot .....	50
Figure 51. Constant Displacement Displacement Plot .....	51
Figure 52. (90) Element 1 in Longitudinal Compression .....	52
Figure 53. (90) Element 6 in Transverse Tension .....	52
Figure 54. (90) Element 13 in Shear .....	53
Figure 55. (90) Element 38 in Transverse Tension .....	53
Figure 56. (90) Element 65 in Transverse Tension .....	54
Figure 57. ( $\pm 45$ ) Element 1 in Transverse Compression .....	54
Figure 58. ( $\pm 45$ ) Element 6 in Longitudinal Tension .....	55
Figure 59. ( $\pm 45$ ) Element 13 in Shear .....	55
Figure 60. ( $\pm 45$ ) Element 38 in Longitudinal Tension .....	56
Figure 61. ( $\pm 45$ ) Element 65 in Longitudinal Tension .....	56



# List of Tables

	page
Table 1. Stress Concentration Factor (SCF) Comparison .....	21

## Abstract

Most advanced composite materials have nonlinear stress versus strain curves—grossly so in the lamina's shear direction. If linear approximations are used, overly conservative design will result. This thesis expands the usefulness of the Automated Structural Optimization System (ASTROS) finite element (FE) program by incorporating a newly developed capability to include material nonlinearities. By dividing a FE problem into several intervals, and incorporating the changing nature of the nonlinear material properties ( $E_1$ ,  $E_2$ ,  $G_{12}$ , and  $\nu_{12}$ ) within each element, a good approximation of the laminate's actual stresses and strains can be obtained without the undue experimentation involved in testing every individual configuration. Each material property is updated in terms of tension and compression, as appropriate ( $G_{12}$  reacts the same in tension and compression). Updating the FE model's material properties is possible in the material axes through comparison to cubic spline curves made from experimental lamina data. The resulting piecewise linear analysis accurately captures the nonlinear nature of the changing properties. This research considered plane stress flat plates with and without circular discontinuities (holes). Graphite/Polyetheretherketone (GR/PEEK) is an advanced composite material that has good high temperature strength properties and nonlinear material properties.

# **SOLVING NONLINEAR COMPOSITE MATERIAL PROBLEMS USING THE AUTOMATED STRUCTURAL OPTIMIZATION SYSTEM (ASTROS)**

## **I. Introduction**

### ***Motivation***

Imagine designing something complex, such as a house, without the different interests working together. Fortunately, general contractors coordinate the efforts of the varying segments to assure a quality product. Unknowingly, concurrent engineering has been understood by the builders of houses for years. It simply makes sense.

In the Department of Defense, concurrent engineering describes the streamlining and overhauling of the design process. Wright Laboratories, at Wright-Patterson AFB in Ohio uses a concurrent engineering tool for aerospace designers: the Automated Structural Optimization System (ASTROS). ASTROS allows the smooth and successful completion of the roughest of all design phases, that of preliminary design. Figure 1 shows that preliminary design occurs after conceptual design (33).

Although conceptual design is usually very sketchy, preliminary design provides a model that will be within five percent of the actual, or final, design (33). This means preliminary design provides maximum payoff within the design process (33). ASTROS brings together mechanical, aeroelastic, and control system design. Since ASTROS uses finite elements (see Chapter II), it also allows sensitivity analysis and optimization. First delivered in 1987, ASTROS is new and continues to be improved (18).

### ***Purpose***

This present research affords ASTROS nonlinear material capabilities, even for composites.

For clarity, the term composites will be limited here to specifically mean more than just an increase of material properties in desired directions (which would include plywood and reinforced concrete). Here, composite will denote those non-isotropic materials becoming common within

# Elements of Design

Conceptual Design



Preliminary Design



Detail Design



Final Design

*Figure 1. Elements of Design*

the aerospace industry, such as graphite fibers encased in a matrix of epoxy. Advanced composite materials (ACMs) are the next generation of aerospace industry composites—they have even further enhanced strength and stiffness properties. They hold very promising opportunities for the future. Advanced composites either have metallic or organic matrices. Most have organic matrices, which are nonlinear (20). Graphite/Polyetheretherketone (Gr/PEEK) is such a material. It holds special promise for the future, because it adds good high temperature strength to the other advantages of an ACM. It may be used in projects such as the National Aerospace Plane, which will be subjected to high temperatures. Gr/PEEK's nonlinear properties make it an ideal choice for this current research. The term nonlinear means that the normal assumption of Hooke's Law:

$$\sigma = E\epsilon$$

$\sigma$  = stress

$E$  = Modulus of Elasticity

$\epsilon$  = strain

is not valid. This would be due to a non-constant slope,  $E$ , of the stress-strain curve. Kinematic nonlinearity is discarded since most composites cannot sustain more than 5 percent strain before failure

(11). More than being interesting, nonlinear materials hold the key of current and impending design. The tailored composite materials of today and for tomorrow need to be better understood to be fully exploited. Design will be incorrect, possibly much too conservative, when nonlinear materials are approximated as linear (20).

### ***Background and Overview***

As nonlinear laminae, or plies, are stacked to form laminates, errors from using linear theory will compound erratically, and are not intuitively easily accounted for. Although there are many reports on the linear behavior of composite lamina and their interaction as laminates (25,28,29,30) research on nonlinear behavior has been more limited (6,9,10,11,12,16,17,20,23,26,27).

Several experiments have been conducted on the nonlinear properties of composite materials (CMs) and ACMs. First, some attempts successfully disclosed the nonlinear laminae properties from testing laminates, then others determined laminate properties from testing laminae. Early attempts focused on the most nonlinear of moduli, the shear modulus,  $G_{12}$ .

Petit first determined a nonlinear lamina  $G_{12}$  response by testing ( $\pm 45$ )<sub>s</sub> coupons, assuming no coupling of the other two moduli,  $E_1$  and  $E_2$ , which were approximated as linear (20). Hahn and Tsai, still considering  $E_1$  and  $E_2$  linear, considered coupling in their derivation, and also noted the importance of considering variations in  $\nu_{12}$ , Poisson's ratio (11).

Rosen was able to obtain  $G_{12}$  directly from test results, improving accuracy by finding  $G_{12}$  independently of  $E_1$  and  $E_2$  (23).

Lifshitz further refined the results for a nonlinear  $G_{12}$  by only requiring axial strains (16). Transverse strain measurements are avoided since they are quite susceptible to error.  $G_{12}$  was then calculated from known values of  $E_1$ ,  $E_2$  and  $\nu_{12}$ , and measured values of axial strain.

Although Hahn and Tsai initially felt that closed-form representations from laminates were impossible (11), work has progressed in this area. Hahn was able to calculate a nonlinear laminate  $G_{12}$  from lamina data, which he confirmed experimentally (10). Petit and Waddoups were able to produce reasonably good results for  $E_1$ ,  $E_2$  and  $G_{12}$  in nonlinear laminates from their lamina properties (20).

Sandhu has led the efforts in analyzing the nonlinear properties of Gr/PEEK. Under simple loading conditions, Sandhu was able to analytically relate laminate behavior to that in individual laminae (26). Using cubic spline interpolation (see Chapter II) within incremental constitutive equations, he was able to determine the nonlinear  $E_1$ ,  $E_2$  and  $G_{12}$  as well as update  $\nu_{12}$ . Daniels,

Fisher and Martin have confirmed Sandhu's work experimentally with their respective research on the responses of Gr/PEEK to various loading conditions (6,9,17).

This present research will incrementally incorporate all three nonlinear moduli while also updating Poisson's ratio into the convenience and versatility of ASTROS. Although only axial tension will be applied, compression will be felt in some elements, as well in some material directions due to Poisson's effect. The generated tests will consider composite plates loaded in tension, including (0), (90), and ( $\pm 45$ ), laminates using Fisher's high temperature data.

This will be accomplished by the following procedure. First, ASTROS is run with nominal values with an increment of the total load or displacement to be applied. The resulting stresses and strains for each element and angular orientation of the finite element model are compared to experimental data for the moduli. The strain values update  $E_1$ ,  $E_2$ ,  $G_{12}$  and  $\nu_{12}$  for each finite element using cubic spline interpolation through experimental data points. After updating these properties on the ASTROS material cards, ASTROS is run for the successive increment. By summing each element's incremental stresses and strains, the nonlinear data results.

This present research shows the ability to predict nonlinear laminate results in different orientations and ply lay-ups, even with discontinuities, or holes. Other applications include modeling nonlinear materials that are not composites. The overall result is that nonlinear materials can successfully be used to design within the ASTROS framework.

## II. Theory

This thesis made use of several theories and concepts. This chapter's purpose is to discuss those relevant postulates, forming a basis for the application seen in this research. The areas of interest covered include, sequentially: nonlinearity, plane stress elasticity, mechanics of composite materials, finite element mechanics, the ASTROS computer program, the cubic spline, and the presentation of the sum of these theories into the algorithm that this research has proposed to advance—incorporating nonlinear material properties into the Automated Structural Optimization System (ASTROS).

Assume Cartesian coordinates throughout this chapter and throughout the entire report.

### *Nonlinearity*

Nonlinearities can be classified into three categories (3), including 1) Materially nonlinear only; 2) Large displacements, large rotations, but small strains; 3) Large displacements, large rotations and large strains.

This present research considered only material induced nonlinearities, or the first category. By using a sufficiently small increment, the problem can be considered piece-wise linear, and more easily understood (3). This was the approach taken to evaluate the effect of changing moduli within the Graphite/PEEK Composites considered. This is an appropriate techniques, even for composites, since even nonlinear materials will retain their orthotropic nature (4). This means that the moduli are uncoupled, that is, shear stresses won't cause normal straining and normal stresses won't cause shear straining.

### *Plane Stress Elasticity*

Volumes could be and have been written about elasticity. For the purpose of this present research, it will be sufficient to encapsulate the theory while expounding on one of the tenants of two dimensional elasticity, namely the plane-stress assumption. Elasticity is the study of the changes in length and direction caused by displacement of a line element that joins two infinitesimally close points (24). We will see that elasticity is also behind the theory of the finite element method, which will be discussed shortly. Elasticity defines equations that are basic to finite element modeling.

If the planes initially normal to an axis remain normal to it after a deformation, including the

straight lines initially parallel to the given axis remaining parallel, plane deformation is encountered (24). Within plane deformation, plane strain or plane stress may result. Plane strain occurs when there are no strains in the axis considered. Plane stress involves zero stresses along the axis in question. Consider plane stress for the out of (the horizontally) plane axis  $X_3$  in Figure 2. Plane stress would involve:

$$\sigma_{33} = \tau_{13} = \tau_{23} = 0$$

Generalized plane stress involves thin plates whose stress tensor and displacement vector are evaluated in this horizontal plane. For isotropic (having no preferred directions) and isothermal conditions, plane stress can be represented analytically by:

$$\begin{Bmatrix} E_1 \\ E_2 \\ \gamma_{12} \end{Bmatrix} = \frac{1}{E} \begin{bmatrix} 1 & -\nu & 0 \\ -\nu & 0 & 0 \\ 0 & 0 & E/G \end{bmatrix} \begin{Bmatrix} \sigma_1 \\ \sigma_2 \\ \tau_{12} \end{Bmatrix}$$

The plane stress assumption is well suited for two dimensional problems. However, it could be invalidated by compression-induced buckling into the third dimension. Because of this limitation,

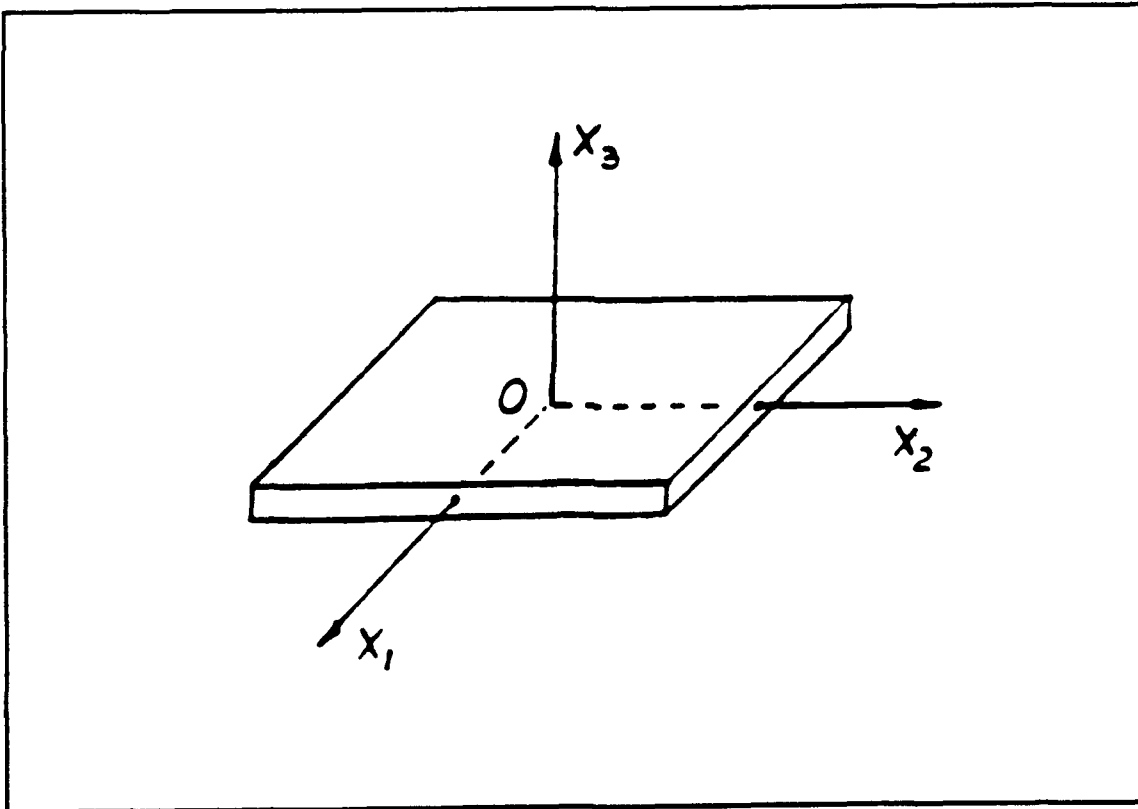


**Figure 2. Flat Plate**



the present research is restricted to axial tension loading and displacements only. The plane stress relations for a composite material will be developed in the next section.

### ***Mechanics of Composite Materials***

ASTROS has been utilized in this research for analysis of both isotropic and anisotropic materials. Composites are not isotropic. The fiber and matrix composites considered in this research are generally orthotropic. As shown in Figure 3, orthotropic means that along the fiber axis there is symmetry. Also notice in this figure that the fiber direction is aligned with the coordinate axis. This is not required for a material to be orthotropic, but analysis of nonaligned materials requires a transformation.

There are two general approaches to composite materials: considering micromechanical or macromechanical behavior. Micromechanical studies concern themselves with the fiber and matrix materials individually. Macromechanical studies are concerned with the properties of the ply as a whole. This is the interest of the present research. Since our nonlinear model is piece-wise linear, linear elastic mechanics model the behavior of our laminates.

***Lamina Behavior.*** Within each linear segment, Hooke's Law holds:

$$\sigma = E\varepsilon$$

$$\varepsilon = G\sigma$$

In matrix or tensor notation, Hooke's Law can be conveniently written:

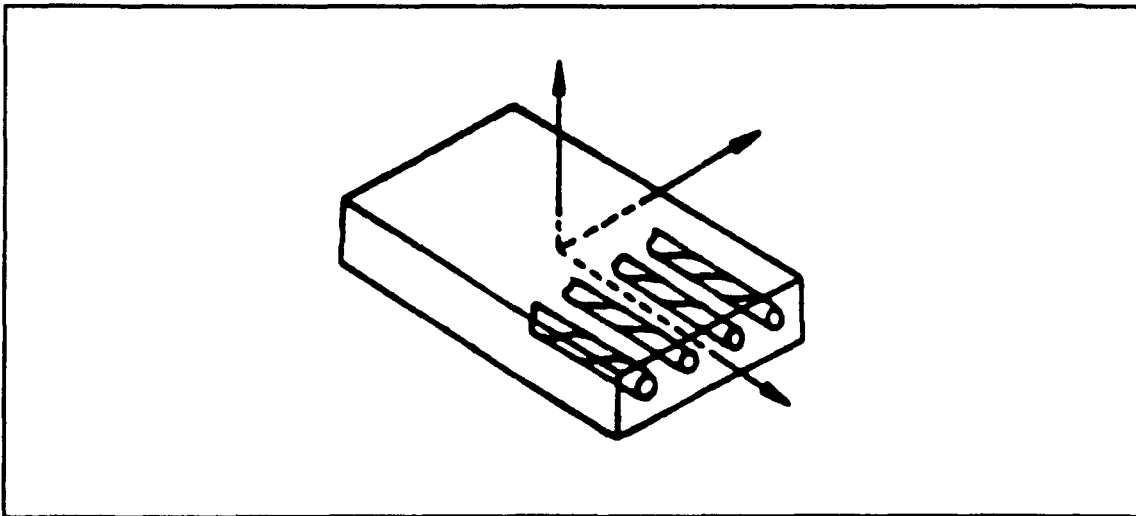


***Figure 3. Lamina with Unidirectional Fibers (15)***

$$\sigma_i = C_{ij} E_j \text{ or}$$

$$E_i = S_{ij} \sigma_j$$

for  $i \text{ \& } j = 1, 2, 3, 4, 5, 6$

where  $C$  is the stiffness matrix and  $S$  is the compliance matrix.

When the coordinate axes correspond to the symmetry axes of the material, the matrices can be written as:

$$\begin{Bmatrix} \sigma_1 \\ \sigma_2 \\ \sigma_3 \\ \tau_{23} \\ \tau_{31} \\ \tau_{12} \end{Bmatrix} = \begin{bmatrix} C_{11} & C_{12} & C_{13} & 0 & 0 & 0 \\ C_{12} & C_{22} & C_{23} & 0 & 0 & 0 \\ C_{13} & C_{23} & C_{33} & 0 & 0 & 0 \\ 0 & 0 & 0 & C_{44} & 0 & 0 \\ 0 & 0 & 0 & 0 & C_{55} & 0 \\ 0 & 0 & 0 & 0 & 0 & C_{66} \end{bmatrix} \begin{Bmatrix} \epsilon_1 \\ \epsilon_2 \\ \epsilon_3 \\ \gamma_{23} \\ \gamma_{31} \\ \gamma_{12} \end{Bmatrix}$$

(where  $\epsilon_{ij}$  = engineering strain =  $2\gamma_{ij}$ )

which reduces to the following in plane stress ( $\sigma_{33} = \tau_{13} = \tau_{23} = 0$ )

$$\begin{Bmatrix} \sigma_1 \\ \sigma_2 \\ \tau_{12} \end{Bmatrix} = \begin{bmatrix} C_{11} & C_{12} & 0 \\ C_{12} & C_{22} & 0 \\ 0 & 0 & C_{66} \end{bmatrix} \begin{Bmatrix} \epsilon_1 \\ \epsilon_2 \\ \gamma_{12} \end{Bmatrix}$$

or equivalently

$$\begin{Bmatrix} \epsilon_1 \\ \epsilon_2 \\ \gamma_{12} \end{Bmatrix} = \begin{bmatrix} S_{11} & S_{12} & 0 \\ S_{12} & S_{22} & 0 \\ 0 & 0 & S_{66} \end{bmatrix} \begin{Bmatrix} \sigma_1 \\ \sigma_2 \\ \tau_{12} \end{Bmatrix}$$

In the above equations,  $C_{ij}$  and  $S_{ij}$  have been found to equal:

$$C_{11} = \frac{E_1}{1 - \nu_{12} \nu_{21}}$$

$$C_{12} = C_{21} = \frac{\nu_{21} E_1}{1 - \nu_{12} \nu_{21}}$$

$$C_{22} = \frac{E_2}{1 - \nu_{12} \nu_{21}}$$

$$C_{66} = G_{12}$$

$$S_{11} = \frac{1}{E_{11}}$$

$$S_{12} = \frac{-\nu_{12}}{E_{11}} = \frac{-\nu_{21}}{E_{22}} = S_{21}$$

$$S_{22} = \frac{1}{E_{22}}$$

$$S_{66} = \frac{1}{G_{12}}$$

The stiffness matrix, C, is also referred to as Q.

When the coordinate axes and fiber (or material) axes are not aligned, as in Figure 4, a transformation must rotate the above equations into the coordinate axes:

$$\begin{Bmatrix} \sigma_x \\ \sigma_y \\ \tau_{xy} \end{Bmatrix} = \begin{bmatrix} \bar{Q}_{11} & \bar{Q}_{12} & \bar{Q}_{16} \\ \bar{Q}_{12} & \bar{Q}_{22} & \bar{Q}_{26} \\ \bar{Q}_{16} & \bar{Q}_{26} & \bar{Q}_{66} \end{bmatrix} \begin{Bmatrix} \epsilon_x \\ \epsilon_y \\ \gamma_{xy} \end{Bmatrix}$$

where

$$\bar{Q}_{11} = Q_{11}\sigma^4 + Q_{22}i^4 + 2(Q_{12} + 2Q_{66})i^2\sigma^2$$

$$\bar{Q}_{22} = Q_{11}i^4 + Q_{22}\sigma^4 + 2(Q_{12} + 2Q_{66})i^2\sigma^2$$

$$\bar{Q}_{12} = (Q_{11} + Q_{22} - 4Q_{66})i^2\sigma^2 + Q_{12}(i^4 + \sigma^4)$$

$$\bar{Q}_{66} = (Q_{11} + Q_{22} - 2Q_{12} - 2Q_{66})i^2\sigma^2 + Q_{66}(i^4 + \sigma^4)$$

$$\bar{Q}_{16} = (Q_{11} - Q_{12} - 2Q_{66})\sigma^3i - (Q_{22} - Q_{12} - 2Q_{66})i^3\sigma$$

$$\bar{Q}_{26} = (Q_{11} - Q_{12} - 2Q_{66})\sigma^3i - (Q_{22} - Q_{12} - 2Q_{66})i^3\sigma$$

where  $i = \sin\phi$

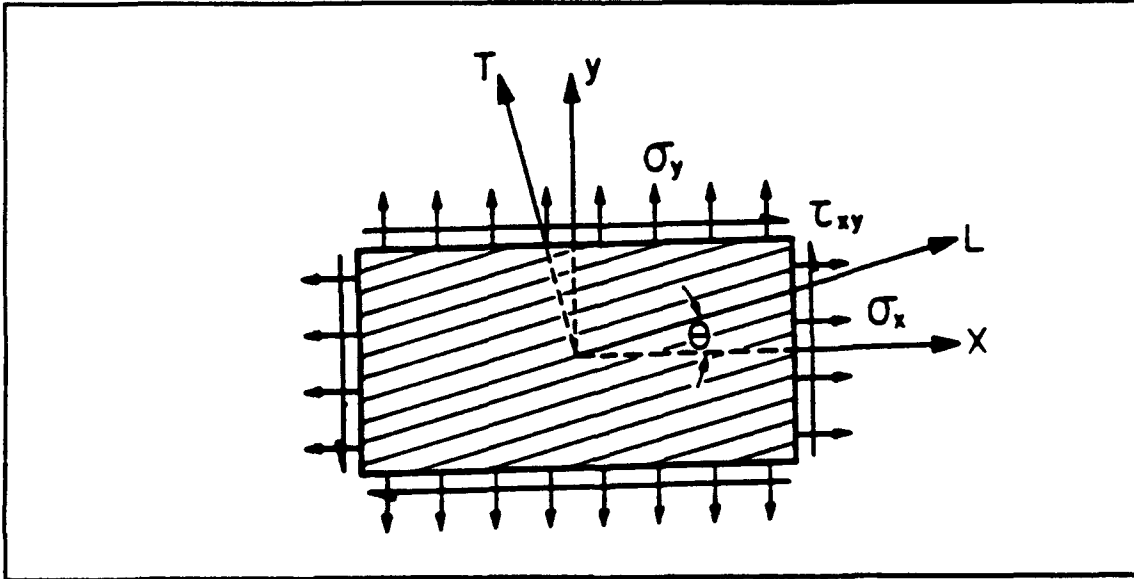


**Figure 4. Principal Material Axes Oriented at Angle  $\theta$  with Reference Coordinate Axes**

$$o = \cos \phi$$

$\phi$  = transformation angle

**Laminate Behavior.** On the macromechanical scale, laminate behavior depends on the summation of individual lamina behavior. However, individual plies cannot deform independently, so equation (1) must be satisfied by each layer. The interaction of the plies is accounted for in the next section, within the finite element's equivalent stiffness matrix. Neighboring plies of different orientation usually cause out of plane stresses, appropriately called interlaminar stresses.

### **Finite Element Modeling (FEM)**

The finite element method is a numerical procedure for analyzing structures and continua. Usually the problem addressed is too complicated to be solved satisfactorily by classical analytical methods. The problem may concern stress analysis, heat conduction, or any of several other areas. The finite element procedure produces many simultaneous algebraic equations, which are generated and solved on a digital computer. Finite element calculations are performed on personal computers, mainframes, and all sizes in between. Results are rarely exact. However, errors are decreased by processing more equations, and results accurate enough for engineering purposes are obtainable at reasonable cost. (5)

With that introduction, Cook has set the stage for further discussion of this technique. The finite element method is used in designing. FEM can be used in the design of any conceivable structure—the U.S. Air Force uses FEM exhaustively. Although it is possible to use FEM without a computer (FEM dates back to 1906), FEM has come of age because of the vast numerical abilities of modern computing equipment.

The main divisions of FEM include: strain-displacement relations, stress-deformation relations, stress-strain relations, stiffness equations, element formulation, and convergence. Although not separately addressed, the theory of elasticity will be evident in the following discussion.

**Strain Displacement Relations.** Figure 5 shows the deformation caused by loading - - 01 and 02 become 0'1' and 0'2'. Recall

$$\epsilon_x = \frac{L0'2' - L0'2'}{L02} = \frac{dx + \left(u + \frac{\partial u}{\partial x} dx\right) - u - dx}{dx}$$

$$\epsilon_x = \frac{\partial u}{\partial x}$$

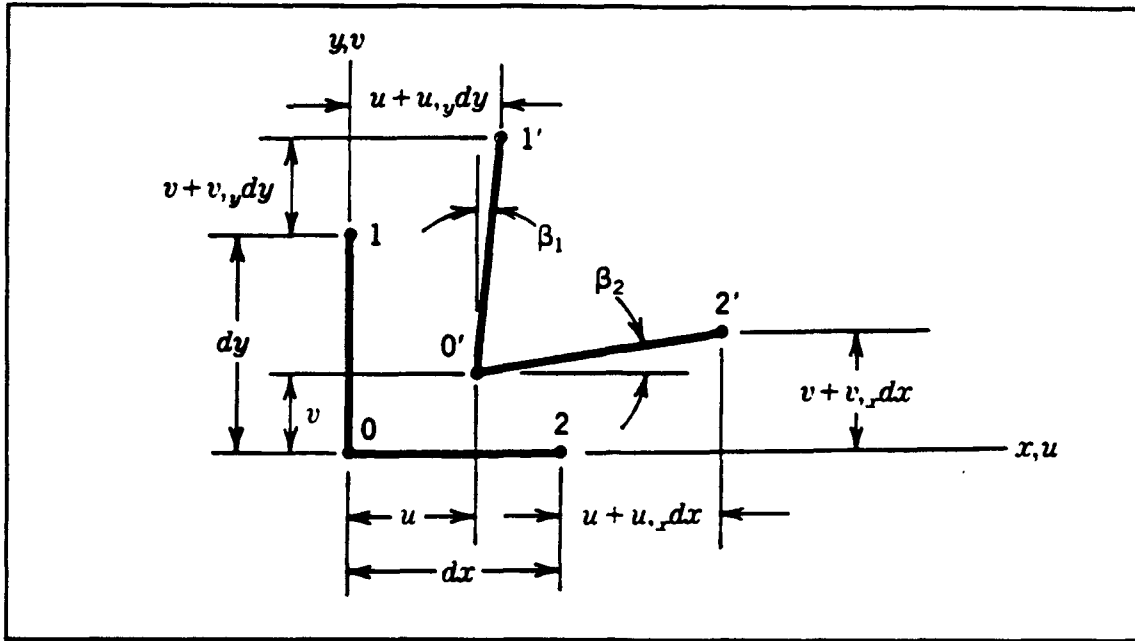


Figure 5. Displacement and Distortion of Differential Lengths  $dx$  and  $dy$

$$\text{Similarly, } \epsilon_y = \frac{\partial v}{\partial y}$$

Engineering shear strain is defined as the amount of change from a right angle. Assuming small angles,  $\beta$ , approximately equals  $\tan\beta$ , likewise for  $\beta_2$ . Therefore, Cook shows that:

$$\gamma_{xy} = \beta_1 + \beta_2 = \frac{\partial u}{\partial y} + \frac{\partial v}{\partial x}$$

The above three equations are the two dimensional strain displacement relations, which can be written as:

$$\{E\} = [\partial] \{U\}$$

where  $U$  represents displacements.

**Stress-Deformation Relations.** This section could formally be entitled "Elasticity." Equilibrium, compatibility and the boundary conditions must be satisfied within the finite element method for a correct solution, just as in elasticity. Equilibrium is satisfied when the forces from the stresses on the differential element's edges and from its body forces are in equilibrium (which is that the sum of all forces equals zero for a statics problem).

From Figure 6, we see this must give the following:

$$\sigma_{xx} + \tau_{xy,y} + F_x = 0 \quad (x \text{ direction})$$

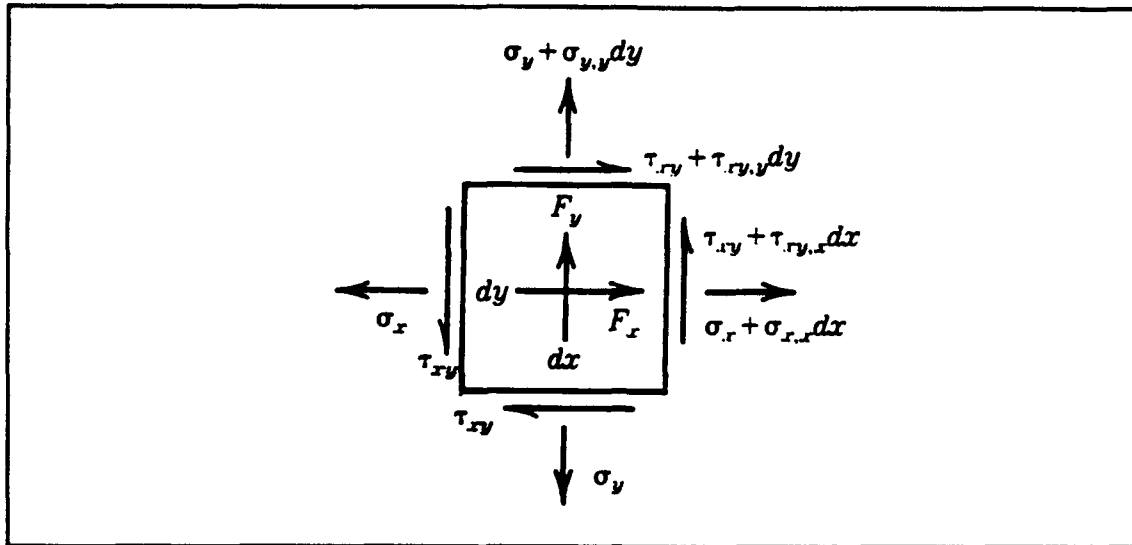


Figure 6. Stresses and Body Forces

$$\tau_{xy,x} + \sigma_{y,y} + F_y = 0 \quad (\text{y direction})$$

where  $\tau_{xy,y}$  notation denotes  $\frac{\partial \tau_{xy}}{\partial y}$ , and  $F_x$  and  $F_y$  respectively represent the body forces in the  $x$  and  $y$  directions.

Compatibility is best explained by example. If we consider a Rubik's cube, we realize that there will not be gaps or overlaps between elements. This also must be computationally true on the infinitesimal level.

The enforcement of boundary conditions translates into prescribed displacements and/or stresses. Again, boundary conditions are easily comprehended by example. If you analyze a cantilevered beam, the inability of displacements at the wall form a boundary condition for the specimen.

**Stress-Strain Relations.** Ignoring the effects of temperature change,

$$\{\epsilon\} = [S] \{\sigma\} \quad \text{or equivalently}$$

$$\{\sigma\} = [C] \{\epsilon\}$$

Where  $[S]$  is called the compliance tensor, and  $[C]$  represents the stiffness tensor, and:

$$[S] = [C]^{-1}$$

As you may recall from the previous section, the plane stress assumption was written as a function of stress and strain.

**Element Formulation.** Stepping back, into the bigger picture of finite element modeling, it would be useful to realize that the problem is solved as several smaller blocks are solved. These blocks are interconnected, like the face of the Rubik's cube mentioned earlier, except that there can be thousands of these smaller pieces. They are interconnected at their boundaries in terms of the constitutive equations, which represent each block physically.

Before considering the elements as a set, a single two dimensional element will be developed. Although three-sided or triangular elements were first used, this present research was conducted using a quadrilateral (rectangular) plate element. This research could not be done with membrane (i.e. two dimensional) elements. ASTROS, as well as other finite element programs require plate elements to capture the thickness which needs to be considered for a composite laminate. The program PLSTR was used to show the accuracy of the developed algorithm. Although ASTROS and PLSTR formulate their plate elements differently, the two programs gave answers which correlated to the sixth decimal place when a isotropic material was considered with the same membrane element.

The plate elements in ASTROS and PLSTR are formulated with the same objectives in mind, but there are a few differences (although they are not very significant).

Dr. Sanhu's element is equivalent to another type of ASTROS element. They are formulated by breaking the quadrilateral into four triangles after generating a fictitious node in the middle (32). This type of element can then consider a quadrilateral as four constant strain triangles. The polynomial which describes each triangular element is of the form:

$$U = ax + by + c$$

It is complete, meaning that when the strain is calculated, the only terms remaining after the partial differentiation are the constants a and b, since

$$E_x = \frac{\partial u}{\partial x}$$

$$E_y = \frac{\partial v}{\partial y}$$

This results in four triangular elements whose strain remains constant throughout each. The fictitious central node is then removed to reform the quadrilateral element.

The element ASTROS used in this study is isoparametric, with slightly better stiffness properties

than the constant strain elements considered above. ASTROS evaluates the quadrilateral element using a displacement equation of the form:

$$U = ax + by + cxy + d$$

When strains are found, there remains a term which is either a function of  $x$  or  $y$ ; these strains are said to vary linearly. Results are found using numerical integration across the remaining variable.

The following discussion will be in terms of this isoparametric four-sided element, although for very simple structures a one dimensional bar or rod element may be used as shown in Figure 7. The linear strain quadrilateral plate element (shown in Figure 8) has eight degrees of freedom (DOF): each of the 4 nodes can move in the  $x$  or  $y$  directions. A displacement in the  $x$  or horizontal direction is called  $u$ , whereas a displacement in the  $y$  direction is in the node's  $v$  direction.

Shape functions are used to determine the response of a DOF. A matrix of shape functions,  $[N]$ , determines how each displacement,  $u$  and  $v$ , varies with  $x$  when the corresponding DOF has unit value and the other is zero.  $[N]$  describes how to interpolate each DOF over the elements.

$$u = [N] \begin{Bmatrix} u_1 \\ u_2 \\ u_3 \\ u_4 \end{Bmatrix}$$

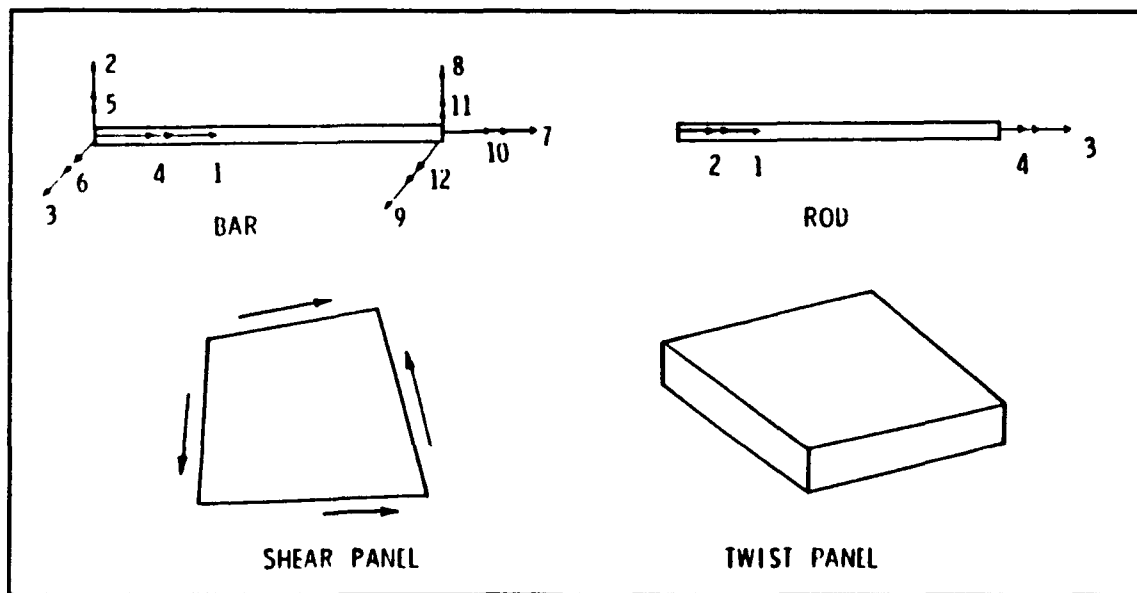


**Figure 7. Structural Elements**



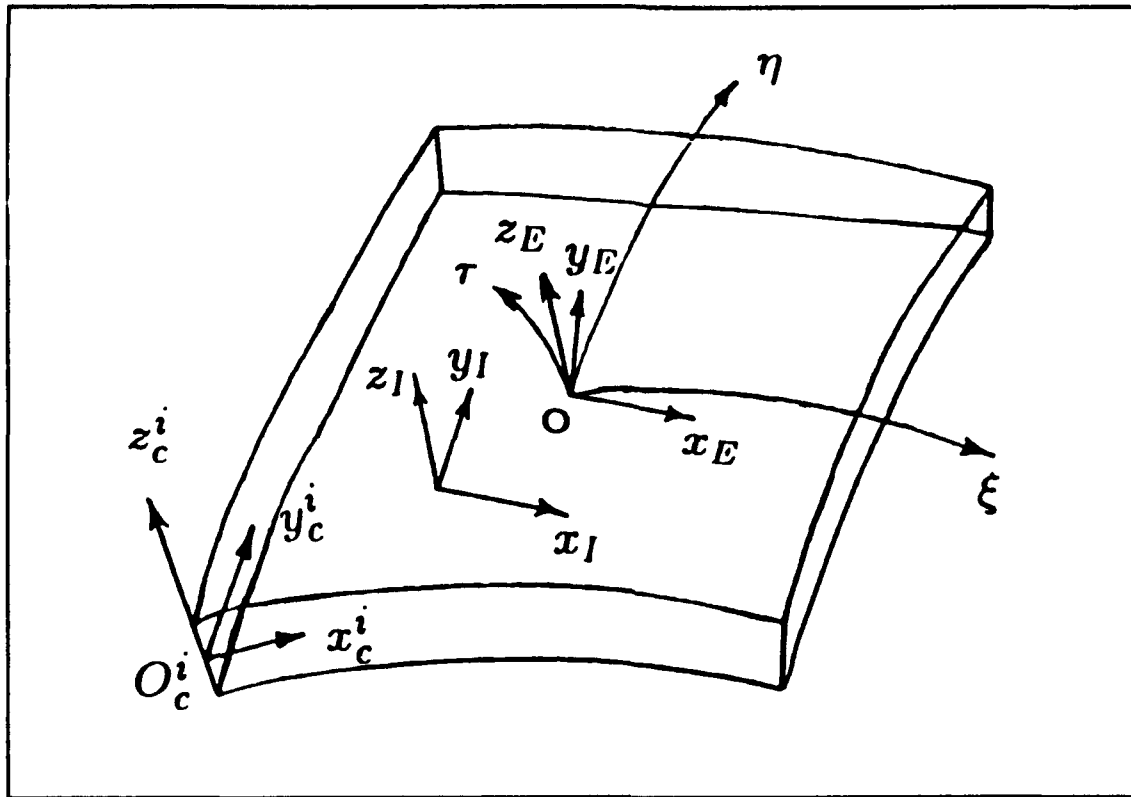


Figure 8. QUAD 4 Element

$$v = [N] \begin{Bmatrix} v_1 \\ v_2 \\ v_3 \\ v_4 \end{Bmatrix}$$

Strains can be found from the strain-displacement matrix,  $[B]$ , and the displacement vector:

$$\begin{Bmatrix} \epsilon_x \\ \epsilon_y \\ \gamma_{xy} \end{Bmatrix} = [B] \begin{Bmatrix} u_1 \\ u_2 \\ u_3 \\ v_1 \\ v_2 \\ v_3 \\ v_4 \end{Bmatrix}$$

An individual element stiffness matrix,  $[k]$ , is now achievable:

$$[k] = \int_{area} [B]^T [E] [B] t \, da$$

$$[k] = [B]^T [E] [B] t A$$

where:

$$[E] = \frac{E}{1-\nu^2} \begin{bmatrix} 1 & \nu & 0 \\ \nu & 1 & 0 \\ 0 & 0 & \frac{1-\nu}{2} \end{bmatrix}$$

(in plane stress)

In composites,  $[Q]$  is parallel to  $[E]$ ; therefore for each composite element:

$$[k] = [B]^T [Q] [B] tA$$

$[k]$  is an equilibrium set of forces from the nodes, or corners, associated with the activation of that DOF. The global stiffness matrix,  $[K]$ , is an interlinked combination of all the element's  $[k]$ .

$$[K] \{D\} = \{R\}$$

where

$\{D\}$  = Global DOF matrix

$\{R\}$  = Global force matrix.

The discussion of finite elements would not be complete without the practical application. There are several important concepts worth mentioning. First, the elements must be chosen to have low aspect (i.e. length to width) ratios and the angles at the corners of each element should not be too extreme, but instead stay around ninety degrees. The elements must be small enough to accurately model the actual situation (this is known as convergence), yet as the number of elements increase, so does computation time and complexity. Each element and its nodes are numbered (according to the specific program's instructions) to keep track of them, specifically those representing areas of heightened interest. Finally, and most importantly, it is essential to be sure the model you give to the computer is what you think it is. Wrong answers can be generated to extreme accuracy, but they will still be wrong.

## ASTROS

The computer software base for this research is the Automated Structural Optimization System, or ASTROS. It is versatile and powerful. Specifically, ASTROS' purpose is to "provide an automated tool for the preliminary design of aerospace structures which emphasizes the interdisciplinary requirements of the design task" (13). It has been developed to meet the concurrent engineering objectives of the defense industry: improved, cost-effective, yet quick design.

Although concurrent engineering may be considered a soft science by some, its basic concepts have been overlooked for so long that their application has been very beneficial. Concurrent engineering may be summarized as the systematic improvement of product design, manufacturability, and quality while reducing time to market (31). Considering these advantages, reduced cost and improved customer satisfaction should also follow. In government terms, concurrent engineering supports Total Quality Management (TQM). As Turino defines in *Managing Concurrent Engineering*, concurrent engineering consists of the following five activities:

- Designing for performance
- Designing for manufacturability
- Designing for testability
- Designing for serviceability
- Designing for compliance

As you can see, concurrent engineering does more than include the design process; the design process is at the heart of it. It is well known that, "Decisions made during the design phase of a product have the biggest impact on product cost over the life of a product." (30). Figures 9 and 10 graphically show this (31).

The Department of Defense is also interested in fielding equipment faster. Figure 11 shows that concurrent engineering saves time by eliminating the redesign and reverify loops from the engineering process.

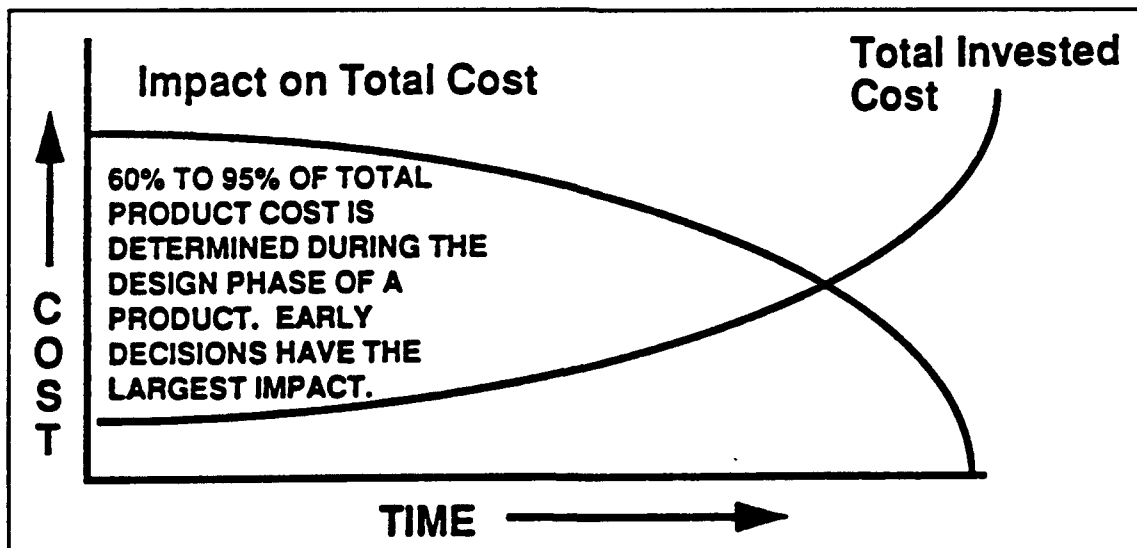


**Figure 9. Impact of Design Decisions on Total Product Life Cycle Cost**

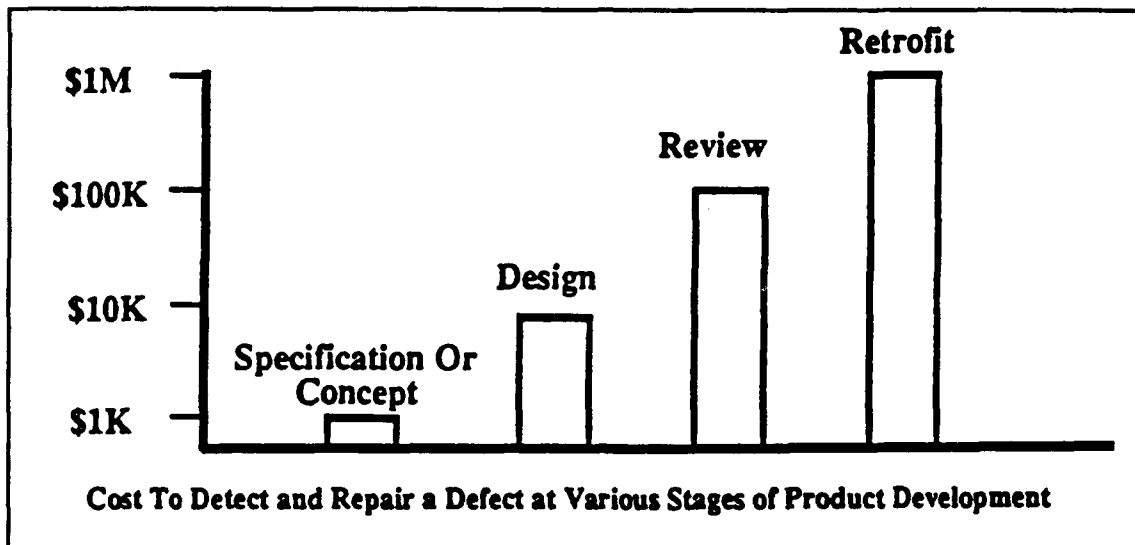


*Figure 10. Concept, Design, Review, and Retrofit Costs*

Finger and Dixon have thoroughly reviewed mechanical engineering design. They feel "An important area that has received little attention to date is the creation of design environments that integrate available tools into a consistent system to support the designer." (7,8). This brief summary of concurrent engineering motivates this research which improves the capabilities of ASTROS, a concurrent engineering tool for designers.

ASTROS is designed to handle aerodynamics, optimization, control systems and the subject of

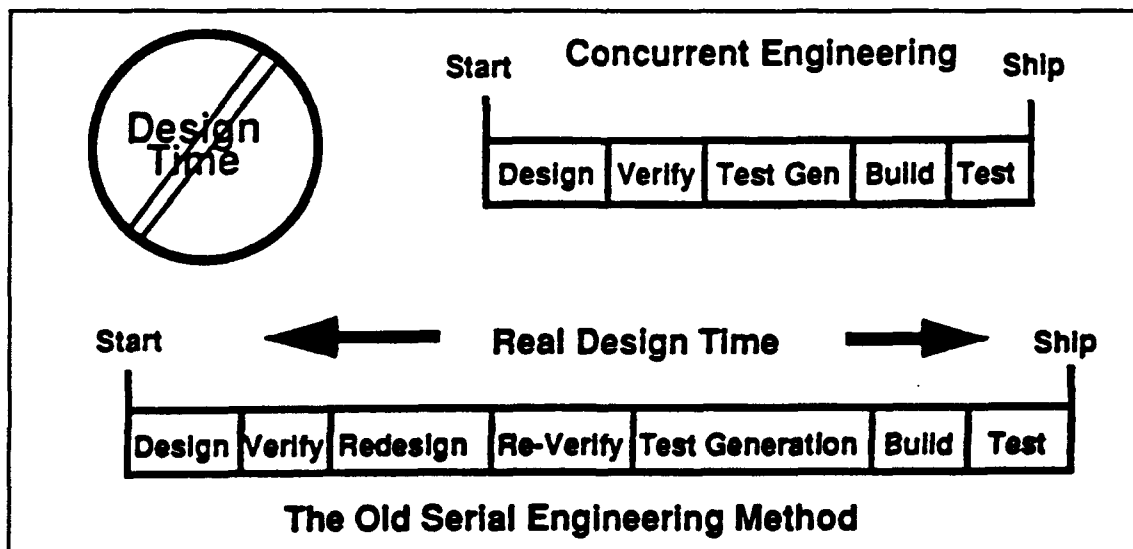


*Figure 11. Time to Market*

this research: static structural analysis (see Figures 12 and 13). Figure 14 shows the organization of this system.

Users interface with ASTROS in three possible ways. First, it is possible to communicate with ASTROS through bulk data entries, which would represent: the element and node sequencing, boundary conditions, and forces and/or displacements. Second, the solution control commands are used to direct the computer exactly how to process the bulk data. This includes possible optimization strategies, titles for later data manipulation, control numbers for boundary condition and load cases, and other options such as printing instructions. Third, there is access into the program software, the Matrix Analysis Problem Oriented Language (MAPOL).

The structural analysis portion of ASTROS is a program similar to NASTRAN in terms of pre- and post-processor interfaces. Neither have had a nonlinear materials feature for composites.

For laminates, ASTROS calculates a material property matrix,  $[G]$ .  $[G]$  is an expression combining all moduli of each layer, such that

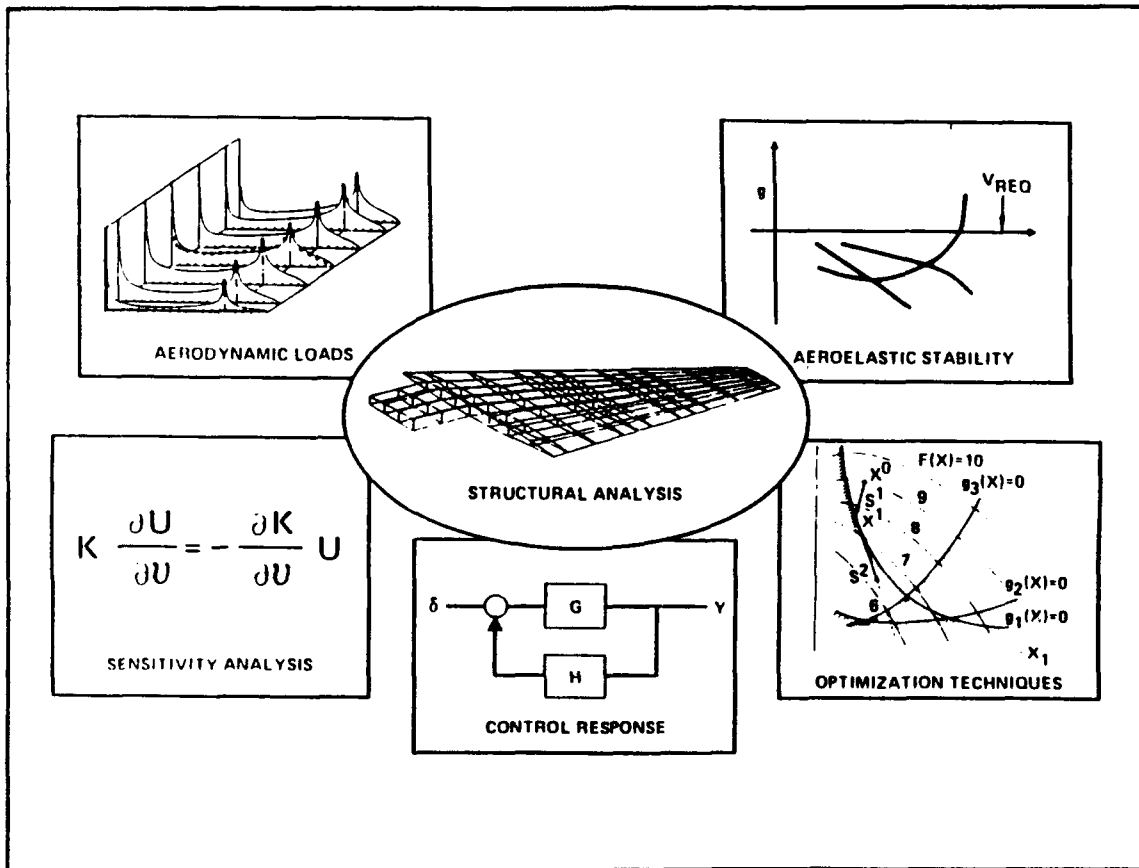


**Figure 12. ASTROS' Engineering Disciplines**

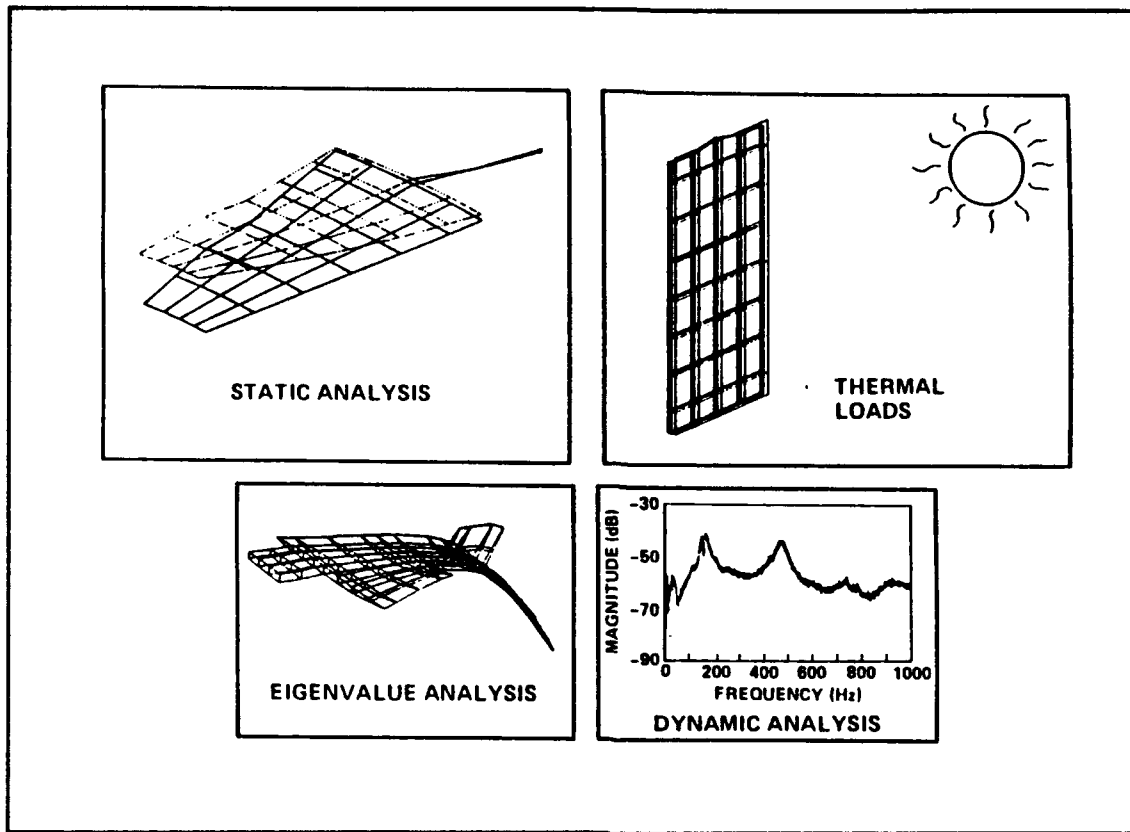


*Figure 13. ASTROS' Structural Analyses*

$$\begin{Bmatrix} \sigma_1 \\ \sigma_2 \\ \tau_{12} \end{Bmatrix} = \begin{bmatrix} G_{11} & G_{12} & G_{13} \\ G_{12} & G_{22} & G_{23} \\ G_{13} & G_{23} & G_{33} \end{bmatrix} \begin{Bmatrix} \epsilon_1 \\ \epsilon_2 \\ \gamma_{12} \end{Bmatrix}$$

This makes it possible to consider a laminate with plies in several directions as a conglomerated ply—with this new ply's material axes coinciding with the stress coordinate system. The  $(\pm 45)$ , laminate has been successfully considered under this arrangement with the stress coordinate system aligned with the global, or  $x$  and  $y$ , axes. However, until more FE programs adopt this standard, comparing results outside of ASTROS will be limited.

### ***Cubic Spline***

The cubic spline is used to generate continuous function values, first derivatives, second derivatives and integrals from a set of data points. This is done by mapping the points to sections of cubic curves and forcing the first and second derivatives to be equal at the joining of each of these sections. They have been found to be quite superior to polynomials of interpolation (2). Simply put, it is possible to solve a system of linked equations, such as those generated to solve a

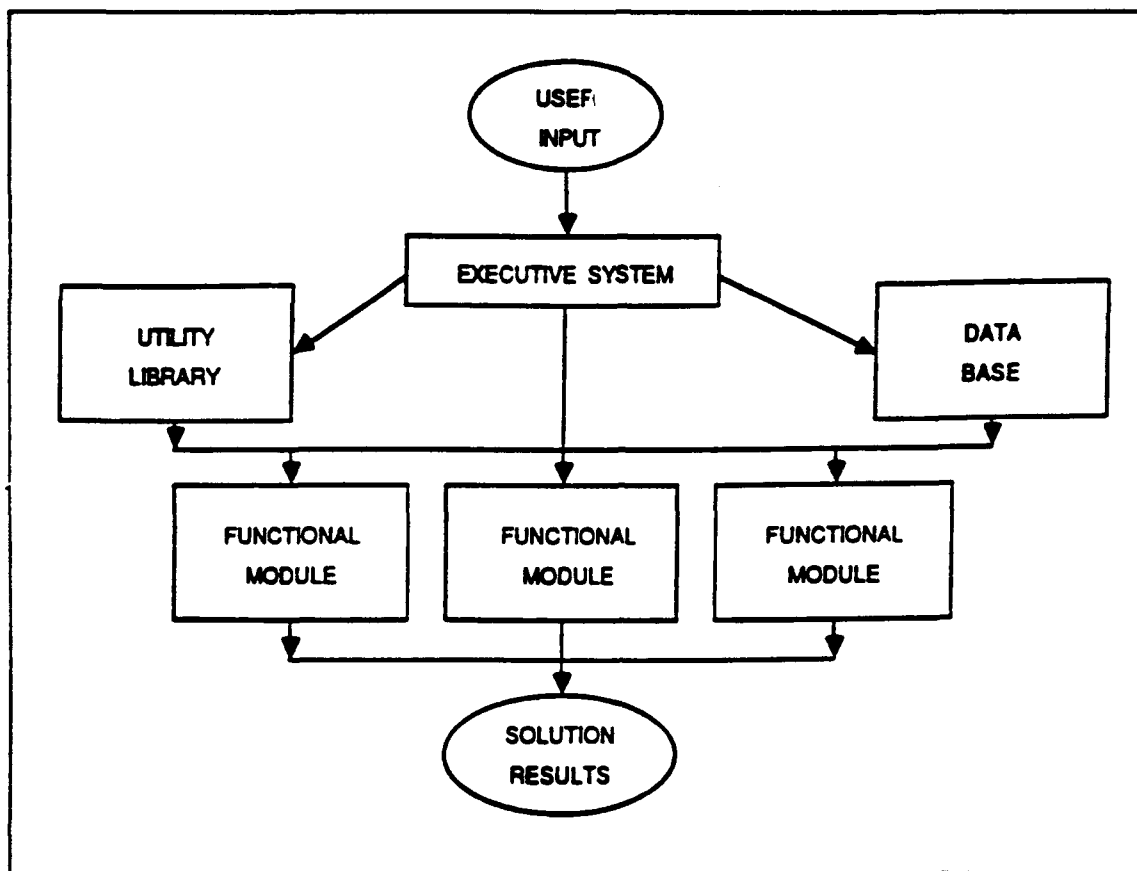


*Figure 14. The ASTROS System Architecture (14)*

spline, if two additional variables are known. By setting the second derivatives of the first and last data points equal to a constant, say zero, the entire system could systematically be solved. In order to eliminate any effect of this forced zero second derivative, an additional data point has been generated. This additional point increases the accuracy of the last few regions by allowing a smooth curve, through even the last data point. No calculations will be performed in the additional range.

The spline is used in this research to find the slopes, or moduli,  $E_1$ ,  $E_2$  and  $G_{12}$  from their respective stress-strain curves.

The updated Poisson's ratio,  $\nu_{12}$ , is the function value, or zeroth derivative of the  $\nu_{12}$  versus  $\epsilon_1$  (longitudinal strain) curve. For  $E_1$ ,  $E_2$ , and  $\nu_{12}$  separate splines were used for tensile and compressive conditions.

These curves can be generated for any material from experimental data.

As a basis for the nonlinear material properties updating, a computer algorithm (22) for a basic

spline was modified to accomplish this material properties research for each of the seven possible curves (see Appendix A). Five of these curves plot stress versus strain and consider the slope or modulus. These five curves include the longitudinal material direction in both tension and compression, the transverse material direction in tension and compression, and the shear direction. The last two curves consider the changing nature of Poisson's ratio for elements in tension and compression. These last two curves plot Poisson's ratio as a function of strain in the material's longitudinal direction. The actual value for Poisson's ratio is desired and not the slope of these curves.

A zero degree composite laminate plate without a hole in tension will only use three of these seven curves in a constant stress analysis in tension. These include the longitudinal tension curve, the transverse compression curve and the Poisson's ratio curve (in tension as well since it is a function of the longitudinal strain).

### *Summary*

This research was made possible and is widely applicable mainly due to the flexibility of ASTROS' bulk data deck. By assigning a material card to each element, the changing nature of the moduli and Poisson's ratio were captured. By putting in a composite property, or PCOMP, card for each layer of each element, a layered composite was able to be considered nonlinearly.

An initial run with very small forces or imposed displacements set the appropriate beginning material property values for the first increment. This initial iteration was not included in the summation of resulting stresses, strains, displacements and reaction forces.

This research considered both incremental imposed displacements and edge pressures. Forces on loaded edge nodes were used to represent a pressure or stress on the edge of the plate. Displacements were imposed directly to the edge nodes.

Every iteration of each test case ran the spline program to update the material properties, which in turn were used to evaluate the next increment of the imposed stress or displacement. The cycle was completed as the new strains were used to find the updated material property values from the experimental data using the spline program. This constituted the piecewise linear solution to the nonlinear properties problem.

Recall from finite elements:

$$[K] d = R$$



where  $[K] = \Sigma [k]_{el}$

$$[k]_{el} = \int \int \int_{vol} [B]^T [D] [B] dz da$$

where  $[D]$  relates  $\sigma$  to  $\epsilon$

$[B]$  relates  $\epsilon$  to the  $DOF$

Therefore:

$$[k]_{el} = \int \int [B]^T \left[ \int_{-t/2}^{t/2} [\bar{Q}_{ij}]_{ply} dz \right] [B] dA$$

$$[k]_{el} = \int \int [B]^T [A_{ij}] [B] dA$$

$$\text{where } [A_{ij}] = \sum_{ply=1}^n \bar{Q}_{ij} \cdot t$$

$$\bar{Q}_{ij} = F(E_1, E_2, \nu_{12}, G_{12}, \sin \theta, \cos \theta)$$

$$Q_{ij} = F(E_1, E_2, \nu_{12}, G_{12})$$

Incrementally:

$$[K] \Delta d = \Delta R$$

$$\Delta d = [K]^{-1} \Delta R$$

$$d\epsilon = [B] \Delta d$$

In global axes:

$$\begin{Bmatrix} d\epsilon_x \\ d\epsilon_y \\ 1/2 d\gamma_{12} \end{Bmatrix} = [B] \Delta d \text{ (constant thickness due to plane stress)}$$

In material coordinates:

$$\begin{Bmatrix} d\epsilon_x \\ d\epsilon_y \\ 1/2 d\gamma_{xy} \end{Bmatrix} = \begin{Bmatrix} d\epsilon_L \\ d\epsilon_T \\ 1/2 d\gamma_{LT} \end{Bmatrix} = [T] \begin{Bmatrix} d\epsilon_x \\ d\epsilon_y \\ 1/2 d\gamma_{xy} \end{Bmatrix}$$

$$\text{where } [T] = \begin{bmatrix} \cos^2\theta & \sin^2\theta & 2 \sin\theta \cos\theta \\ \sin^2\theta & \cos^2\theta & -2 \sin\theta \cos\theta \\ -\sin\theta \cos\theta & \sin\theta \cos\theta & \cos^2\theta - \sin^2\theta \end{bmatrix}$$

$$\epsilon_{xy} = \text{engineering strain} = 1/2 \gamma_{xy}$$

Therefore:

$$\begin{Bmatrix} \epsilon_1 \\ \epsilon_2 \\ \epsilon_{12} \end{Bmatrix}_{\text{total}} = \begin{Bmatrix} \epsilon_1 \\ \epsilon_2 \\ \epsilon_{12} \end{Bmatrix}_{\text{previous}} + \begin{Bmatrix} d\epsilon_1 \\ d\epsilon_2 \\ \frac{1}{2} d\gamma_{12} \end{Bmatrix}_{\text{current increment}}$$

Notice that the total strain for each element in the material axes is the summation of the current increment's strain with the strains from the previous increments. This is similarly true for stress, reaction forces and displacements.

Error results from the previous value for  $[K]$  being used to evaluate the current strains, stresses, reaction forces and displacements. To minimize error, increments must be kept small.

### III. Results and Discussion

This section summarizes the thesis research. It is divided into four logical units which represent the process and proper procedures for validating and using this research's results.

#### *Finite Element Model Verification*

**Mesh Size.** There were two models used in this research, although four were initially considered. Figure 15 shows that one of these models does not contain a hole. This simple flat plate was used to verify the FE and spline programs, as well as to easily contrast constant stress versus constant displacement loadings. The other three models included meshes of varying coarseness, but each of these had similar overall dimensions. They were 6.0 inches long, 1.2 inches wide, .084 inches thick and each had a central circular discontinuity of 0.4 inch diameter. Figures 16 through 18 are quarter plates of these three models.

To validate the accuracy of these models, an isotropic material was considered with a 2000 PSI stress applied through forces on edge nodes furthest from the hole. The actual stress concentration factor for a plate of this geometry is 3.46 (9). Table 1 shows the stress and SCF generated by the element closest to the hole and perpendicular to the applied force.

Model Number			
	1	2	3
Number of elements	36	66	72
Maximum Stress	10992	6194	6479
SCF	5.50	3.10	3.24
Error	59.0%	10.4%	6.4%

*Table 1. Stress Concentration Factor (SCF) Comparison*

Table 1 shows that model 1 is too coarse to converge. The answers gained by this model are not valid. Models 2 and 3 are actually variations of the same mesh. They have been used to show that although stress concentrations perpendicular to the hole are best modeled by the smallest possible element there, it should not be the only consideration in choosing a model. The mesh is an important factor, but not the only factor.

**Constant Stress Versus Constant Displacement Increments.** The rectangular quarter

3	0	0	12	15	18	21	24	27	30	33	36	39	42	45	48	51	54	57	60	63	66
2	0	5	11	14	17	20	23	26	29	32	35	38	41	44	47	50	53	56	59	62	65
1	0	0	7	10	13	16	19	22	25	28	31	34	37	40	43	46	49	52	55	58	61

4	0	0	13	16	19	22	25	28	31	34	37	40	43	46	49	52	55	58	61	64	67
3	0	5	11	14	17	20	23	26	29	32	35	38	41	44	47	50	53	56	59	62	65
2	0	0	8	11	14	17	20	23	26	29	32	35	38	41	44	47	50	53	56	59	62
1	0	0	0	3	6	9	12	15	18	21	24	27	30	33	36	39	42	45	48	51	54

**Figure 15. Plate without Hole**

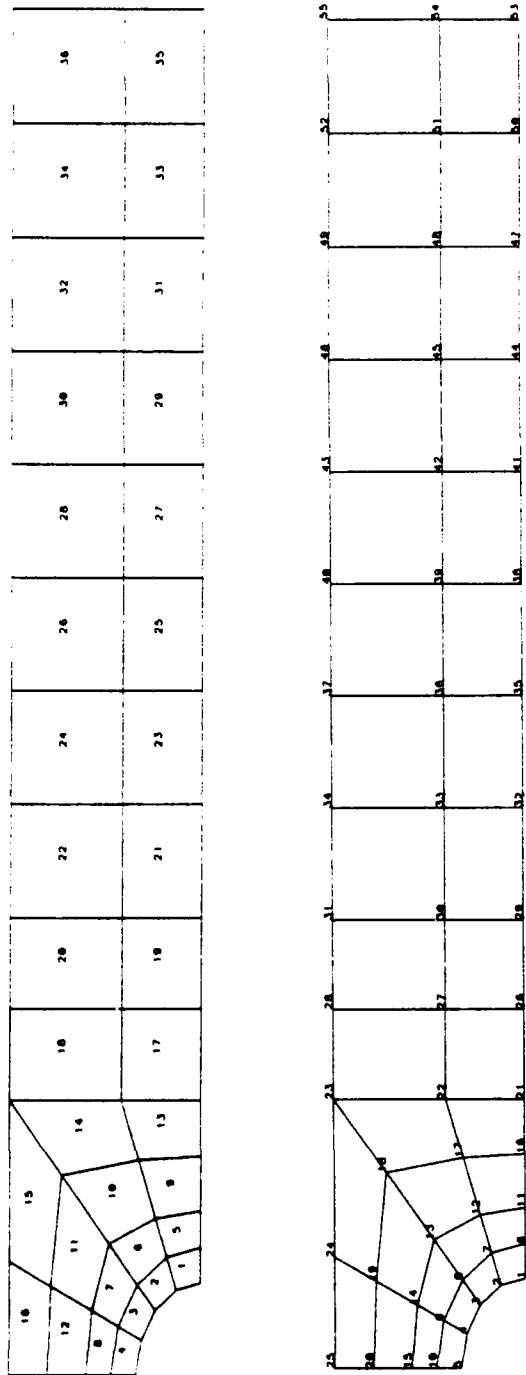


**Figure 16.36 Element Model**



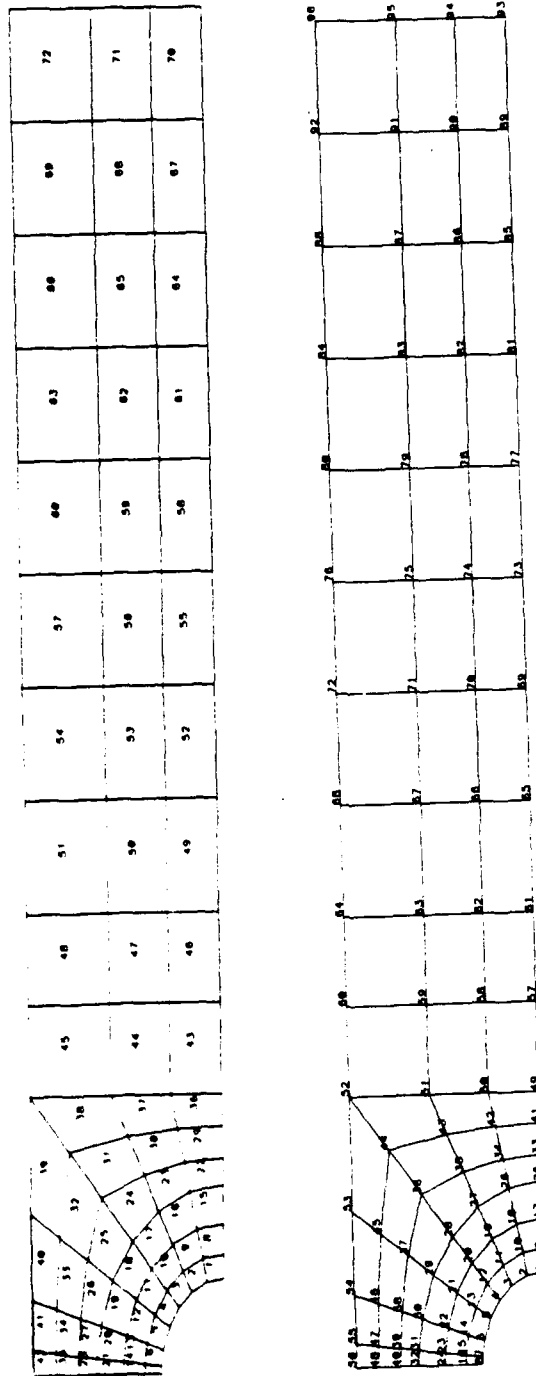


**Figure 18.72 Element Model**

plate without a hole is ideally suited to bring to light another important consideration in model selection. The loading conditions must also be considered to determine the accuracy of a FE model. Figures 19 and 20 show that even in the model without a hole (and therefore without complicated stress fields) there are slight stresses in the farfield in the nonloaded directions. This being true at the boundary, where stresses must equal the boundary conditions and applied stresses, shows a limitation of the constant displacement model. This makes sense, since the constant stress model, which should not produce stresses in the nonloaded axes at the farfield, has a different displacement and therefore stress situation than this constant displacement model. With constant stress, the edge region parallel to the discontinuity moves more than the originally parallel edge regions, due to the weakness from the discontinuity.

The constant displacement loading will produce small erroneous stresses in the nonloaded directions, but internal to the ASTROS model, the benefits of the ease of comparison of the linear to the nonlinear case have made both constant stress and constant displacement applications appropriate.

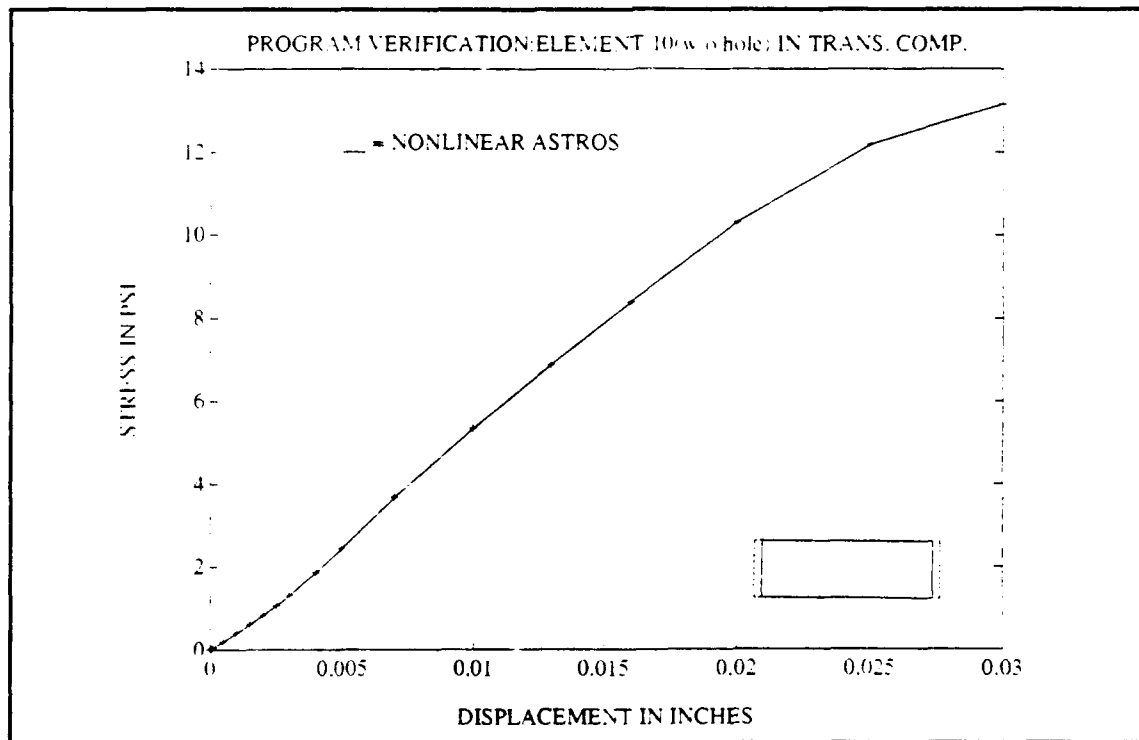


**Figure 19. (0) Rectangular Plate without Hole in Transverse Compression**



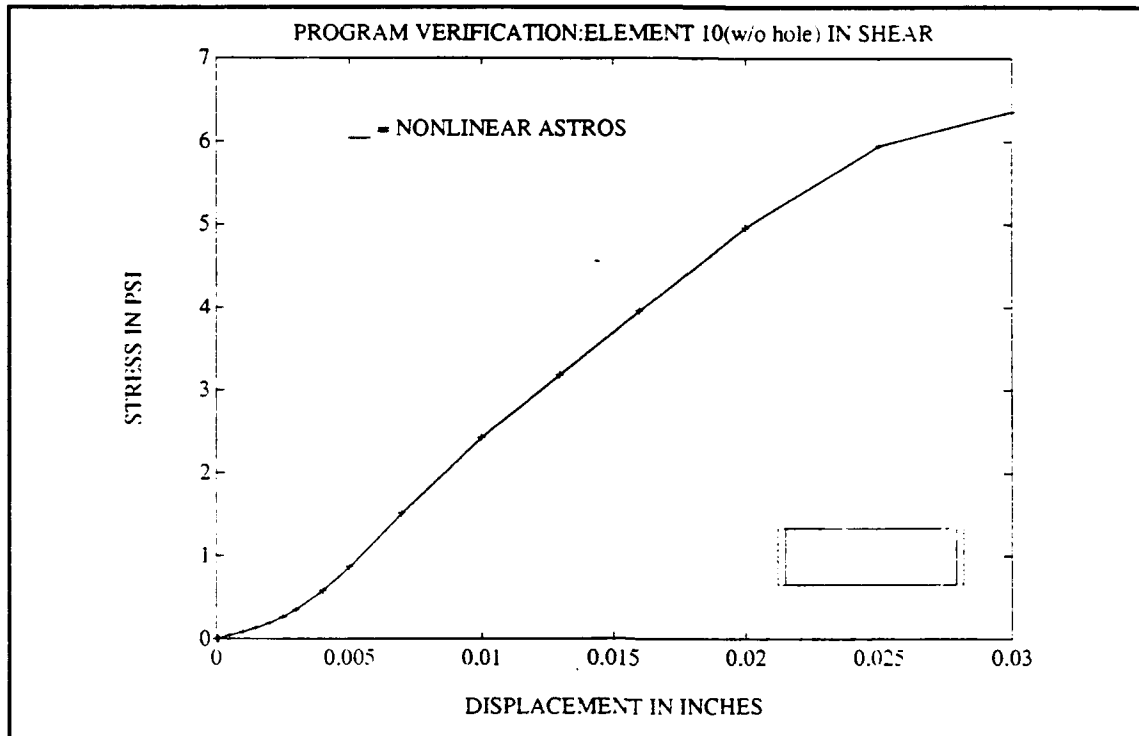


**Figure 20. (0) Rectangular Plate without Hole in Shear**

### ***Nonlinear Program Verification***

To verify that the developed nonlinear material capability worked as designed, comparisons were made to a validated nonlinear material solver. The first comparison modeled a 16 layer (0) plate without a hole, using generated spline data (see Appendix B). Figures 19, 20 and 21 are results of this comparison for the nonlinear ASTROS, showing the stresses resulting from the applied incremental displacements in the x direction. Contrast the magnitude of the nonloaded axes stresses in Figures 19 and 20 to that in Figure 21.

To validate the nonlinear program, this plate without a hole and one with a hole were each compared to Dr. Sandhu's nonlinear PLSTR program. Figure 22 shows the comparison between the newly developed nonlinear ASTROS, linear ASTROS and PLSTR. The linear version of ASTROS, represented by the dash-dot line, does not account at all for the changing modulus. It is evident that the nonlinear version of ASTROS represented by the solid line is able to correctly model the nonlinear stress-strain curve, which is modeled by the dashed line of the already proven program PLSTR. The differences between nonlinear ASTROS and PLSTR can be attributed to the differences in element formulation and the effect of increment size as discussed in Chapter II.

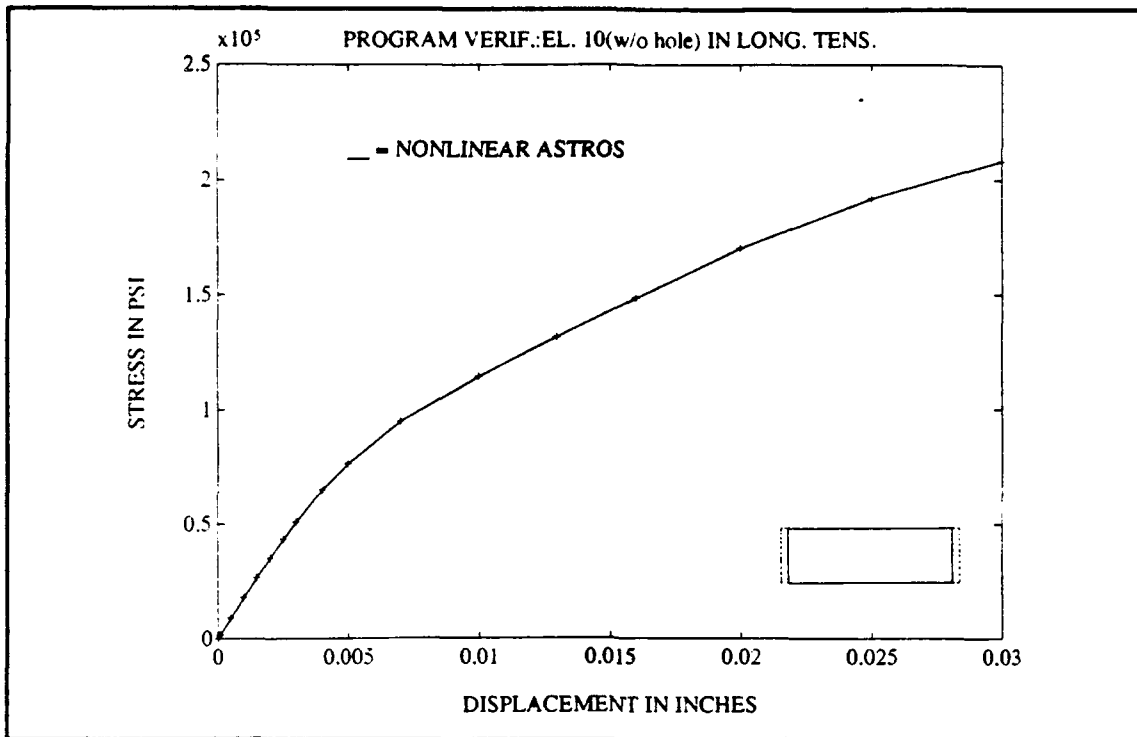


**Figure 21. (0) Rectangular Plate without Hole in Longitudinal Tensile Stress**

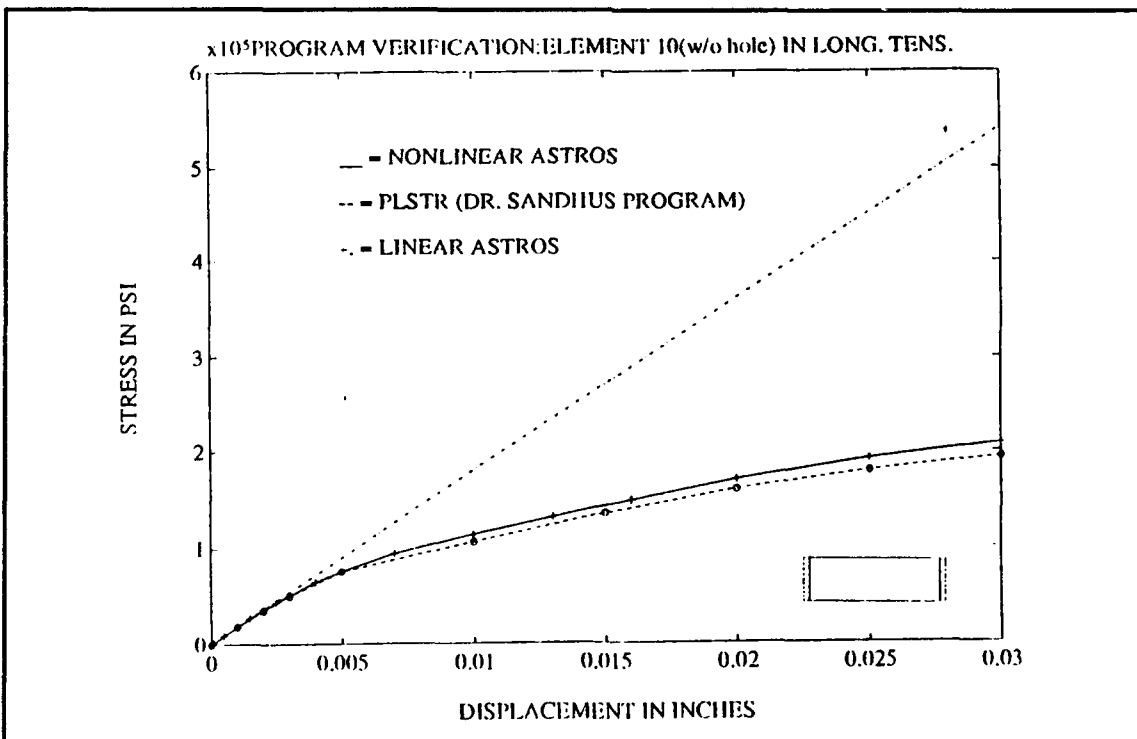


**Figure 22. (0) Rectangular Plate without Hole Comparison**

A plate with a hole comparison completes our program verification. The following series of figures were ran in the 66 element model of Figure 17. This model was used since ASTROS, both the linear and the nonlinear version, had trouble solving the 72 element mesh from Figure 18 in a composite material situation (due to restrictions within ASTROS that have been separately addressed with the ASTROS' Program Management Office personnel).

Since the splines used both in Dr. Sandhu's PLSTR and the nonlinear ASTROS are derived similarly, it is not surprising to see in Figures 23 through 27 that the slope at each data point is the same. Clearly, from this and the preceding example, the nonlinear version of ASTROS is working properly to incorporate the effects of changing material properties. Figures 28 and 29 contrast the amount of displacement incurred on the nonlinear models with that of the linear model at these same stress levels. It is easy here to see the effect of these varying amounts of stress, but in other examples, a displacement plot will not always effectively show these varying effects of the amount of calculated stress. The force predicted through linear approximations that would be required to give the same displacement as actually occurred in the nonlinear material would be 41.1 percent too high.

The nonlinear ASTROS data is shown in the solid lines in Figures 23 through 27. It is evident

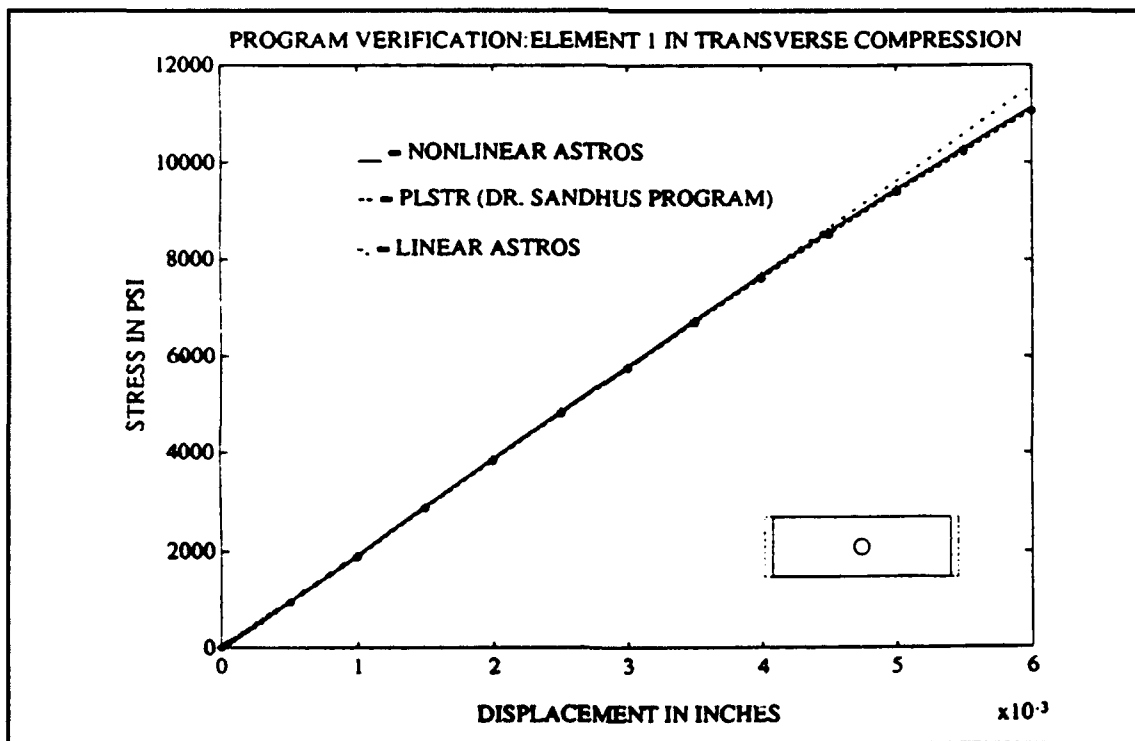


**Figure 23. Program Verification—Element 1 in Transverse Compression**

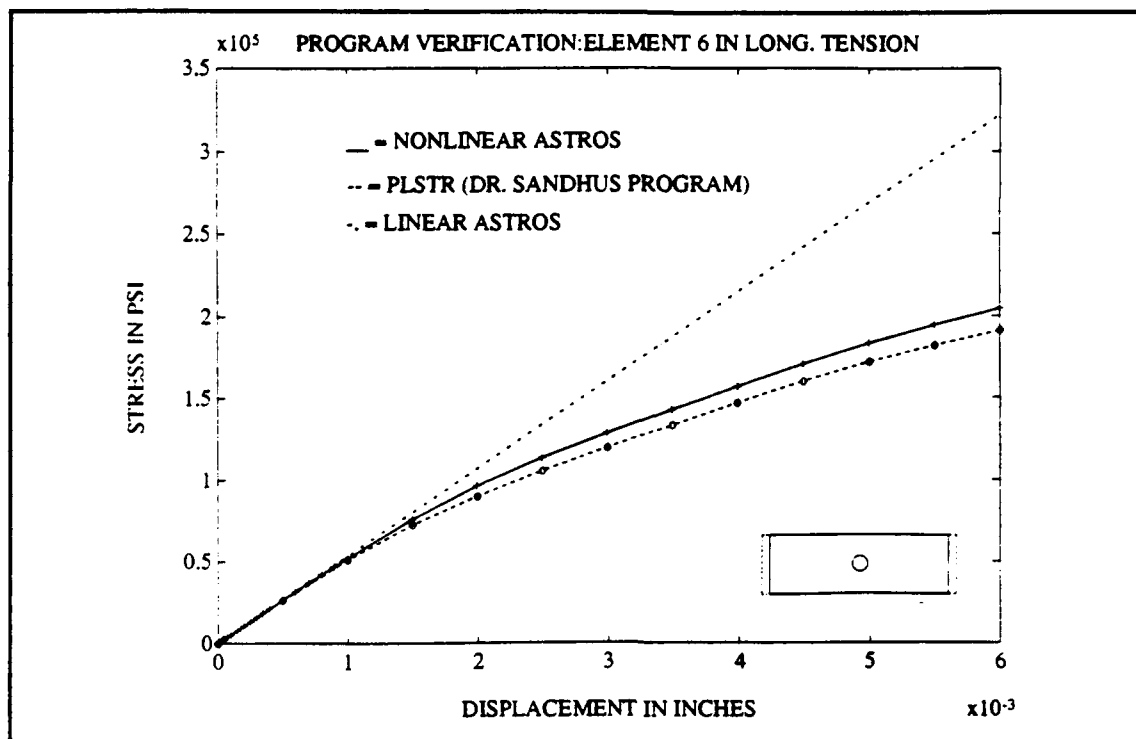


**Figure 24. Program Verification—Element 6 in Longitudinal Tension**

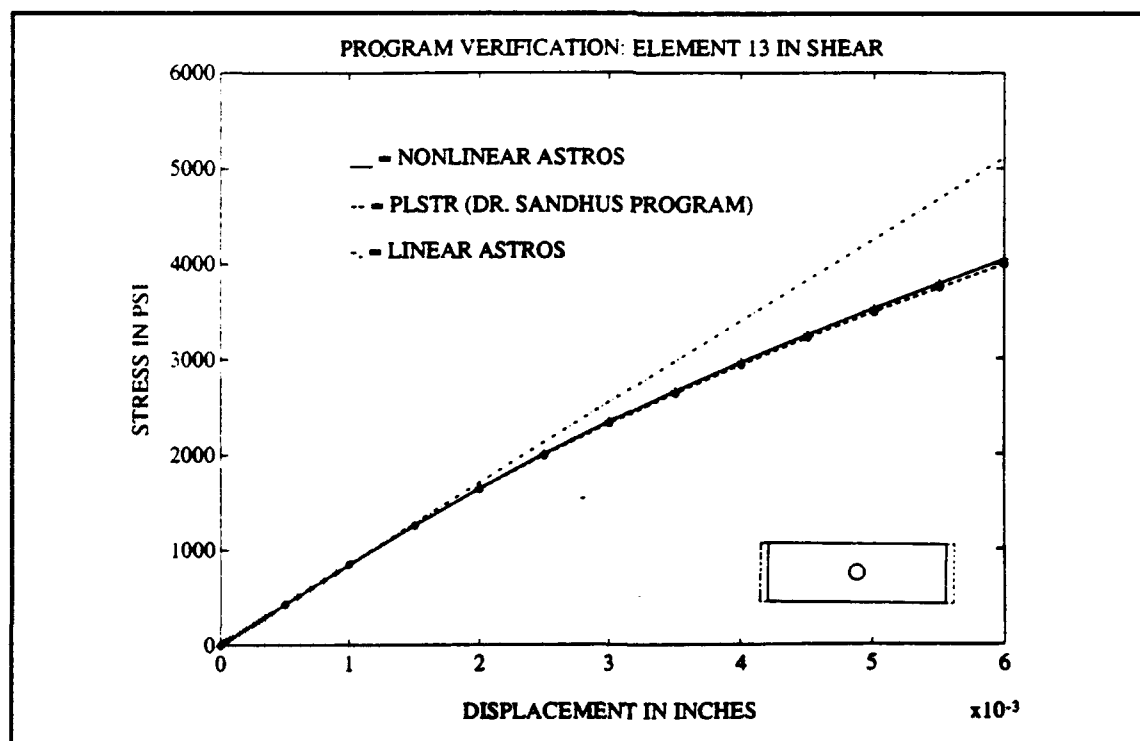


**Figure 25. Program Verification—Element 13 in Shear**

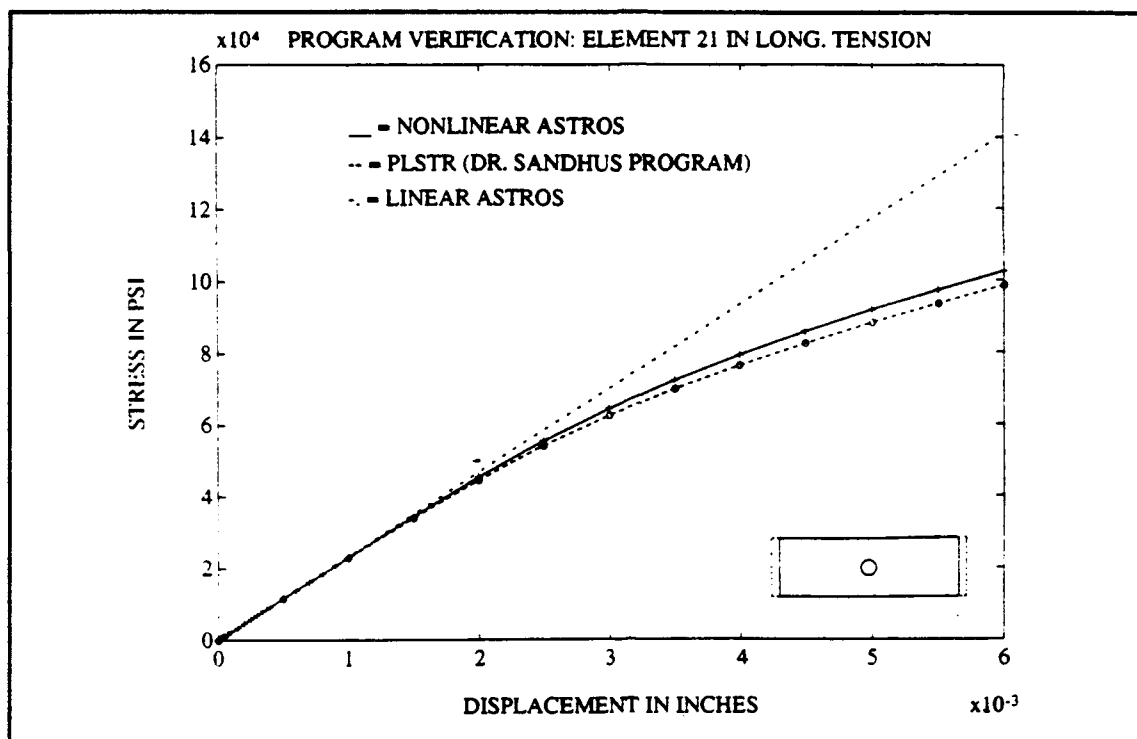


Figure 26. Program Verification—Element 21 in Longitudinal Tension

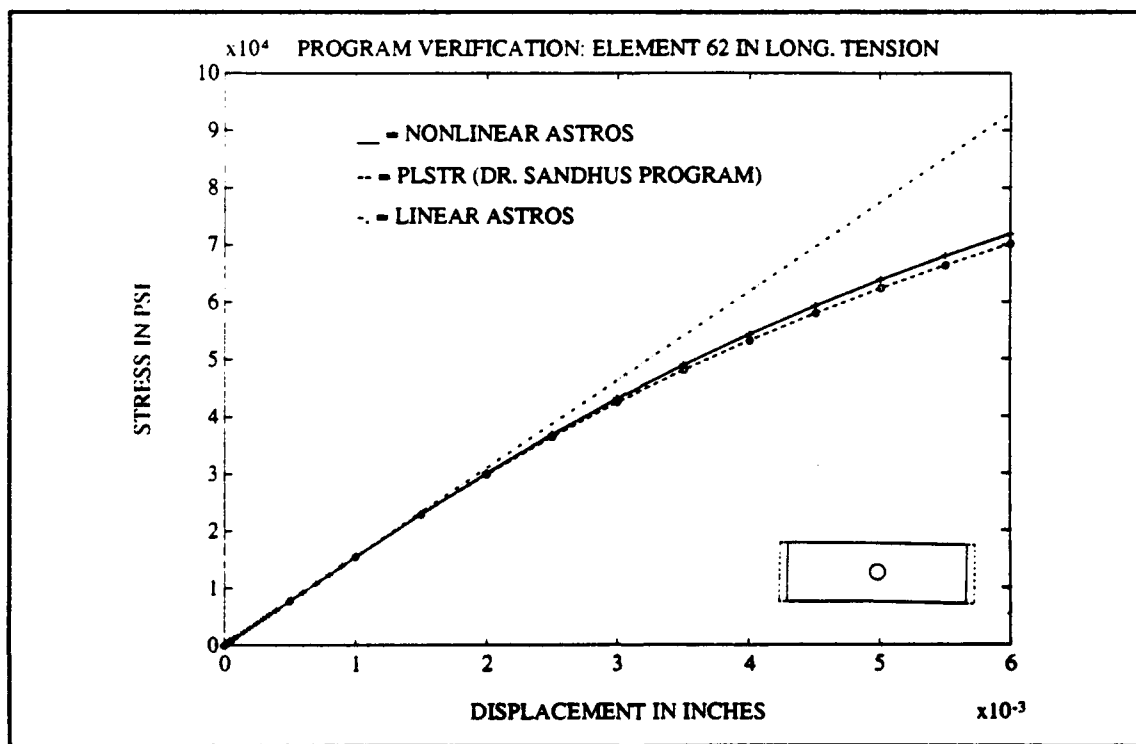
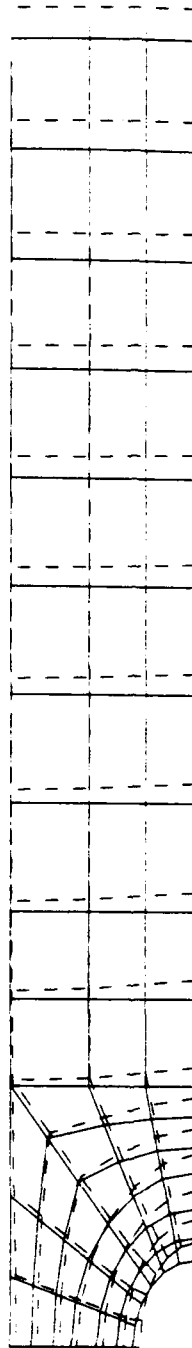
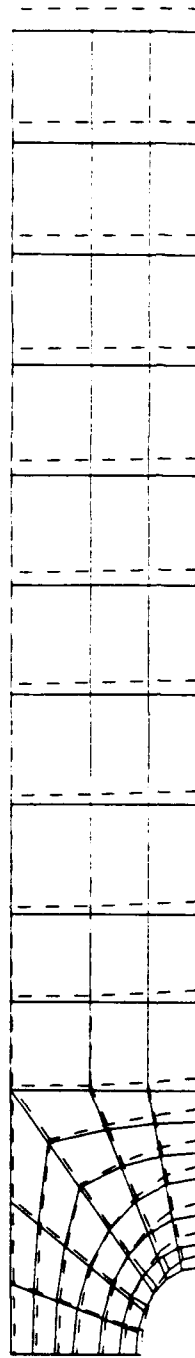


Figure 27. Program Verification—Element 62 in Longitudinal Tension



NONLINEAR ASTROS 16 PLY AT 0 DEG AT .007 ENFORCED DISPLACEMENT (X10)

**Figure 28. Program Verification—Nonlinear Displacement Plot**



LINEAR ASTROS 16 PLY AT 0 DEG LOADED WITH EQUIVALENT FORCES

**Figure 29. Program Verification—Linear Displacement Plot**

that nonlinear ASTROS models the changing nature of the moduli. These figures also show the importance of appropriate increment sizes. The increments must sufficiently model the changing nature of the moduli or error in the amount of total stress will accumulate. The error in total stress accumulates—this means that error induced early is not corrected out in the nonlinear ASTROS. The effect of increment size will be discussed in the following section.

### ***Iteration Size Study***

The results of the study of the effect of increment size on accuracy confirmed expectations. Figures 30 through 34 show that as increment size increases, so does the amount of error in resulting stress. Error starts out small, but increases as increment size is increased. Each increment represents a realignment of the actual modulus at a given strain. Notice that as increments occur at the same value of displacement, the curves run parallel to each other. This is due to the modulus, or slope, being corrected in each curve at that value.

Results verified several premises. First, the shape of the curve being modeled is quite important. Each element attempts to follow the spline curve generated from the experimental data. Given an infinite number of increments, each element's curve would trace the spline curve exactly. This is

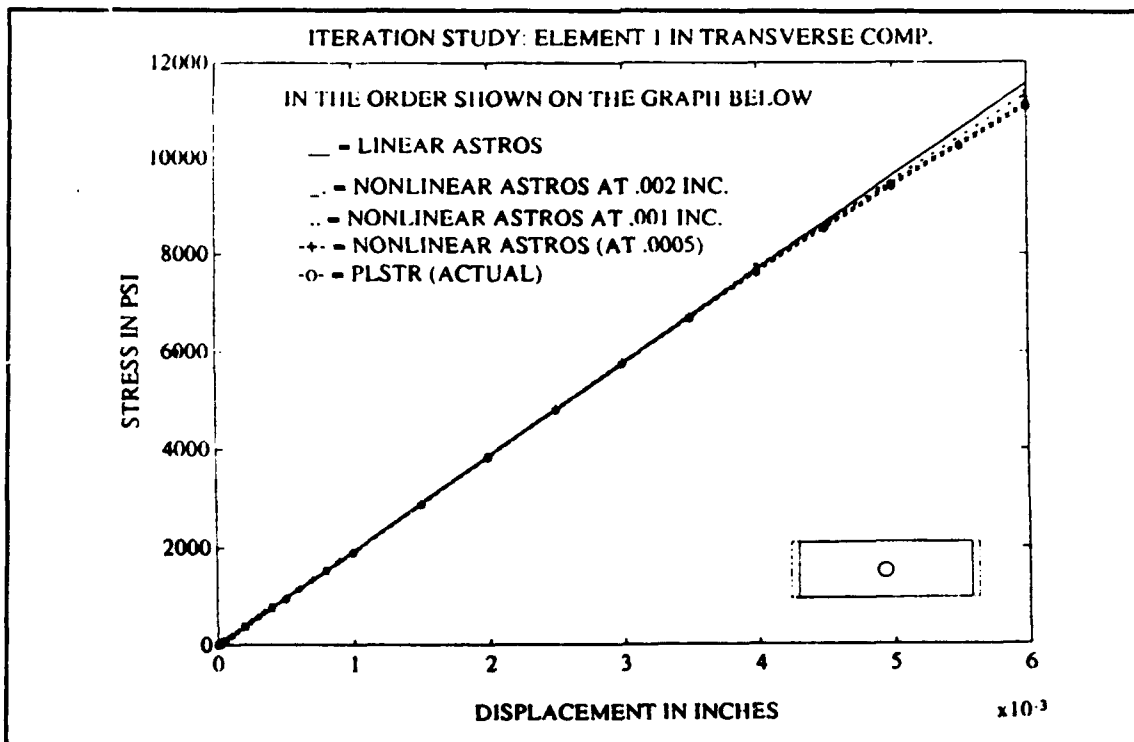


***Figure 30. Effect of Increment Size—Element 1***



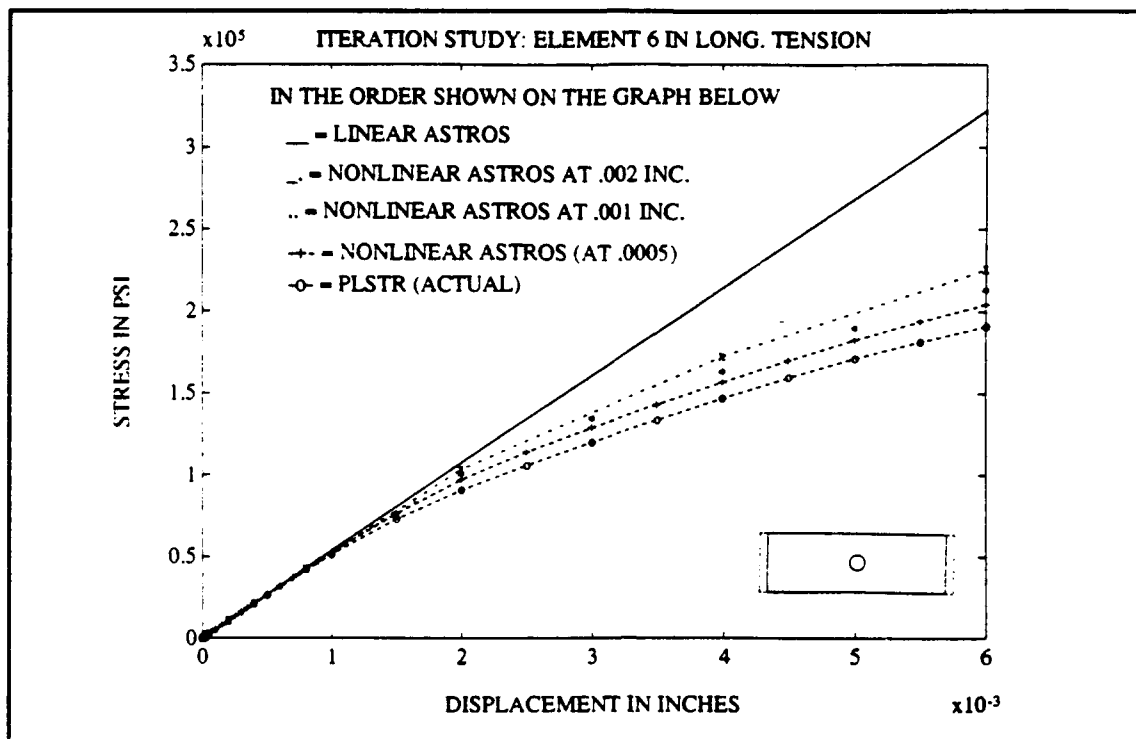


Figure 31. Effect of Increment Size—Element 6

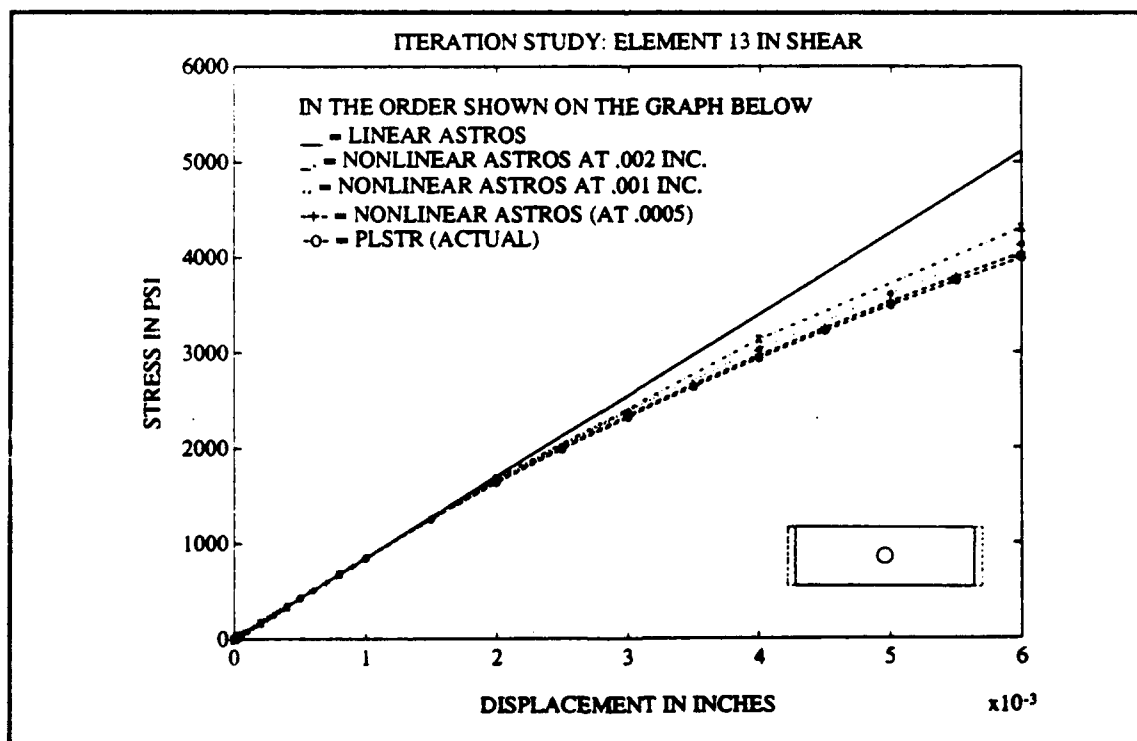


Figure 32. Effect of Increment Size—Element 13

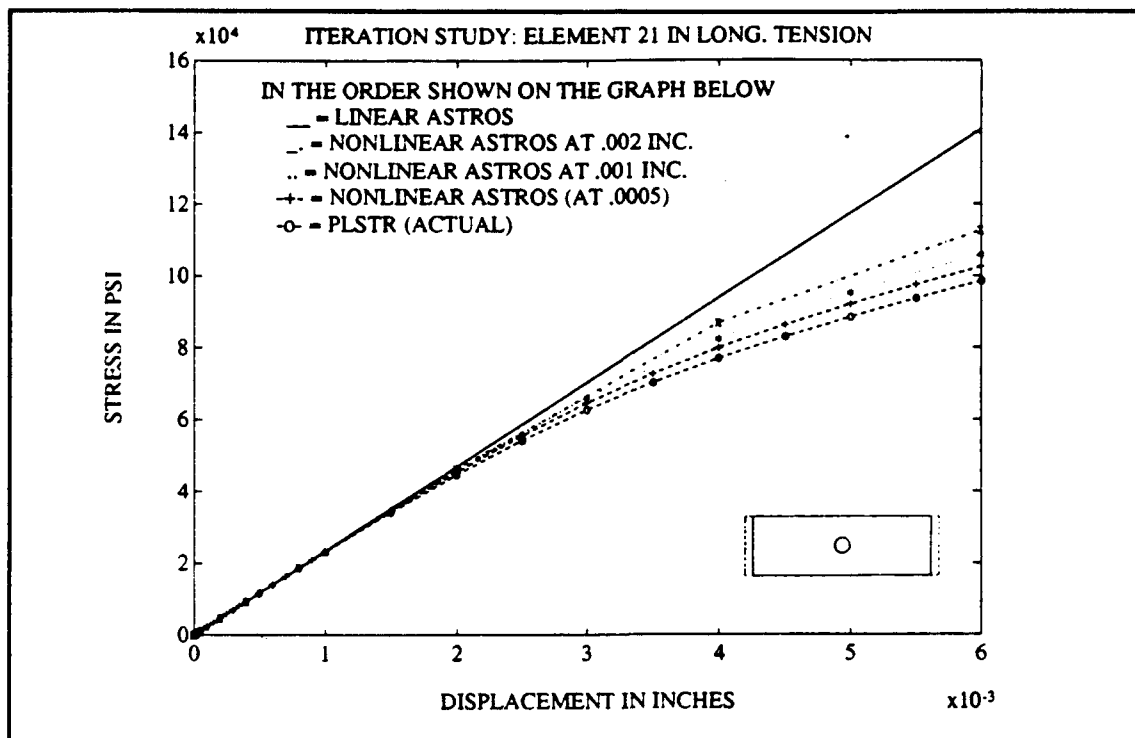


Figure 33. Effect of Increment Size—Element 21

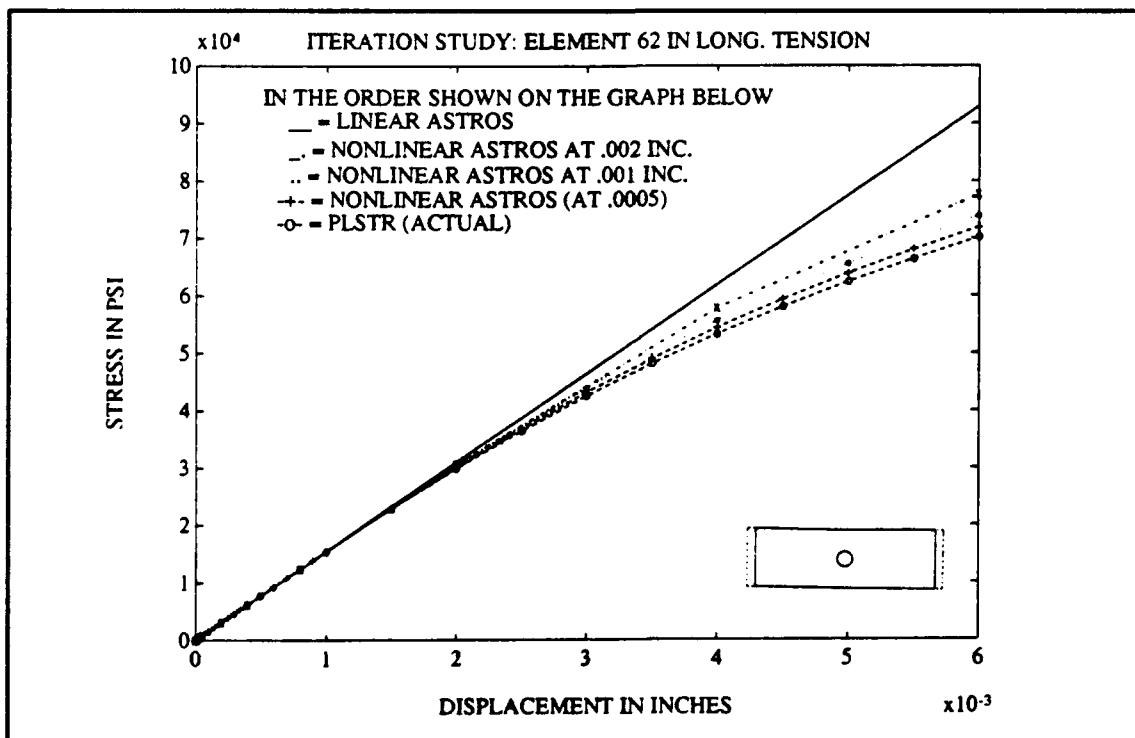


Figure 34. Effect of Increment Size—Element 62

not practical and also not required. Good results are generated from approximately twenty well placed increments. Of course, the actual shape of the curve may warrant an increased number of increments. The first curve to depart from the linear region must be catered to. Second, since error is not corrected out, the rule is that initial increments should stay small to minimize this error. Finally, it has been shown possible to model very linear beginnings of curves in a few steps—this is inversely related to the premise that a quickly changing slope requires more increments to keep stress values accurate.

### ***Linear Versus Nonlinear Analysis***

The finite element model has been found to be acceptable, and this nonlinear version of ASTROS has been shown to accurately model a nonlinear material. This section considers actual Gr/PEEK experimental data for the spline. These curves are shown in Appendix C. This section shows the results of linear ASTROS compared to the newly developed nonlinear ASTROS for (0), ( $\pm 45$ ), and (90) laminates with both constant displacement and constant stress. Gr/PEEK is nonlinear mainly in the transverse and shear directions.

***The (0) Laminate.*** This laminate shows the most apparent nonlinearities. This makes sense since the laminate was loaded in the x direction, corresponding to the material's longitudinal direction—which had the most strength. This allowed for the nonlinearities to develop. Figures 35 through 49 show the developing nonlinear characteristics of the Gr/PEEK. The first set, Figures 35 from 39, has a constant displacement (in the x direction), whereas Figures 40 through 44 are in constant applied stress. Figures 45 through 49 show that these can be compared by considering the average displacement of the constant stress model. Figure 35 shows the effects of the decreasing transverse compressive modulus. Figures 36, 38 and 39 show the slight nonlinearities of the longitudinal modulus in tension. The shear of Figure 37 shows nonlinearities beginning to develop. Notice that not all nonlinearities will result in a decrease of the linearly predicted stress. Since the slightly nonlinear Gr/PEEK longitudinal stress versus longitudinal strain in tension curve actually increases slightly in slope, the actual or nonlinear stress results are greater than the linear in constant displacement. This reveals that the modulus is able to increase as well as decrease. This occurs as the early section of the spline curve arches steeply. The spline curve's modulus starts equivalent to the linear modulus, but increases before decreasing. The above comments also apply to the corresponding constant applied stress model's figures (Figures 40 through 44). The correlation is

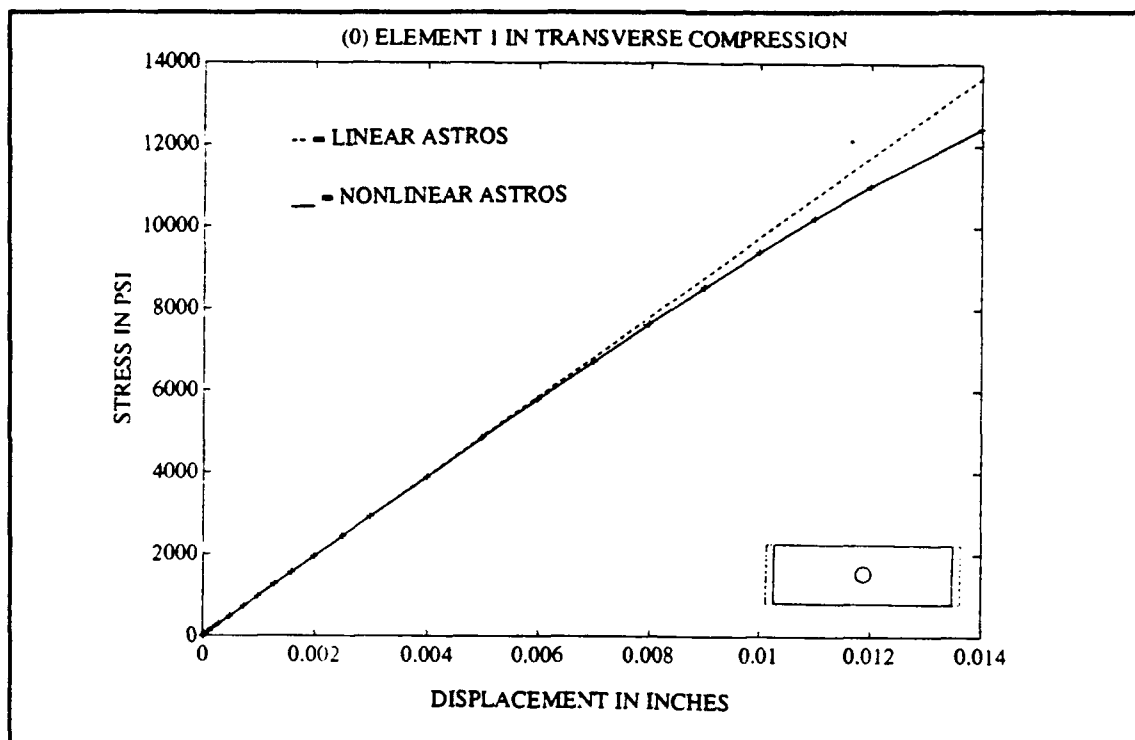


**Figure 35. (0) Element 1 in Transverse Compression**

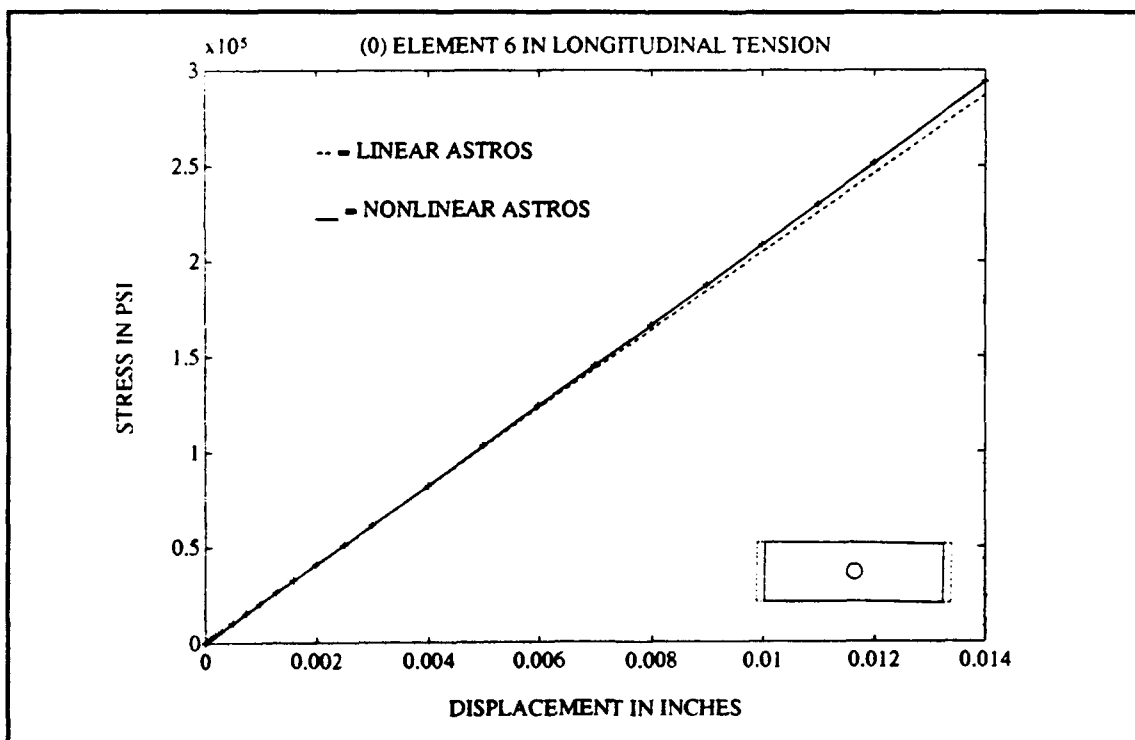


**Figure 36. (0) Element 6 in Longitudinal Tension**

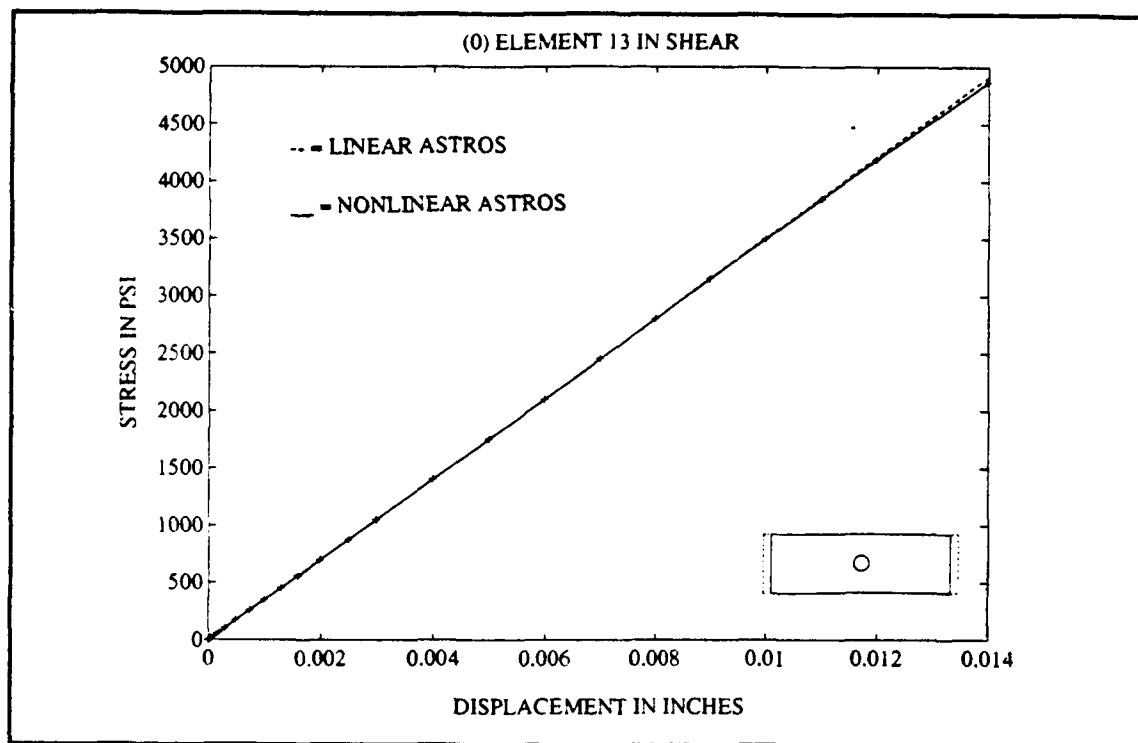


**Figure 37. (0) Element 13 in Shear**

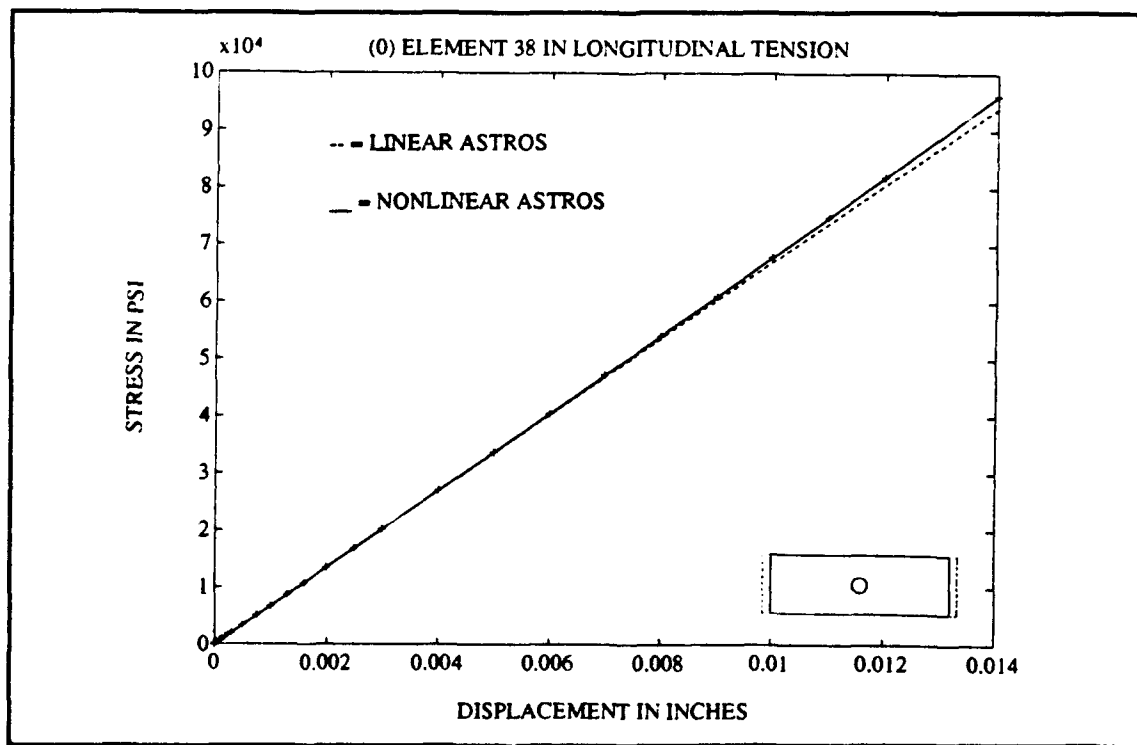


**Figure 38. (0) Element 38 in Longitudinal Tension**

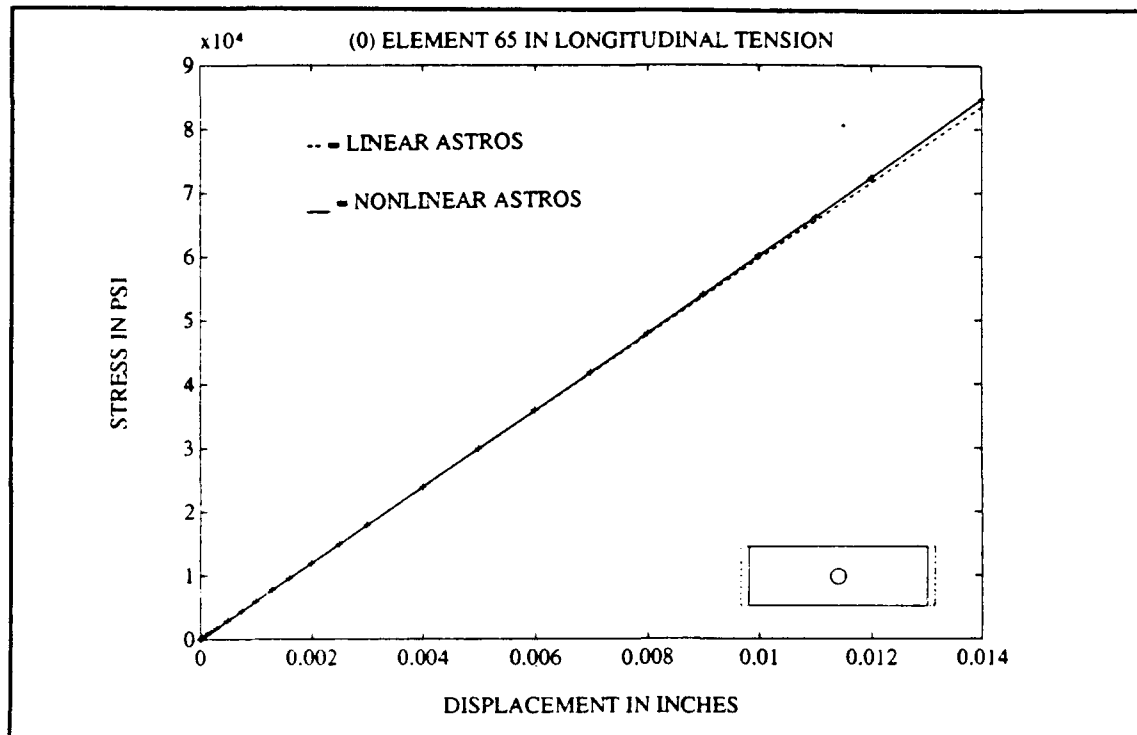


**Figure 39. (0) Element 65 in Longitudinal Tension**

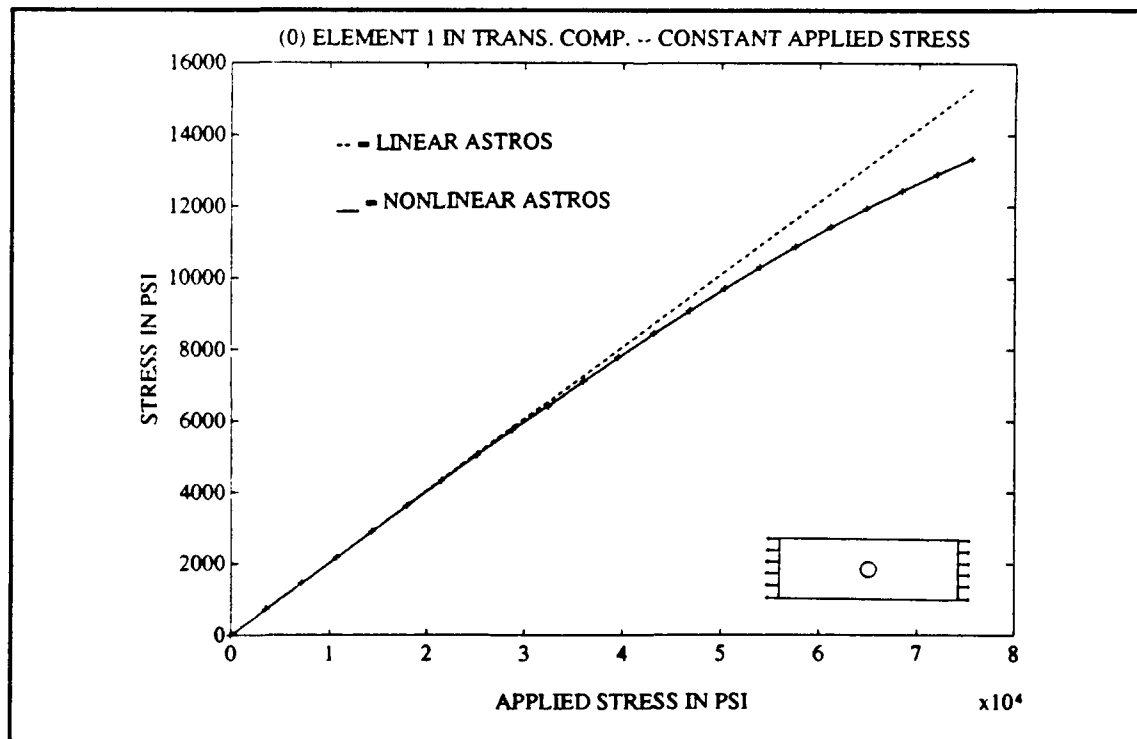


**Figure 40. (0) Element 1 in Transverse Compression—Constant Applied Stress**

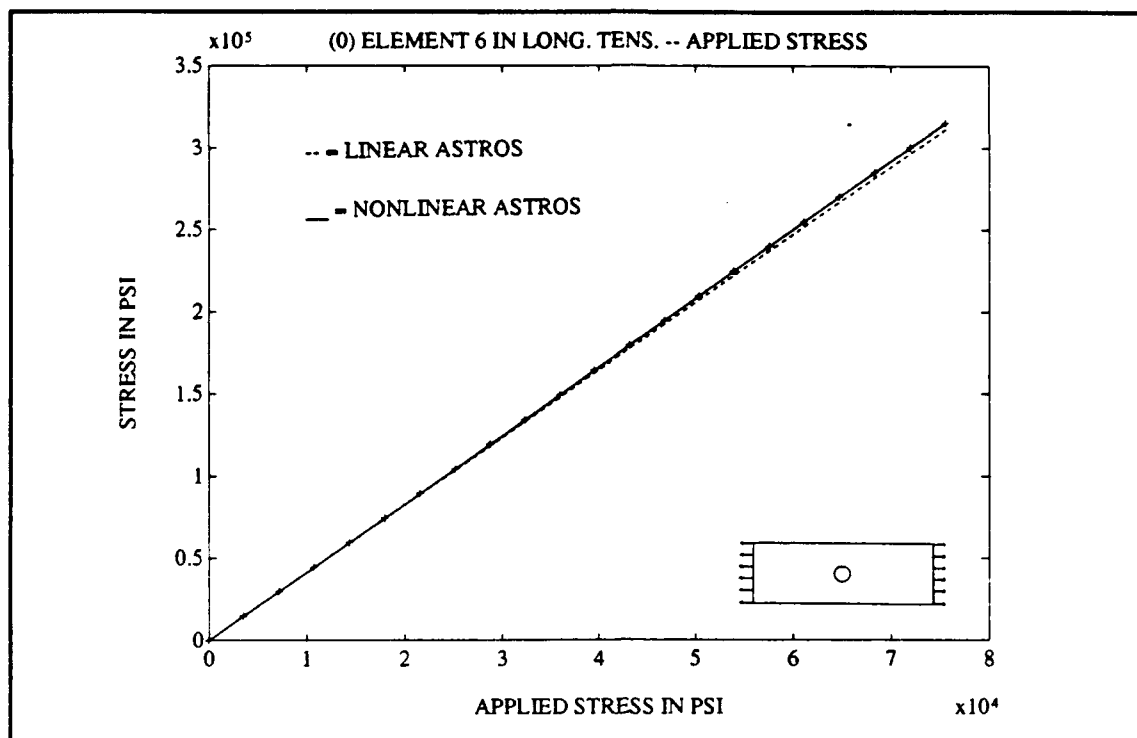


**Figure 41. (0) Element 6 in Longitudinal Tension—Constant Applied Stress**

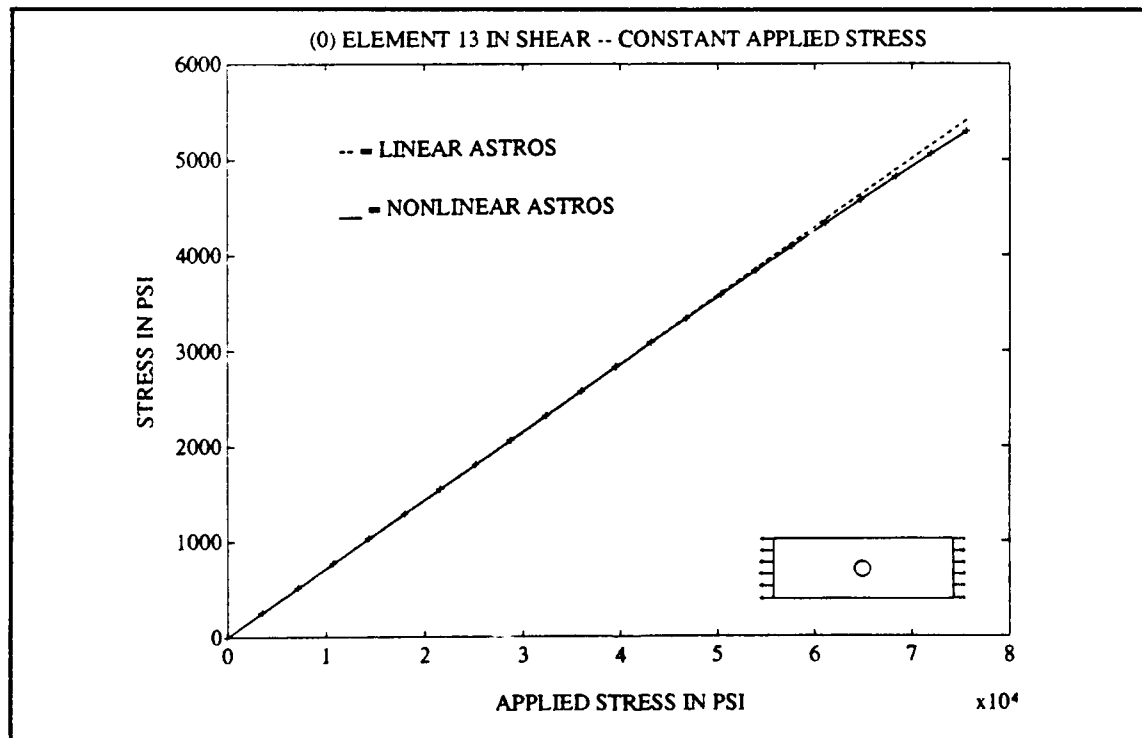


**Figure 42. (0) Element 13 in Shear—Constant Applied Stress**

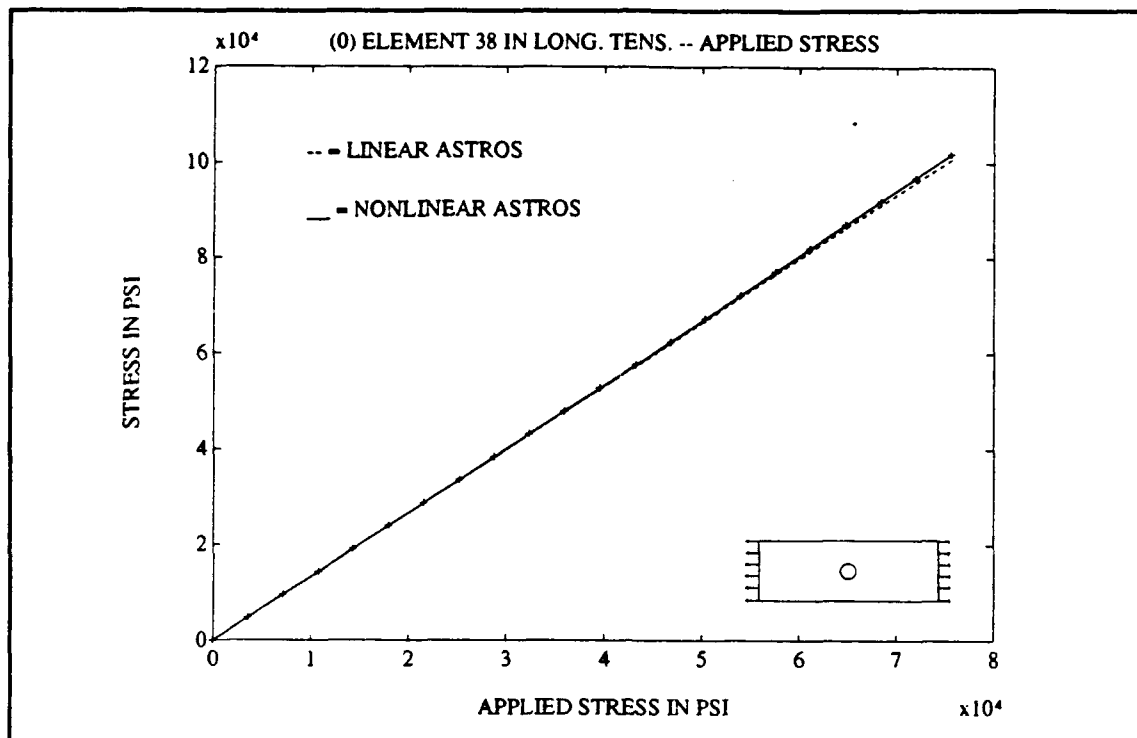


**Figure 43. (0) Element 38 in Longitudinal Tension—Constant Applied Stress**

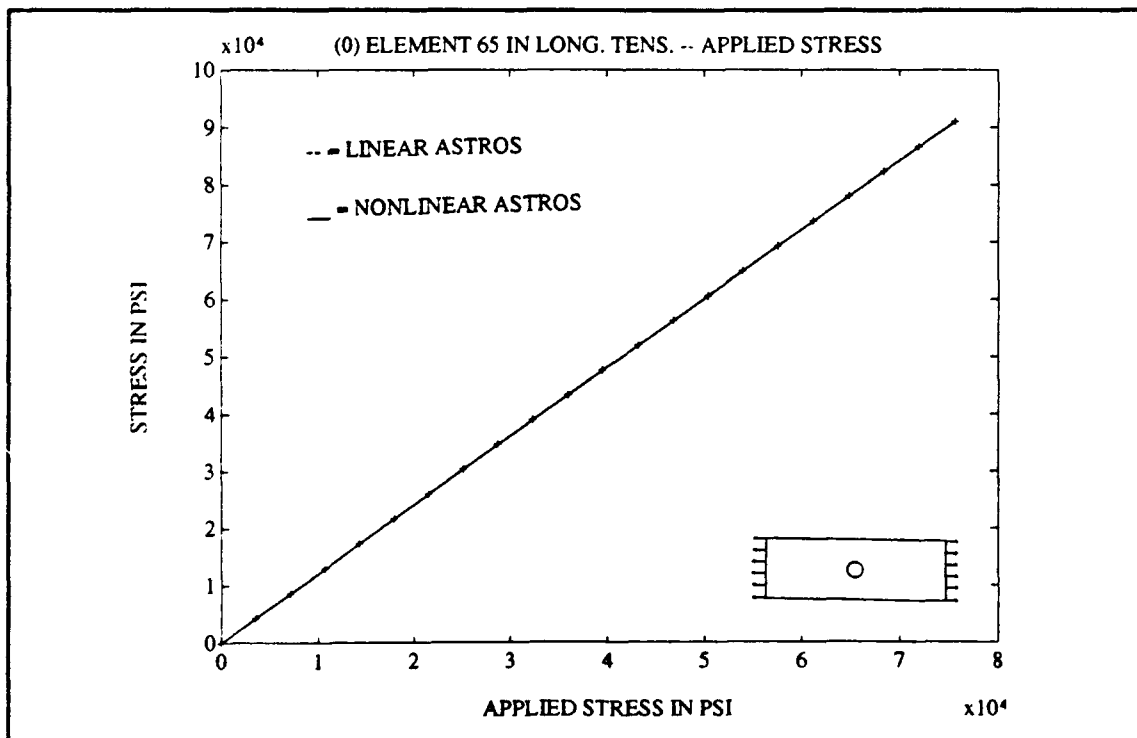


**Figure 44. (0) Element 65 in Longitudinal Tension—Constant Applied Stress**



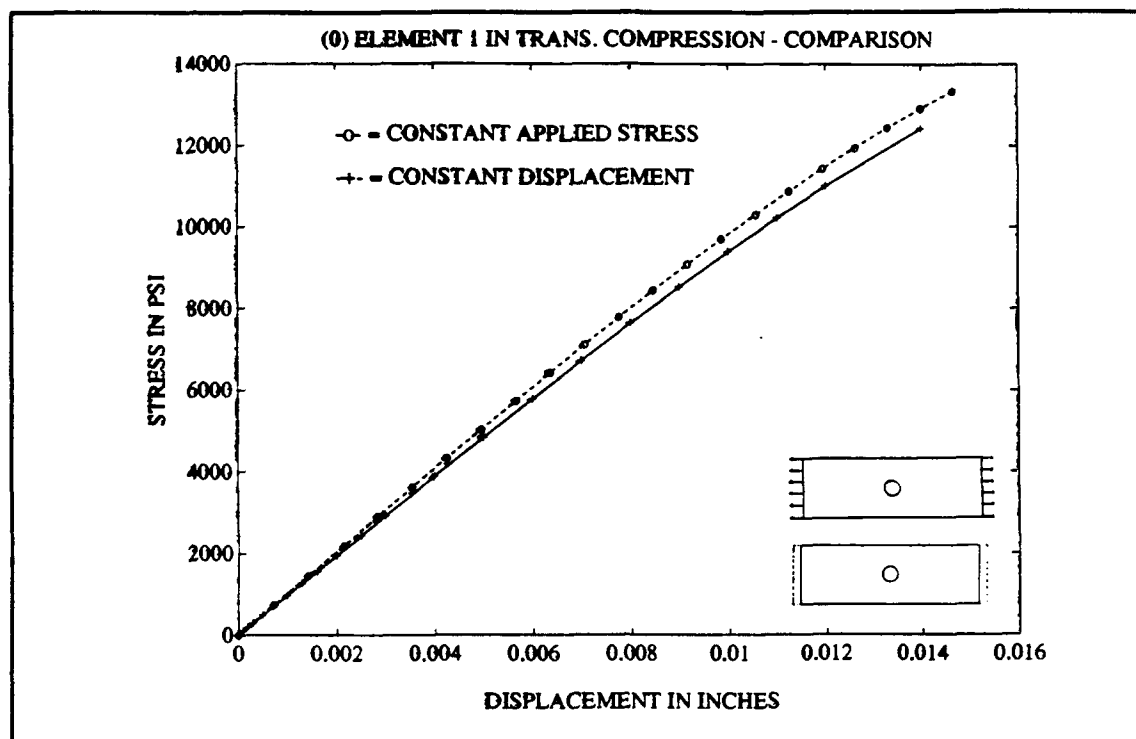


Figure 45. (0) Element 1 in Transverse Compression—Comparison

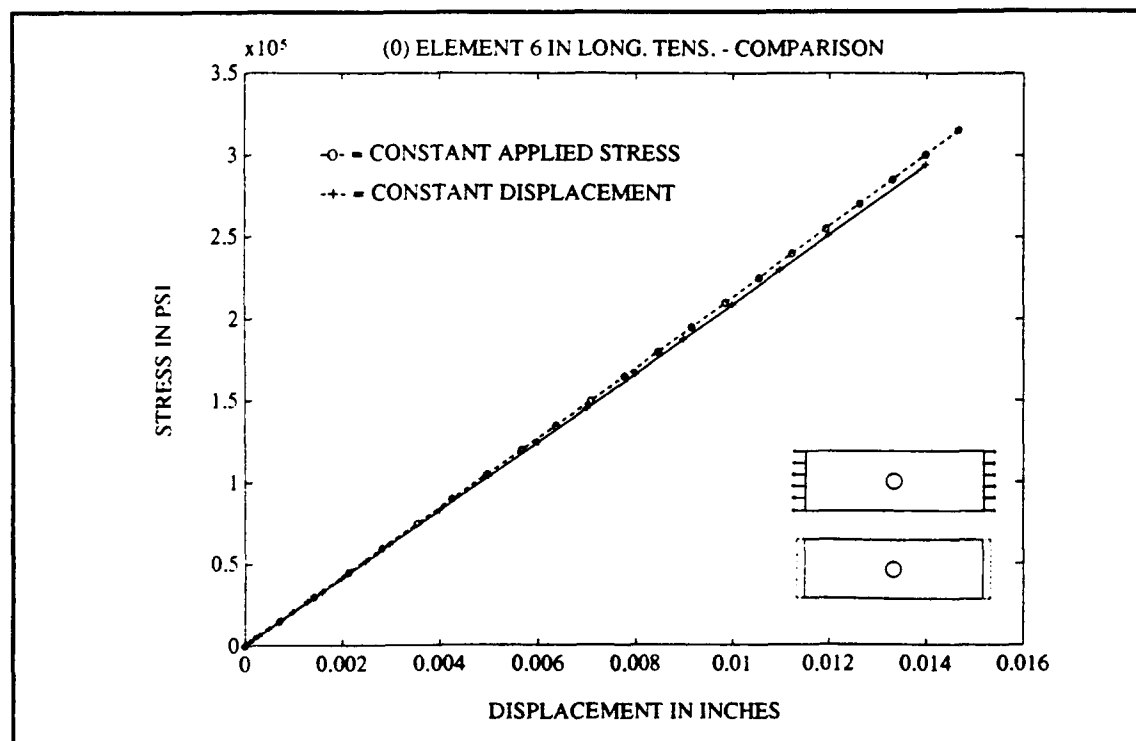
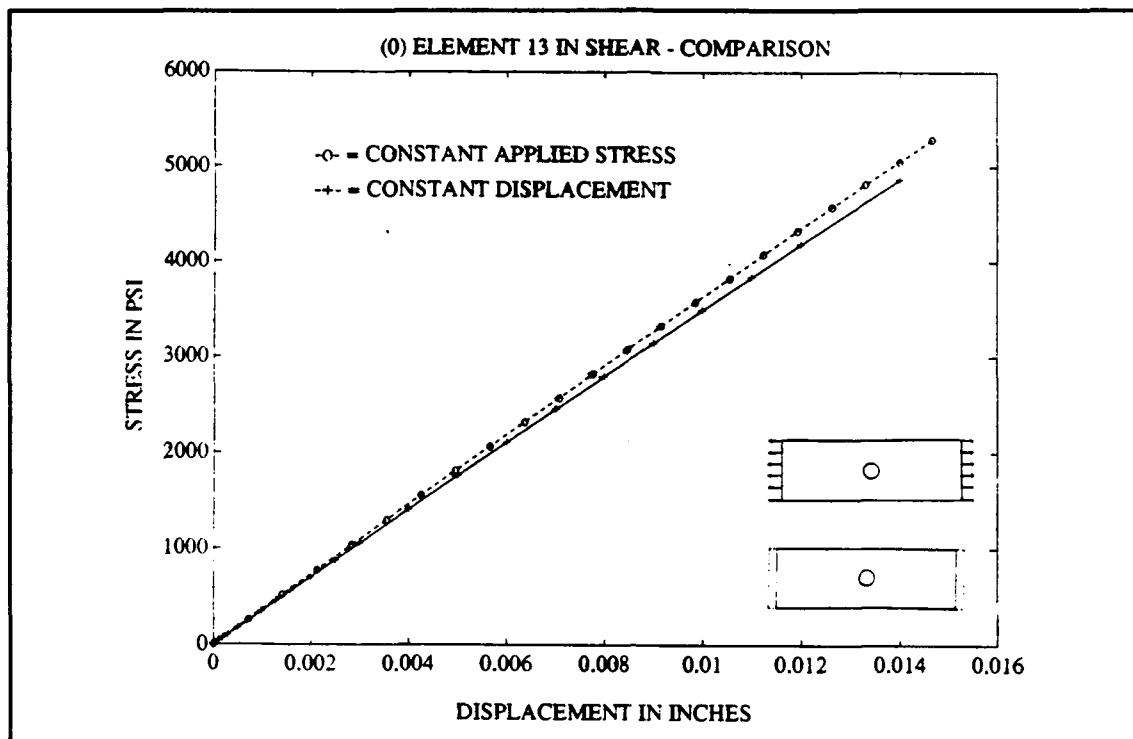
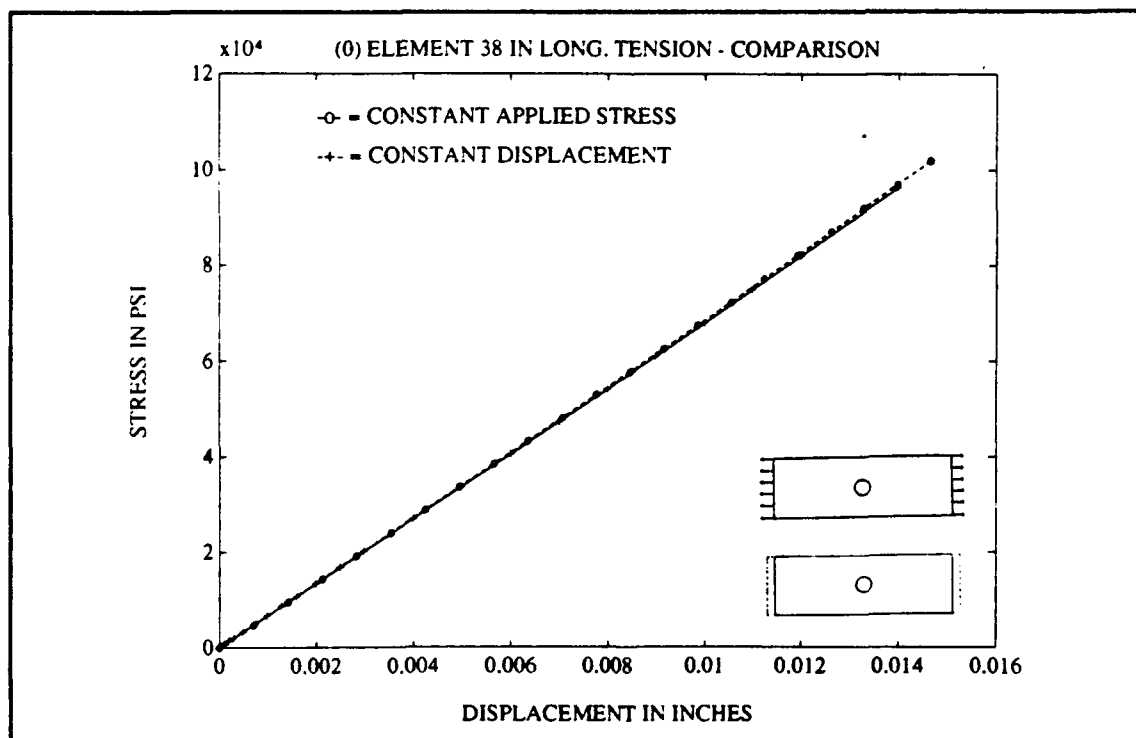


Figure 46. (0) Element 6 in Longitudinal Tension—Comparison



**Figure 47. (0) Element 13 in Shear—Comparison**



**Figure 48. (0) Element 38 in Longitudinal Tension—Comparison**

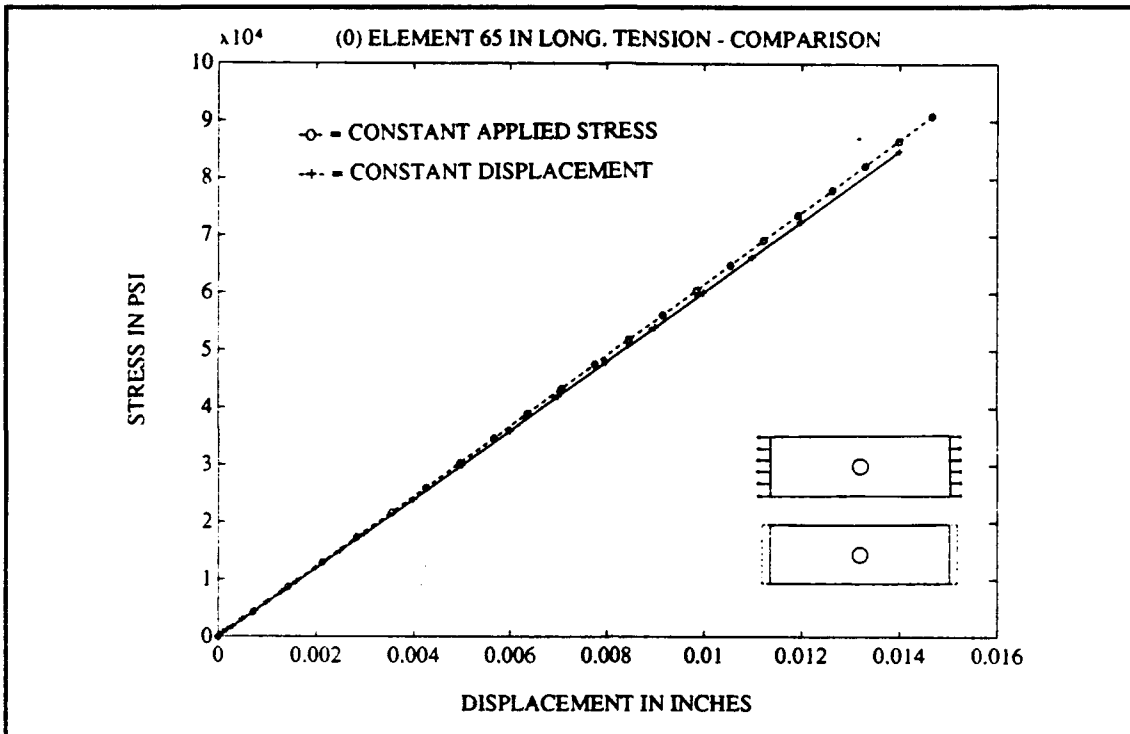


**Figure 49. (0) Element 65 in Longitudinal Tension—Comparison**

shown in Figures 45 through 49. Notice the error that would be expected from linear approximations. This highlights the shortcomings of linear analysis and the need for nonlinear analysis of nonlinear materials. Figures 50 and 51 show the differences between displacements of the constant applied stress and the constant displacement models.

**The (90) Laminate.** The (90) laminate breaks quickly in tensile loading since only the weak matrix (PEEK) withstands the applied displacements. Figures 52 through 56 show a comparison to those elements discussed in the previous cases. Because this (90) laminate fails quickly, or with much less developed stress, the nonlinear curves are closer to the linear approximations. The (90) curves have been presented to enable comparison with the (0) case. For example, this is accomplished by plotting the stresses of Figure 17's element 6 longitudinally for the (0) laminate and transversely for the (90) laminate. Therefore, both are along the global  $x$  axis. However, the longitudinal and transverse stress-strain curves are different, so that the comparisons are different.

**The  $(\pm 45)_s$  Laminate.** None of the moduli for the  $(\pm 45)_s$  laminate showed excessive nonlinearity before failure began. Figures 57 through 61 show the analysis done with increments of displacement.

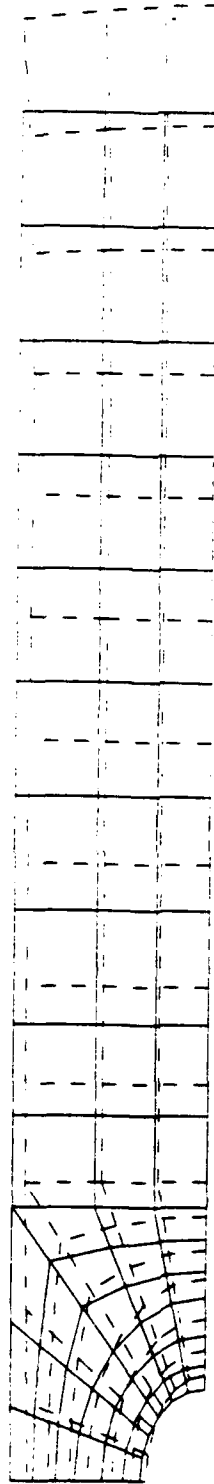


**Figure 50. Constant Applied Stress Displacement Plot**

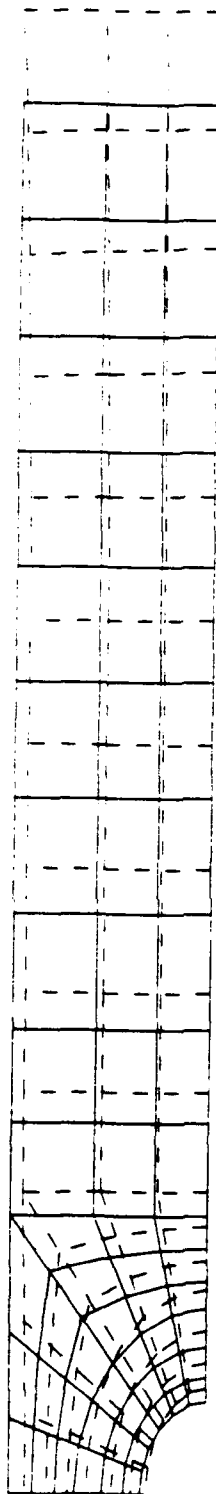


**Figure 51. Constant Displacement Displacement Plot**

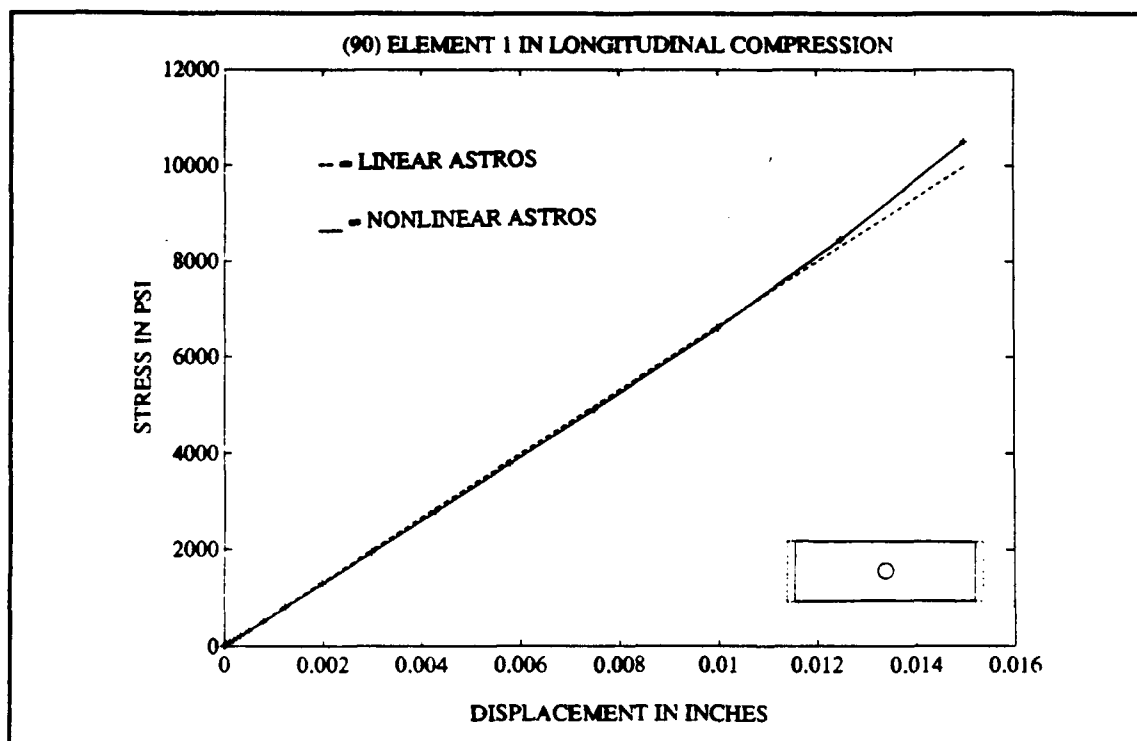


*Figure 52. (90) Element 1 in Longitudinal Compression*

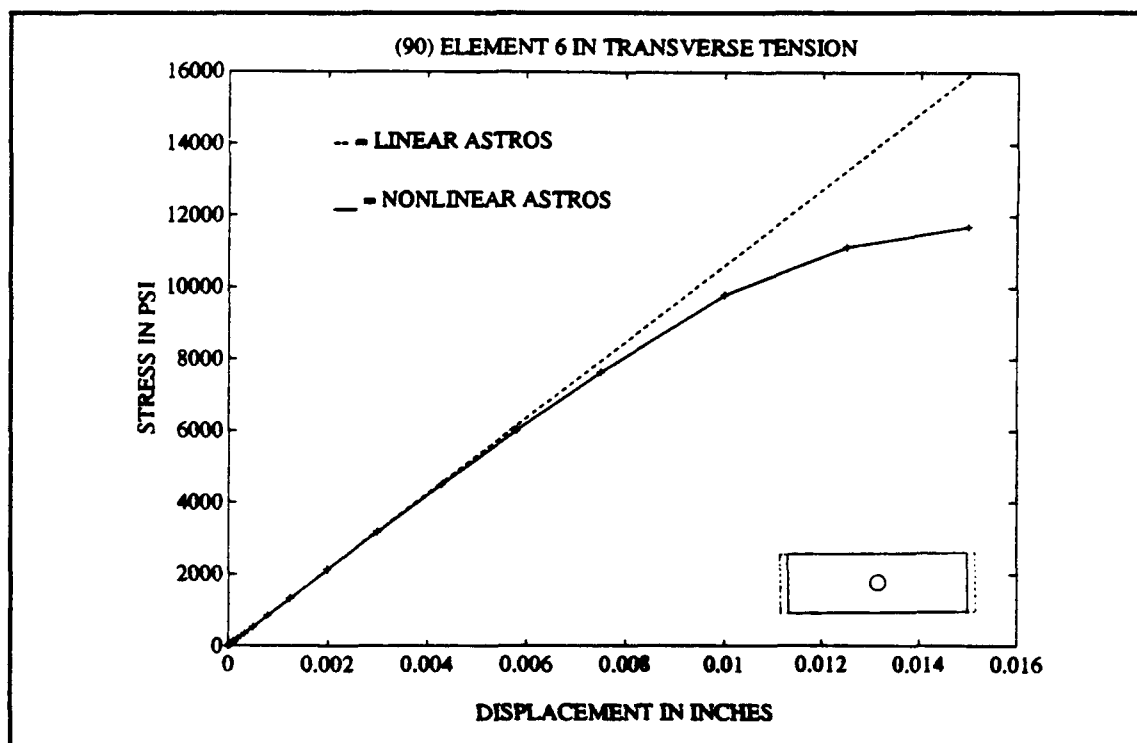


*Figure 53. (90) Element 6 in Transverse Tension*

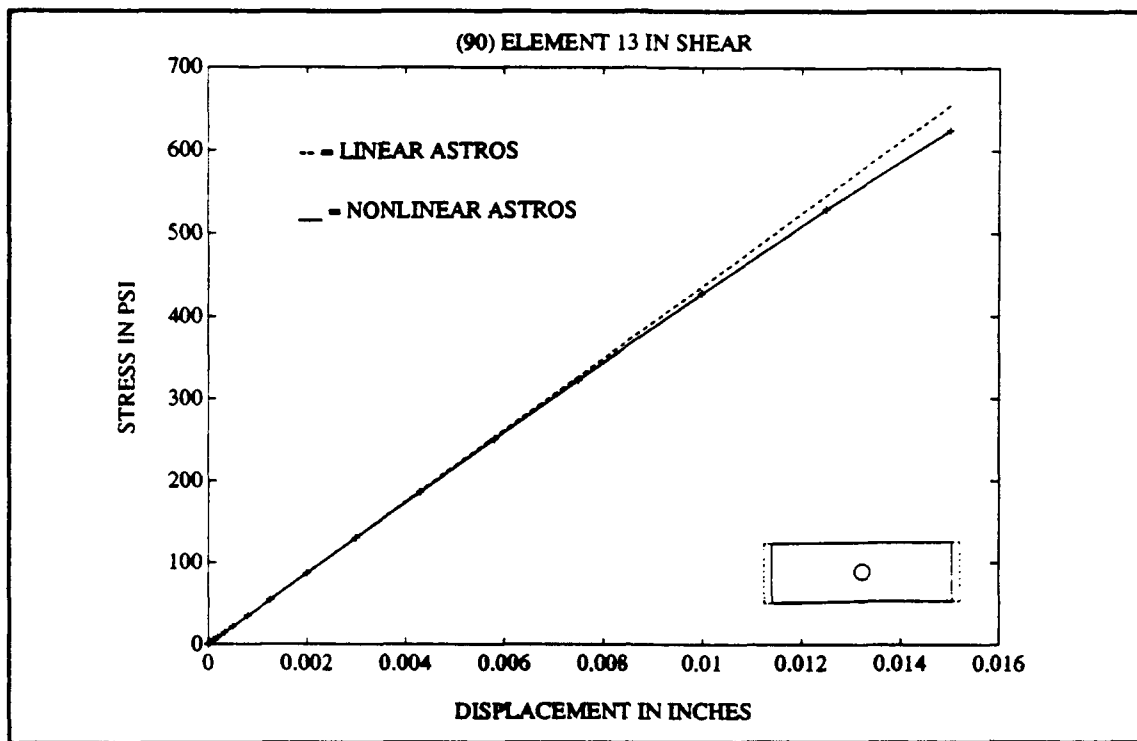


**Figure 54. (90) Element 13 in Shear**

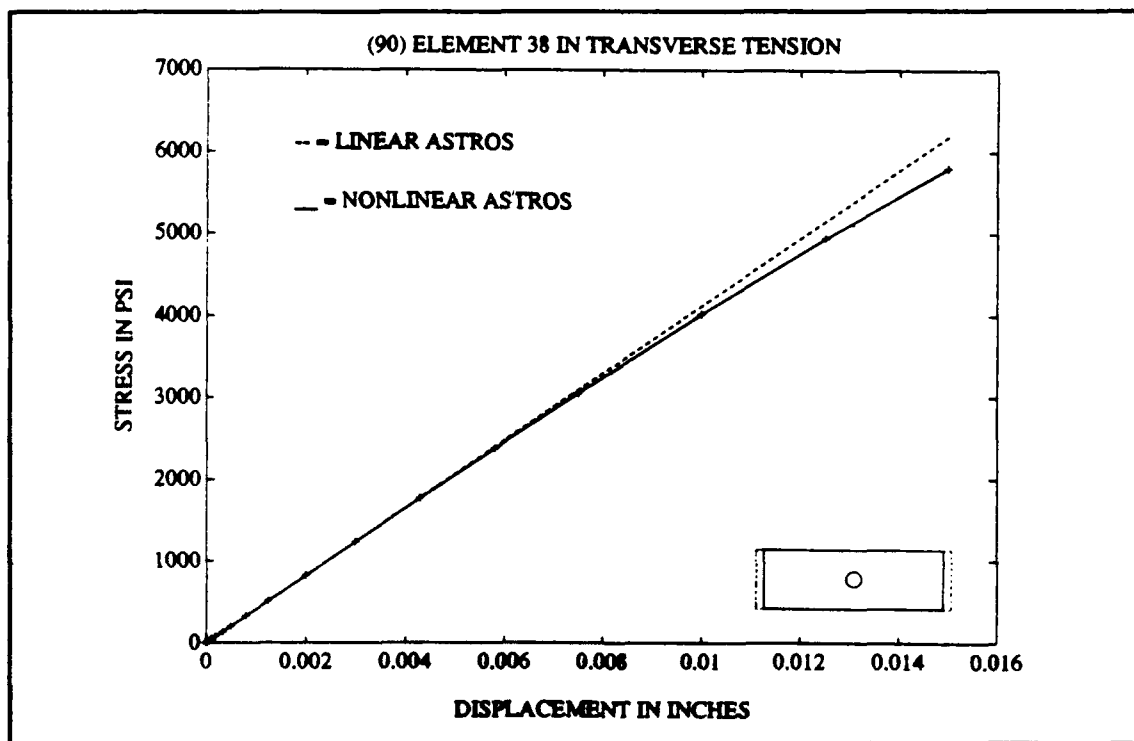


**Figure 55. (90) Element 38 in Transverse Tension**

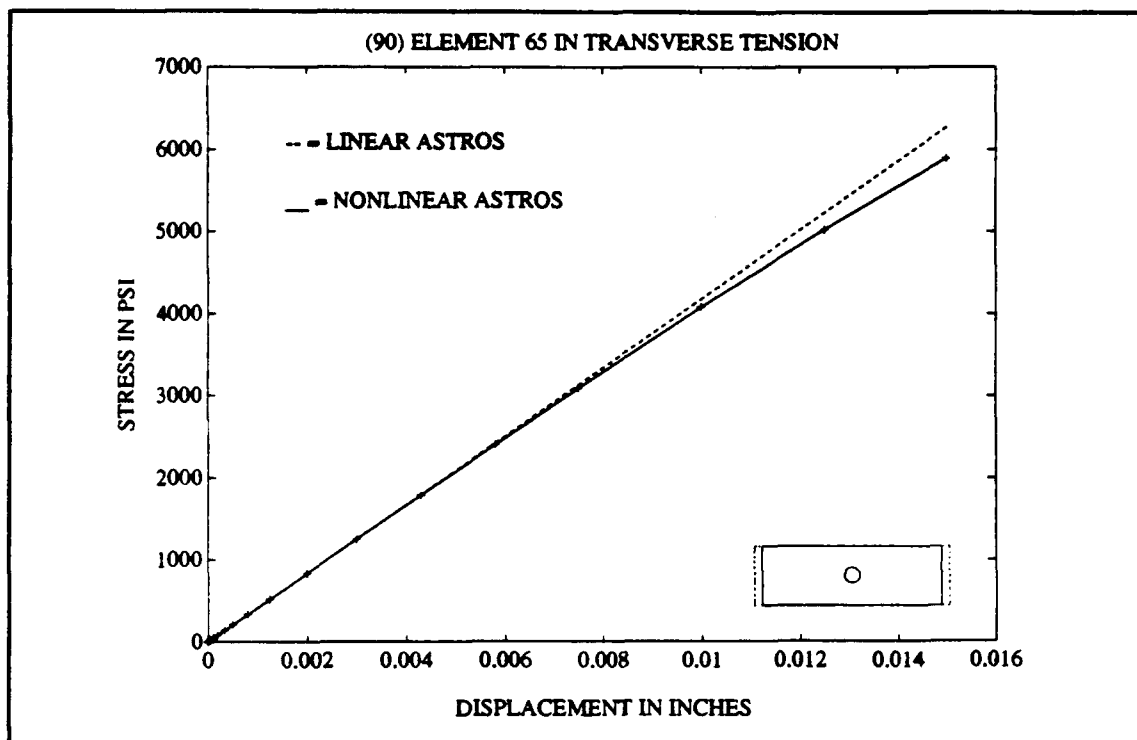


*Figure 56. (90) Element 65 in Transverse Tension*

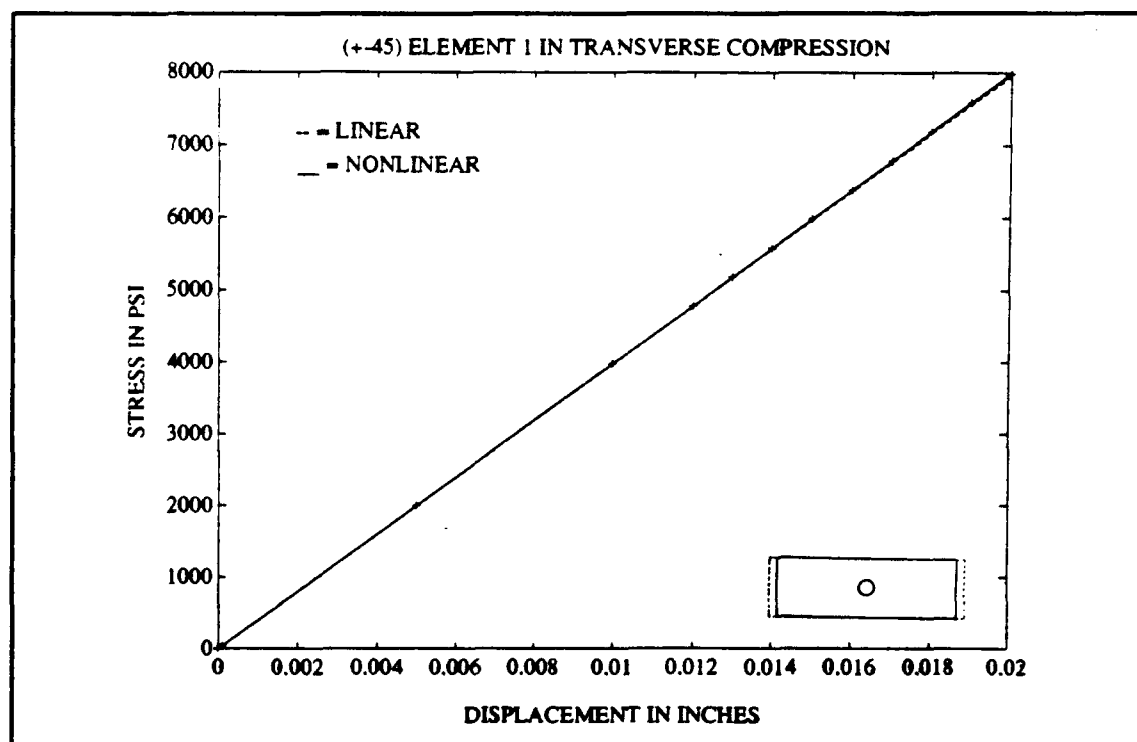


*Figure 57. ( $\pm 45$ ) Element 1 in Transverse Compression*



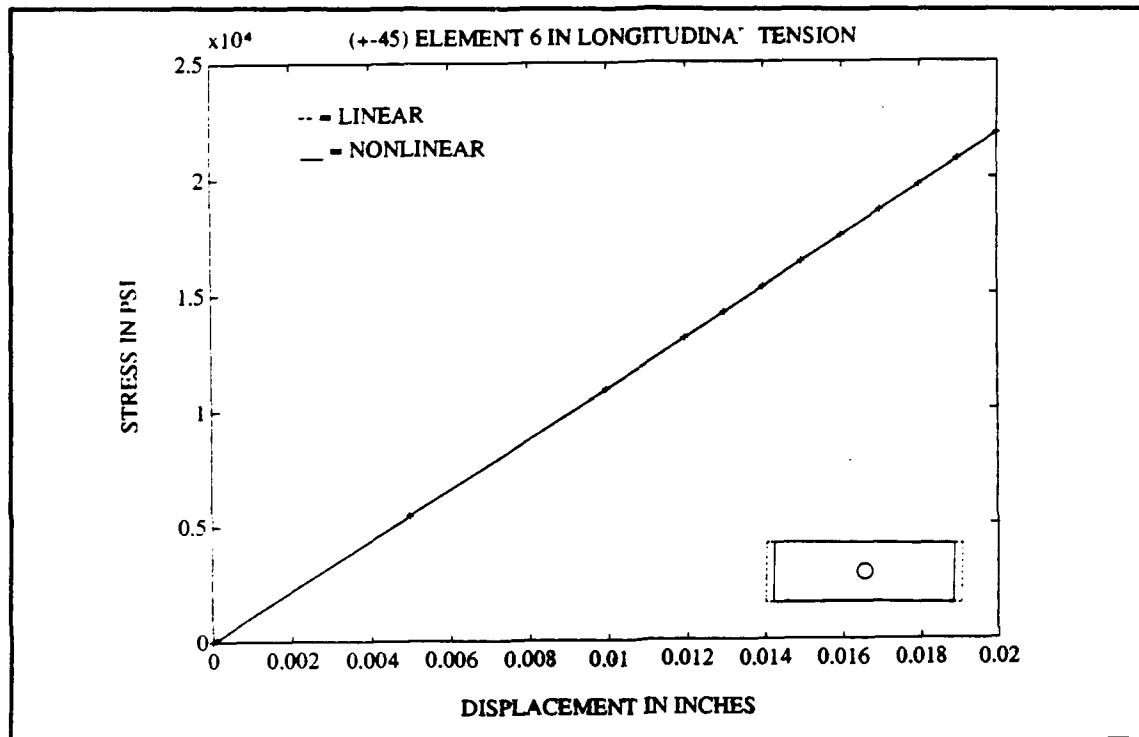


*Figure 58. ( $\pm 45$ ) Element 6 in Longitudinal Tension*

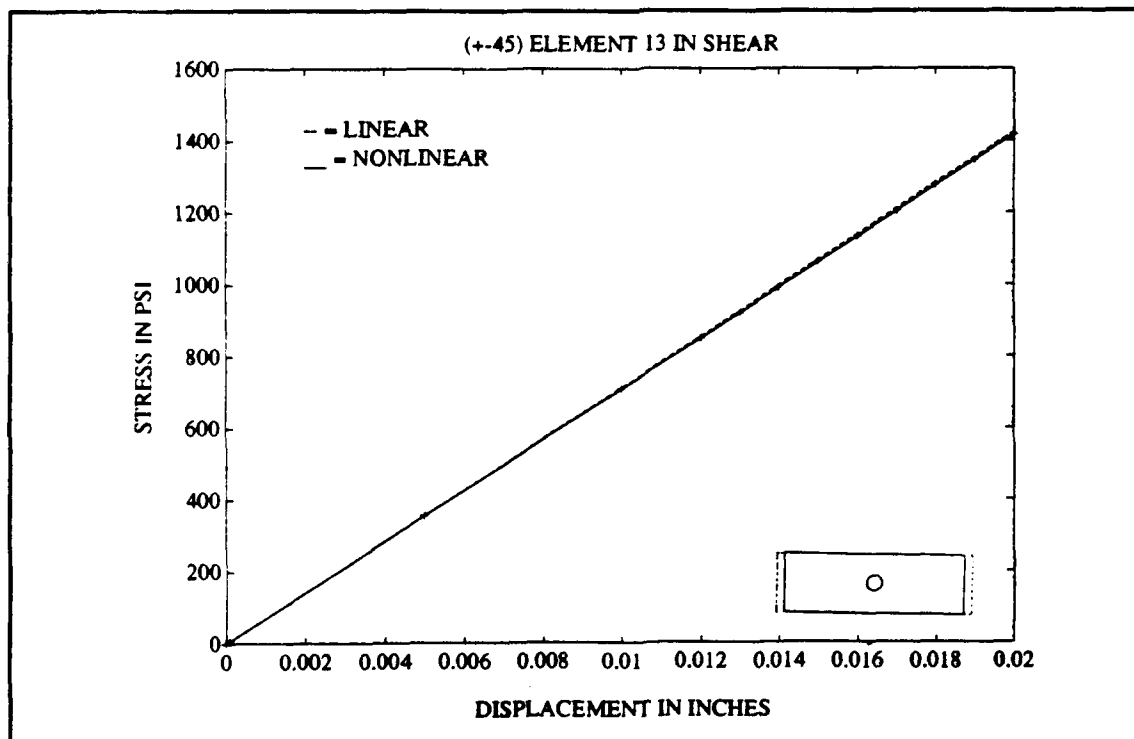


*Figure 59. ( $\pm 45$ ) Element 13 in Shear*

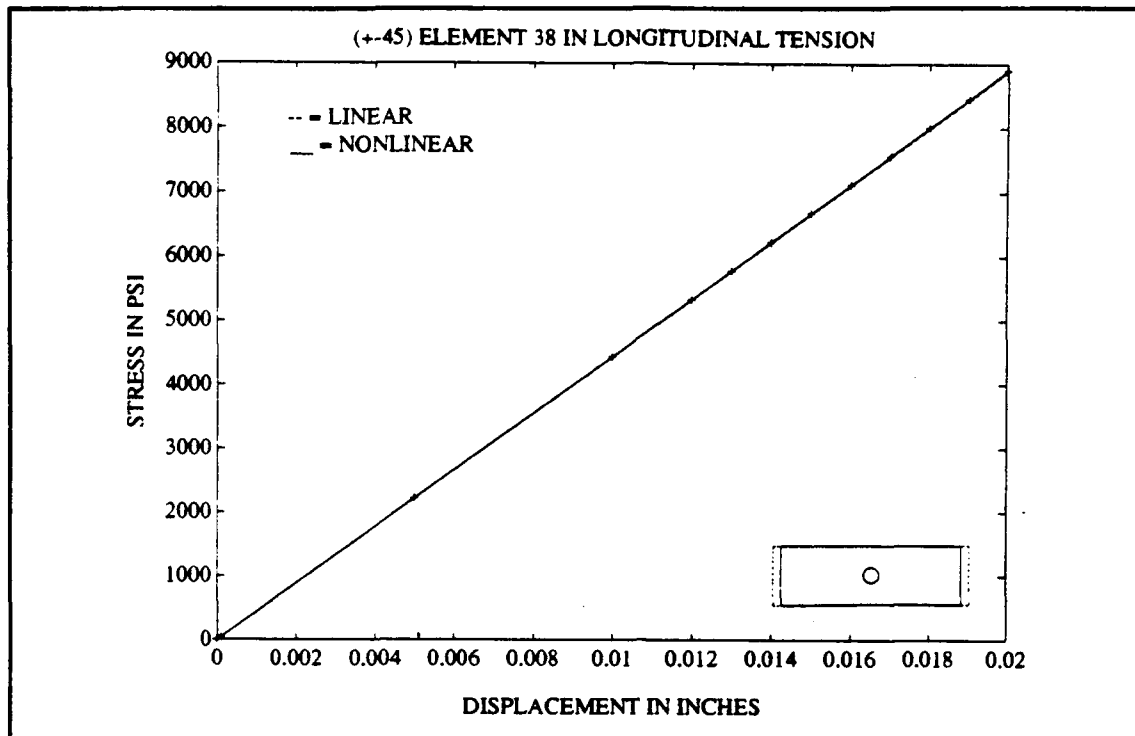


**Figure 60. ( $\pm 45$ ) Element 38 in Longitudinal Tension**

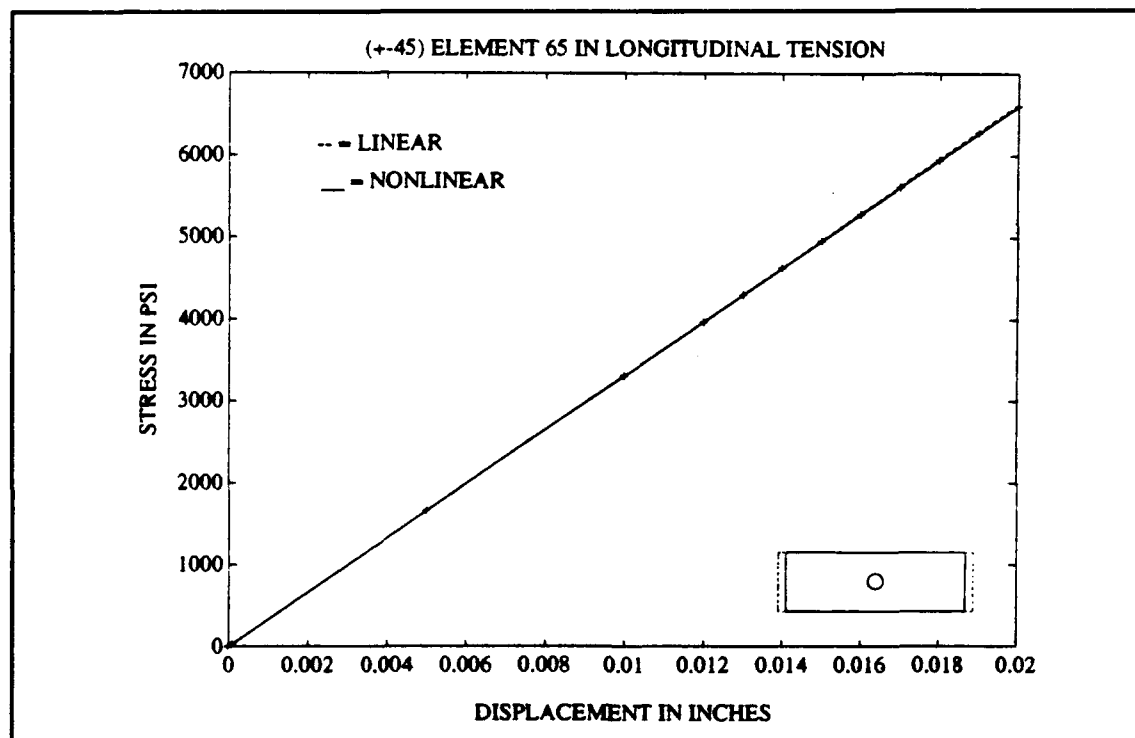


**Figure 61. ( $\pm 45$ ) Element 65 in Longitudinal Tension**

Recall that ASTROS models a layered composite as a summation of each ply's material properties. Figures 57 through 61 show that nonlinear materials can be successfully incorporated within ASTROS. Recall that the material axes for this combined laminate is along the global (the x and y directions) axes.

Note in each of Figures 57 through 61 that for a ( $\pm 45$ )<sub>s</sub> laminate, the combination of the +45 fiber's material properties with the -45 fiber's material properties produce a laminate whose nonlinear effects cancel each other out.

## ***Conclusion***

The effect of increment size on this nonlinear algorithm has revealed that for reasonable accuracy, at least 20 increments should be considered. This of course depends on the second derivation of the spline's stress-strain curves. More linear sections of these curves may be evaluated with less increments, whereas severely nonlinear curves must have many increments. The most nonlinear curve analyzed must be catered to, demanding several small increments.

By analyzing both constant displacements and constant applied stresses, this nonlinear materials capability allows ASTROS users flexibility.

There is benefit in modeling materials nonlinearly; as materials get even more nonlinear than they currently are, this benefit increases. Further research could consider adding failure conditions to this nonlinear finite element model. This research has accomplished what it has proposed to do. It has been possible to model nonlinear materials, including composite laminates, on the automated structural optimization system (ASTROS) and expand the capabilities of this FE analysis tool.

## Appendix A

```

CCCCCCCCCCCCCCCCCCCCCCCCCCCCCCCCCCCCCCCCCCCCCCCCCCCCCCCCCCCC
C   SPLINE FOR THESIS
C   THIS PROGRAM IS PART OF CAPTAIN BOB BOLHA'S THESIS.
C   IT RECEIVES STRAIN, STRESS, REACTION FORCE, AND
C   DISPLACEMENT INFORMATION FROM ASTROS, A FINITE ELEMENT
C   PROGRAM. THIS INPUT DATA IS COMBINED WITH EXPERIMENTAL
C   DATA ON MATERIAL PROPERTIES, TO DETERMINE WHERE ON THE
C   STRESS Vs STRAIN CURVE THE ELEMENT IS AND WHAT THE
C   CURRENT VALUE OF THE MODULUS, OR SLOPE, IS. THESE MODULI
C   ALONG WITH UPDATED POISSON'S RATIO INFORMATION IS THEN
C   OUTPUT, ALONG WITH THE SUM OF THE STRAIN, STRESS, REACTION
C   FORCES AND DISPLACEMENTS. THIS OUTPUT IS FED INTO ASTROS
C   TO EVALUATE THE NEXT LOAD INCREMENT. THE FINAL OUTPUT
C   ACCOUNTS FOR THE NONLINEAR MATERIAL PROPERTIES.
C
PROGRAM SPLINE
DIMENSION B(10,500),C(10,500),DELSQY(10,500),DELY(10,500),
& SS2(10,500),S2(10,500),S3(10,500),T(10,500),FORCE(5),
& Y(10,500),FORCETOT(5),IN(10),IN1(10),W(10),HT1(10),
& HT2(10),PROD(10),DELSQS(10),TNOW(10,500),TTOT(10,500),
& X(10,500),H(10,500),H2(10,500),SS(10,500),SS1(10,500),
& STRESNOW(10,500),STRESTCT(10,500),DISPX(100),DISPY(100),
& DISPZ(100),DISPTOTX(100),DISPTOTY(100),DISPTOTZ(100)
OPEN(UNIT=11,FILE='SPL15E1T.DAT',STATUS='OLD')
OPEN(UNIT=12,FILE='SPL15E2T.DAT',STATUS='OLD')
OPEN(UNIT=13,FILE='SPL15G.DAT',STATUS='OLD')
OPEN(UNIT=14,FILE='SPL15NUT.DAT',STATUS='OLD')
OPEN(UNIT=15,FILE='SPL15E1C.DAT',STATUS='OLD')
OPEN(UNIT=16,FILE='SPL15E2C.DAT',STATUS='OLD')
OPEN(UNIT=17,FILE='SPL15GX2.DAT',STATUS='OLD')
OPEN(UNIT=18,FILE='SPL15NUC.DAT',STATUS='OLD')
OPEN(UNIT=19,FILE='SPLINE170.DAT',STATUS='OLD')
OPEN(UNIT=20,FILE='INPUTCHK.OPT',STATUS='OLD')
OPEN(UNIT=21,FILE='SPL15E1T.OPT',STATUS='OLD')
OPEN(UNIT=22,FILE='SPL15E2T.OPT',STATUS='OLD')
OPEN(UNIT=23,FILE='SPL15G.OPT',STATUS='OLD')
OPEN(UNIT=24,FILE='SPL15NUT.OPT',STATUS='OLD')
OPEN(UNIT=25,FILE='SPL15E1C.OPT',STATUS='OLD')
OPEN(UNIT=26,FILE='SPL15E2C.OPT',STATUS='OLD')
OPEN(UNIT=27,FILE='SPL15GX2.OPT',STATUS='OLD')
OPEN(UNIT=28,FILE='SPL15NUC.OPT',STATUS='OLD')
OPEN(UNIT=29,FILE='SPLINE170.OPT',STATUS='OLD')
OPEN(UNIT=30,FILE='SPTOT170.OPT',STATUS='OLD')
OPEN(UNIT=31,FILE='SPSTRSTOT.IO',STATUS='OLD')
EPSLN=0.01
NODES=89
C   M IS THE NUMBER OF MAT8 CARDS GENERATED
M=66
C   RHO IS MASS DENSITY, IT IS NEEDED FOR MAT8 CARDS
RHO=0.058
WRITE(6,*) ' IF THIS IS THE 1ST ITERATION YOU WILL'
WRITE(6,*) ' NEED TO RUN FRONT HALF TO MAKE'
WRITE(6,*) ' THE TOTAL STRESS & STRAINS ZERO -> TYPE 1 (ELSE 2)'
READ(5,*) ISTART
IF(ISTART NE.1) GOTO 87
ICOUNT=0
DO 101 K9 = 1,4
101 FORCETOT(K9)=0.0
WRITE(31,*) ICOUNT
DO 95 K5=1,M

```

```

      DO 93 K4=1,3
        STRESTOT(K4,K5)=0.0
        TTOT(K4,K5)=0.0
93  CONTINUE
      WRITE(31,*)K5,STRESTOT(1,K5),STRESTOT(2,K5),STRESTOT(3,K5)
      WRITE(31,*) TTOT(1,K5),TTOT(2,K5),TTOT(3,K5)
95  CONTINUE
      WRITE(31,*)FORCETOT(1),FORCETOT(2),FORCETOT(3),FORCETOT(4)
      DO 97 KO=1, NODES
        DISPTOTX(KO)=0.0
        DISPTOTY(KO)=0.0
        DISPTOTZ(KO)=0.0
        WRITE(31,1990)DISPTOTX(KO),DISPTOTY(KO),DISPTOTZ(KO)
97  CONTINUE
      CLOSE(UNIT=31)
      OPEN(UNIT=31,FILE='SPSTRSTOT.IO',STATUS='OLD')
87  CONTINUE
1990 FORMAT(3E15.5)
C
C   THIS PART OF THE PROGRAM LOADS IN THE SPLINE CURVE DATA:
DO 90 IW = 1,8
C   IN IS AN ARRAY TELLING HOW MANY DATA PTS EACH SPLINE CURVE HAS:
  READ(10 + IW,*) IN(IW)
  WRITE(20,*)
  WRITE(20,*) 'FOR INPUT FILE ',IW +10,': #SPLINE PTS=',IN(IW)
  WRITE(20,*) '      X      Y'
  WRITE(6,*) 'IN(',IW,')=',IN(IW)
  DO 70 I=1,IN(IW)
    READ(10 + IW,*) X(IW,I),Y(IW,I)
    WRITE(20,*) X(IW,I),Y(IW,I)
70  CONTINUE
    X(IW,IN(IW)+1)=X(IW,IN(IW))+(X(IW,IN(IW))-X(IW,IN(IW)-1))
    Y(IW,IN(IW)+1)=Y(IW,IN(IW))+(Y(IW,IN(IW))-Y(IW,IN(IW)-1))
    IN(IW)=IN(IW)+1
    IN1(IW)=IN(IW)-1
    DO 51 I=1,IN1(IW)
      H(IW,I)=X(IW,I+1)-X(IW,I)
      DELY(IW,I)=(Y(IW,I+1)-Y(IW,I))/H(IW,I)
51  CONTINUE
    DO 52 I=2,IN1(IW)
      H2(IW,I)=H(IW,I-1)*H(IW,I)
      B(IW,I)=.5*H(IW,I-1)/H2(IW,I)
      DELSQY(IW,I)=(DELY(IW,I)-DELY(IW,I-1))/H2(IW,I)
      S2(IW,I)=2.*DELSQY(IW,I)
      C(IW,I)=3.*DELSQY(IW,I)
52  CONTINUE
      S2(IW,1)=0.
      S2(IW,IN(IW))=0.
      OMEGA=1.0717968
5   ETA=0.
6   DO 10 I=2,IN1(IW)
7   W(IW)=(C(IW,I)-B(IW,I))*S2(IW,I-1)-(.5-B(IW,I))*S2(IW,I+1)-
    & S2(IW,I))*OMEGA
8   IF(ABS(W(IW))-ETA) 10,10,9
9   ETA=ABS(W(IW))
10  S2(IW,I)=S2(IW,I)+W(IW)
13  IF(ETA-EPSLN)14,5,5
14  DO 53 I=1,IN1(IW)
53  S3(IW,I)=(S2(IW,I+1)-S2(IW,I))/H(IW,I)
90  CONTINUE

```

```

WRITE(20,*) 'ICOUNT,K,K3,J, STRESTOT(K3,J),STRESNOW(K3,J)',
& TOTSTRAIN (K3,J)
WRITE(30,*) J, SS1(1,J), SS1(2,J), SS1(3,J), SS(4,J)
WRITE(30,*) 'TTOT(1,J), TTOT(2,J), TTOT(3,J)'
WRITE(30,*) 'TNOW(1,J), TNOW(2,J), TNOW(3,J)'
READ(31,*) ICOUNT
C
C THIS PART OF THE PROGRAM UPDATES THE MATERIAL PROPERTIES:
15 DO 61 J=1,M
READ(19,*) TNOW(1,J), TNOW(2,J), TNOW(3,J)
READ(19,*) STRESNOW(1,J), STRESNOW(2,J), STRESNOW(3,J)
TNOW(4,J)=TNOW(1,J)
STRESNOW(4,J)=STRESNOW(1,J)
READ(31,*) JUNK,STRESTOT(1,J), STRESTOT(2,J),STRESTOT(3,J)
READ(31,*) TTOT(1,J), TTOT(2,J), TTOT(3,J)
STRESTOT(4,J)=STRESTOT(1,J)
TTOT(4,J)=TTOT(1,J)
DO 89 K3=1,4
STRESTOT(K3,J)=STRESTOT(K3,J) + STRESNOW(K3,J)
TTOT(K3,J)=TTOT(K3,J) + TNOW(K3,J)
T(K3,J)=ABS(TTOT(K3,J))
IF (STRESTOT(K3,J).LT. 0. ) k=k3+4
IF (STRESTOT(K3,J).EQ. 0. ) k=k3
IF (STRESTOT(K3,J).GT. 0. ) k=k3
WRITE(20,*) ICOUNT,K,K3,J,STRESTOT(K3,J),STRESNOW(K3,J),TTOT(K3,J)
16 I=1
54 IF(T(K3,J)-X(K,1)) 58,17,55
55 IF(T(K3,J)-X(K,IN(K)-1)) 57,59,58
56 IF(T(K3,J)-X(K,I)) 60,17,57
57 I=I+1
GOTO 56
58 PRINT 44,J
44 FORMAT(14,24HTH ARGUMENT OUT OF RANGE)
WRITE(6,*) J,'ARG OUT OF RANGE IN COL',K,'(IF COL>4, C)=' ,T(K3,J)
WRITE(20,K,*) J,'ARGUMENT OUT OF RANGE IN COL',K,'(IF COL>4, C)'
WRITE(29,*) J,'ARG OUT OF RANGE IN COL',K,'(IF COL>4, C)=' ,T(K3,J)
WRITE(30,*) J,'ARGUMENT OUT OF RANGE IN COL',K,'(IF COL>4, C)'
GOTO 89
59 I=IN(K) -1
60 I=I-1
17 HT1(K)=T(K3,J)-X(K,I)
HT2(K)=t(k3,J)-X(K,I+1)
PROD(K)=HT1(K)*HT2(K)
SS2(K,J)=S2(K,I)+HT1(K)*S3(K,I)
DELSQS(K)=(S2(K,I)+S2(K,I+1)+SS2(K,J))/6.
SS(K3,J)=Y(K,I)+HT1(K)*DELY(K,I)+PROD(K)*DELSQS(K)
SS1(K3,J)=DELY(K,I)+(HT1(K)+HT2(K))*DELSQS(K) +PROD(K)*S3(K,I)/6.
IF(K.EQ. 4) WRITE(24,*) SS(K,J),K,J,ICOUNT,STRESTOT(K,J),
& STRESNOW(K,J), '<-SS(K,J),K,J,ICOUNT,STRESTOT(K,J),STRESNOW(K,J)'
IF(K.EQ. 8) WRITE(28,*) SS(K,J),K,J,ICOUNT,STRESTOT(K,J),
& STRESNOW(K,J), '<-SS(K,J),K,J,ICOUNT,STRESTOT(K,J),STRESNOW(K,J)'
IF(K.LT.4) WRITE(20,K,*) SS1(K,J),K,J,ICOUNT,STRESTOT(K,J),
& STRESNOW(K,J), 'SS1,K,J,ICT,STRESTOT,NOW'
IF((K.LT. 8).AND.(K.GT. 4)) WRITE(20,K,*) SS1(K,J),K,J,ICOUNT,
& STRESTOT(K,J),STRESNOW(K,J), 'SS1,K,J,ICT,STRESTOT,NOW'
WRITE(6,*) 'STRESTOT&NOW(' ,k3, ', ',j, ')=' ,STRESTOT(k3,j),
& STRESNOW(K3,J)
89 CONTINUE
WRITE(29,2000)J,SS1(1,J),SS1(2,J),SS(4,J),J
2000 FORMAT(5HMT8*,17X,I2,3E16.7,3H-C0,I2)

```

```

WRITE(29,2010)J,SS1(3,J),RHO
2010 FORMAT(3H+CO,I2,3X,E16.7,32X,E16.7)
WRITE(30,*)' ',J,SS1(1,J),SS1(2,J),SS1(3,J),SS(4,J)
WRITE(30,*)TTOT(1,J),TTOT(2,J),TTOT(3,J)
WRITE(30,*)TNOW(1,J),TNOW(2,J),TNOW(3,J)
61 CONTINUE
READ(31,*)FORCETOT(1),FORCETOT(2),FORCETOT(3),FORCETOT(4)
READ(19,*)FORCE(1),FORCE(2),FORCE(3),FORCE(4)
FORCETOT(1)=FORCETOT(1)+FORCE(1)
FORCETOT(2)=FORCETOT(2)+FORCE(2)
FORCETOT(3)=FORCETOT(3)+FORCE(3)
FORCETOT(4)=FORCETOT(4)+FORCE(4)
DO 99 K6=1,NODES
  READ(31,1990)DISPTOTX(K6),DISPTOTY(K6),DISPTOTZ(K6)
  READ(19,1990)DISPX(K6),DISPY(K6),DISPZ(K6)
  DISPTOTX(K6)=DISPTOTX(K6)+DISPX(K6)
  DISPTOTY(K6)=DISPTOTY(K6)+DISPY(K6)
  DISPTOTZ(K6)=DISPTOTZ(K6)+DISPZ(K6)
99 CONTINUE
CLOSE(UNIT=31)
OPEN(UNIT=31,FILE='SPSTRSTOT.IO',STATUS='OLD')
ICOUNT=ICOUNT+1
WRITE(31,*)ICOUNT
DO 75 K7=1,M
  WRITE(31,*)K7,STRESTOT(1,K7),STRESTOT(2,K7),STRESTOT(3,K7)
  WRITE(31,*)TTOT(1,K7),TTOT(2,K7),TTOT(3,K7)
75 CONTINUE
WRITE(31,*)FORCETOT(1),FORCETOT(2),FORCETOT(3),FORCETOT(4)
DO 98 K1=1,NODES
98 WRITE(31,1990)DISPTOTX(K1),DISPTOTY(K1),DISPTOTZ(K1)
62 CONTINUE
CLOSE(UNIT=11)
CLOSE(UNIT=12)
CLOSE(UNIT=13)
CLOSE(UNIT=14)
CLOSE(UNIT=15)
CLOSE(UNIT=16)
CLOSE(UNIT=17)
CLOSE(UNIT=18)
CLOSE(UNIT=19)
STOP
END

```

## Appendix B

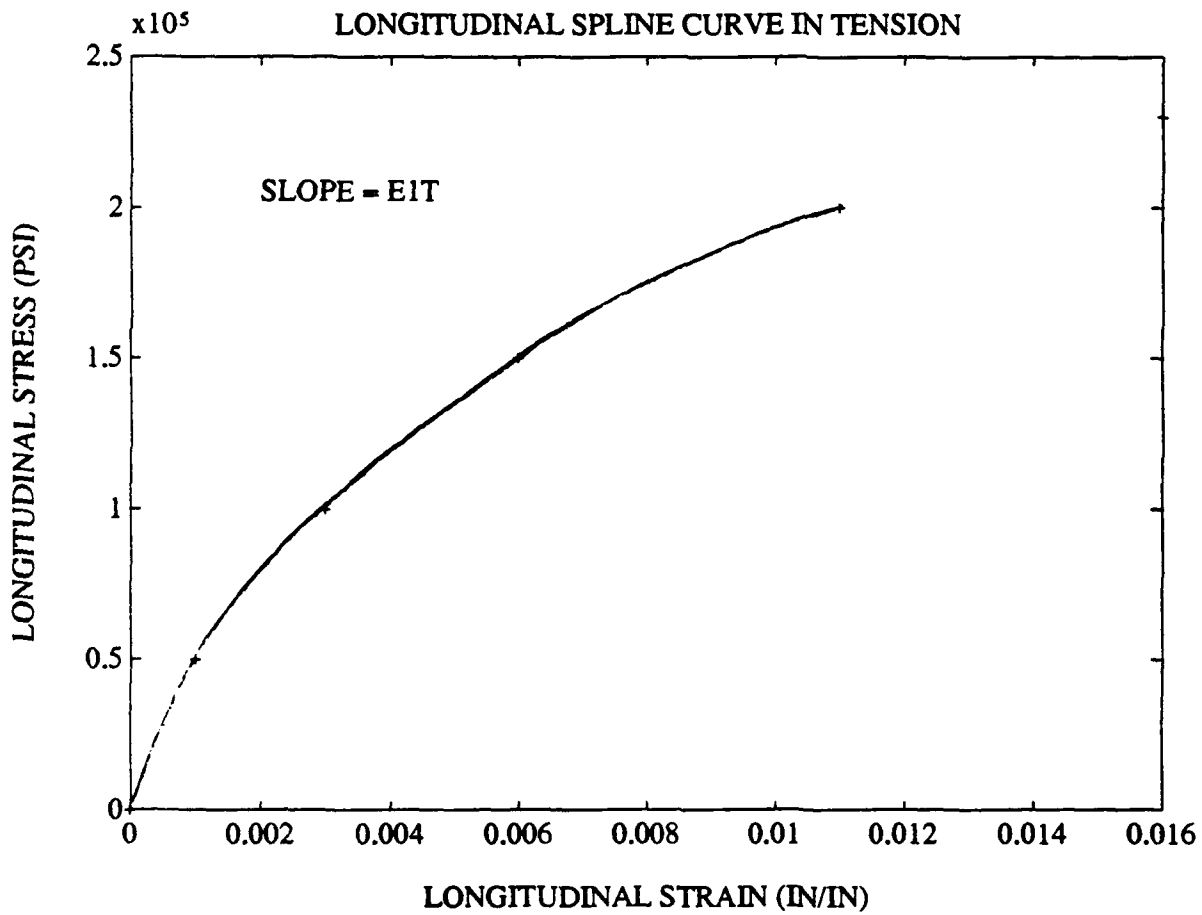


*Figure B-1  $\sigma_1$  (ksi) versus  $\epsilon_1$  (in/in) (tension)*



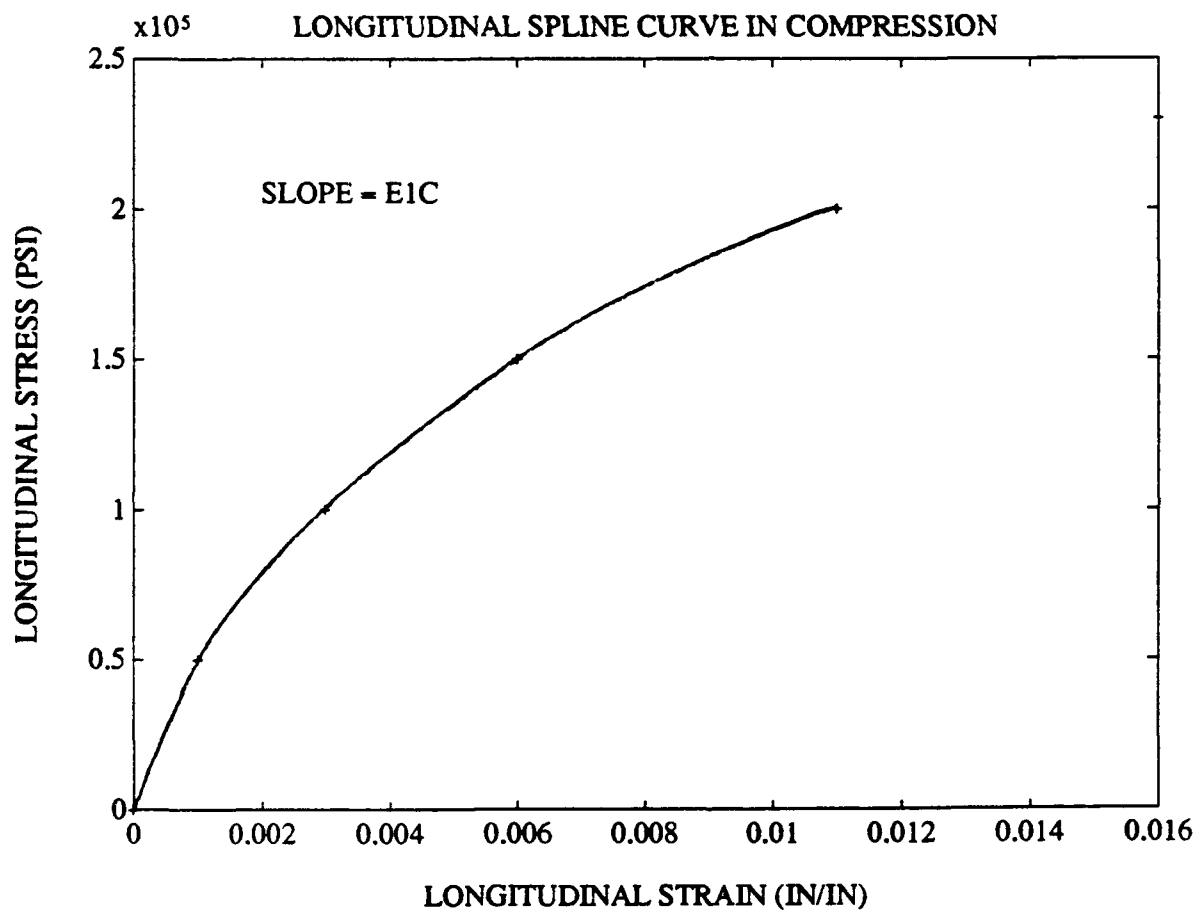


**Figure B-2  $\sigma_1$  (ksi) versus  $\epsilon_1$  (in/in) (compression)**

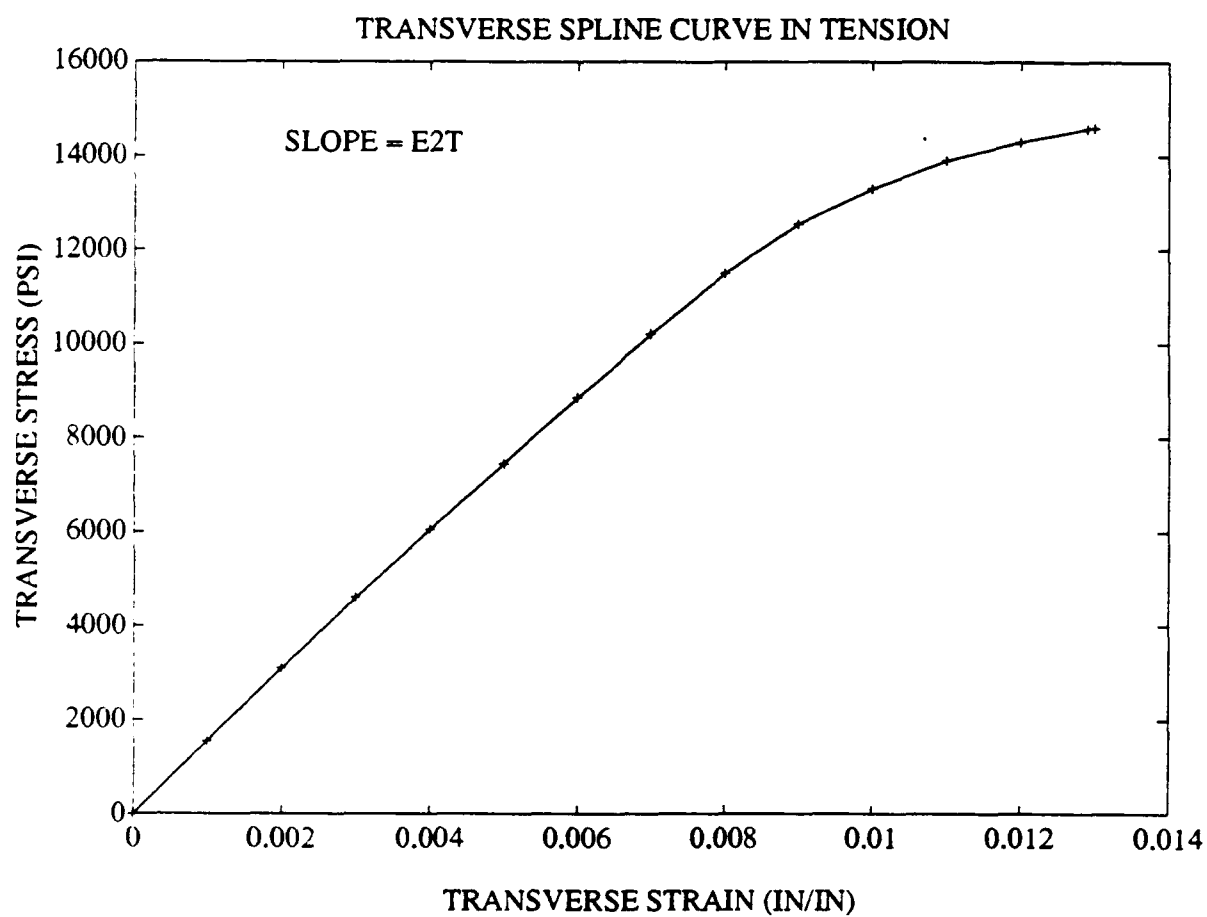


**Figure B-3  $\sigma_2$  (ksi) versus  $\epsilon_2$  ( $\frac{in}{in}$ ) (tension)**

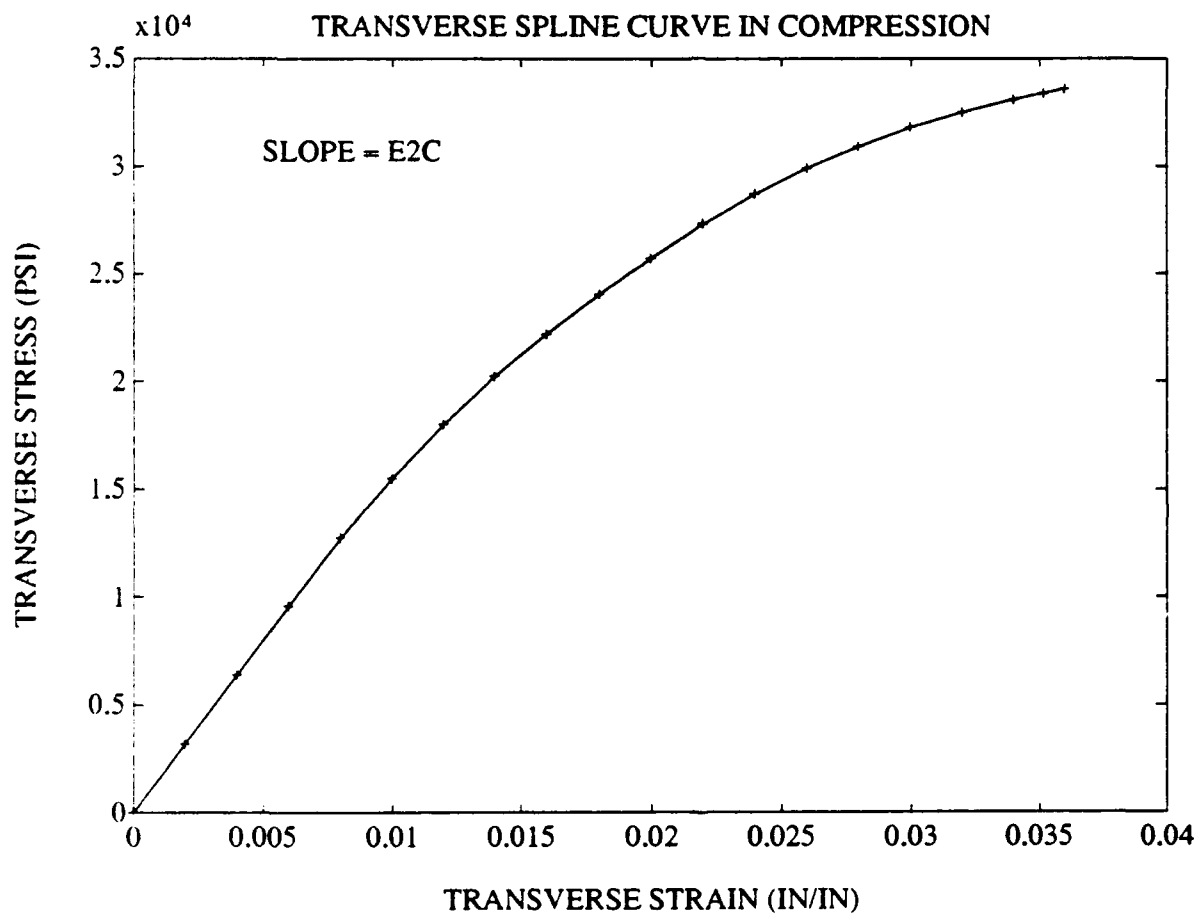


**Figure B-4  $\sigma_2$  (ksi) versus  $\epsilon_2$  (in/in) (compression)**

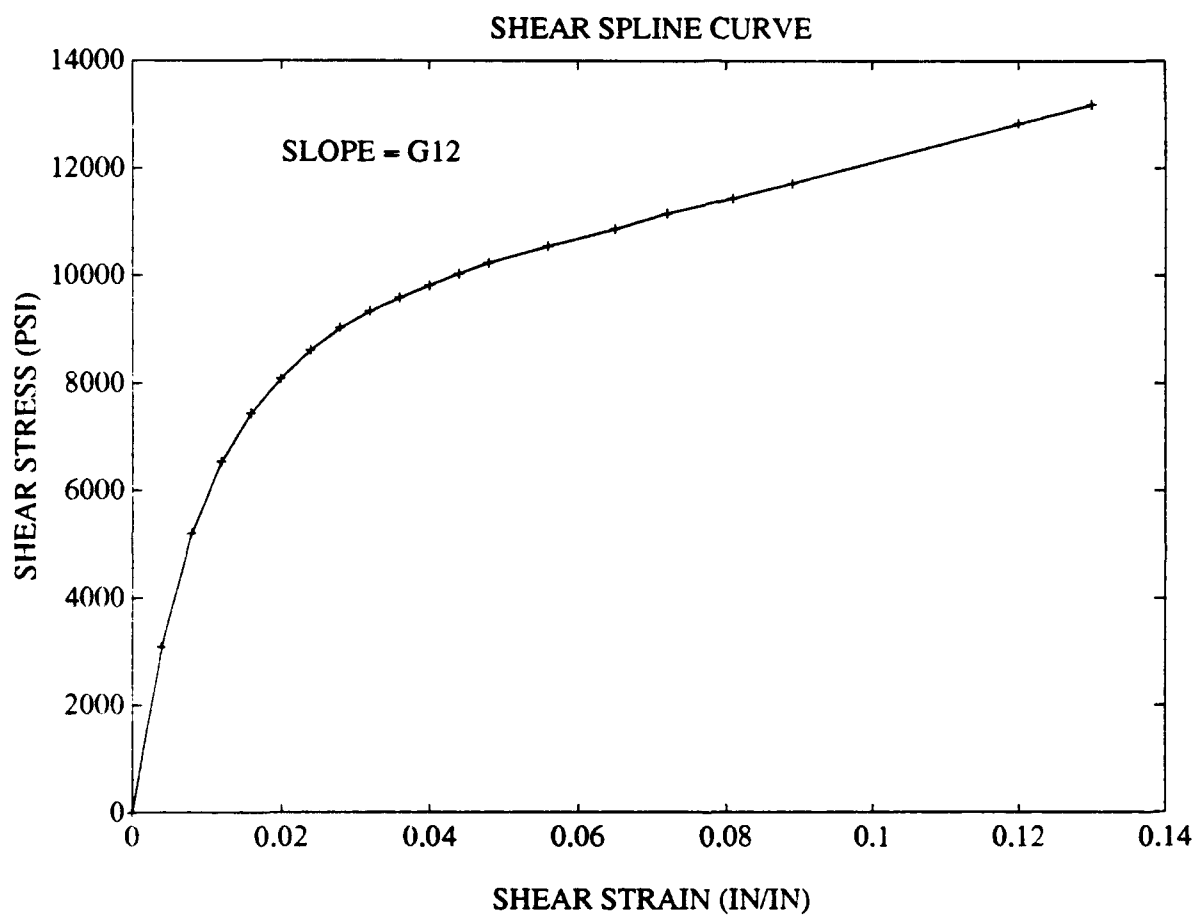


**Figure B-5  $\tau_{12}$  (ksi) versus  $\gamma_{12}(\pm 45)$**

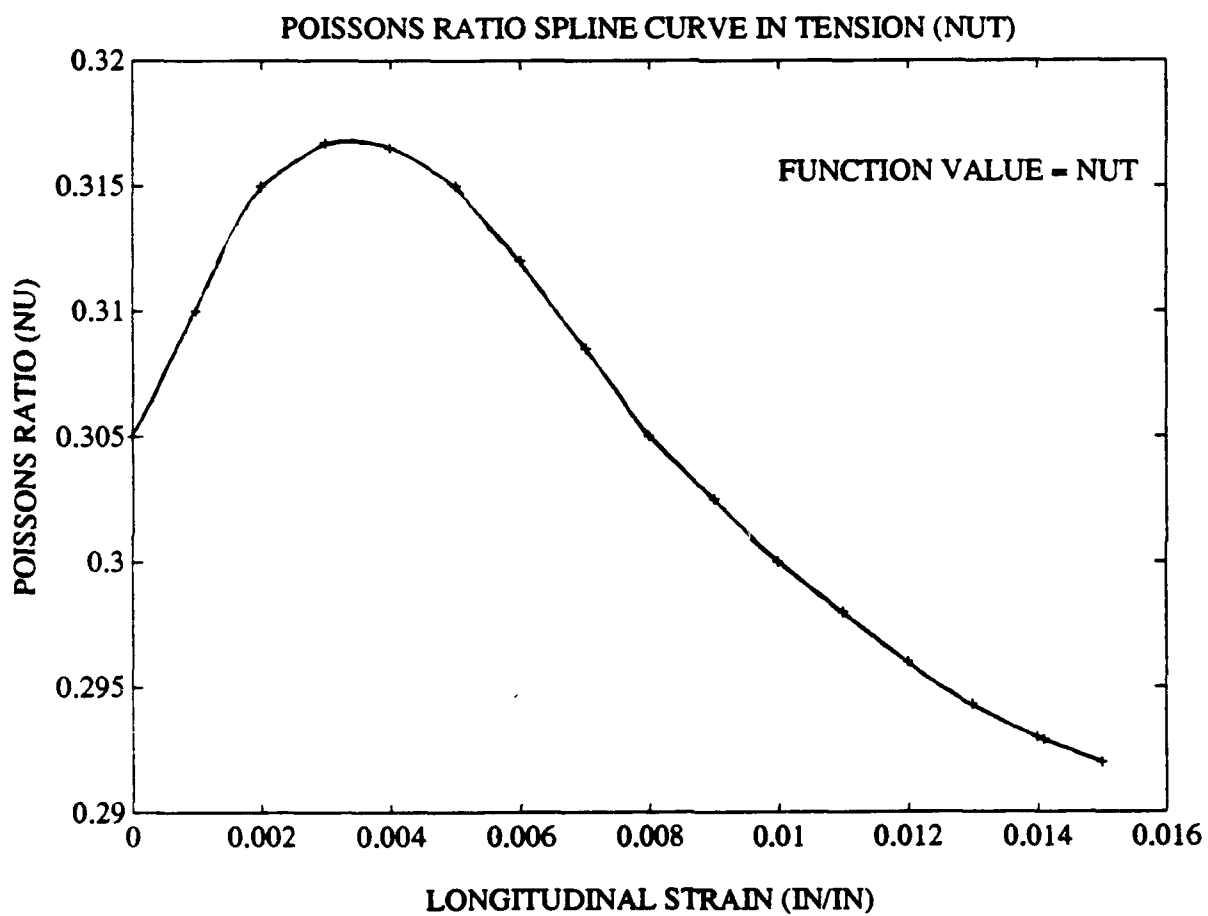


*Figure B-6  $\nu_{12}$  (ksi) versus  $\epsilon_1$  (tension)*

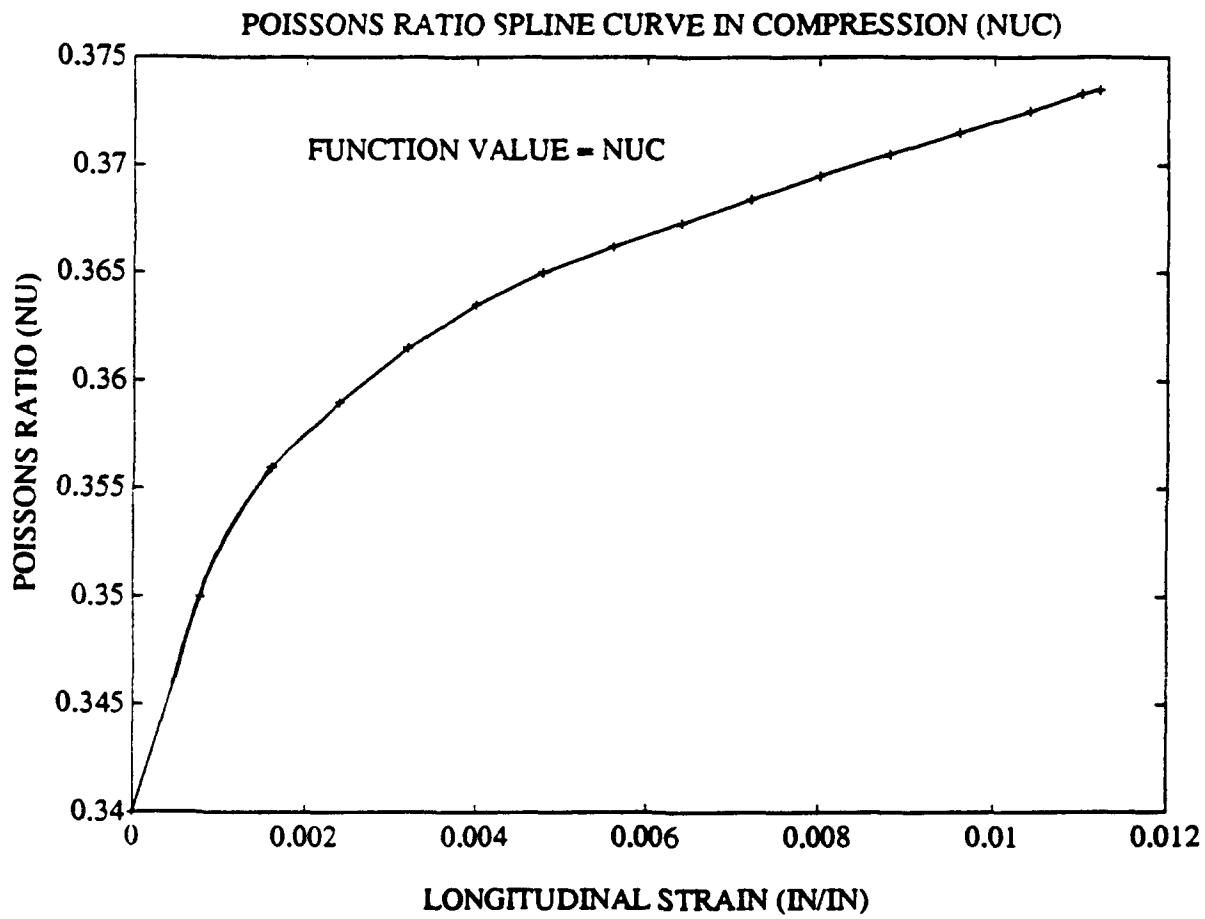


**Figure B-7  $\nu_{12}$  (ksi) versus  $\epsilon_1$  (compression)**

## Appendix C

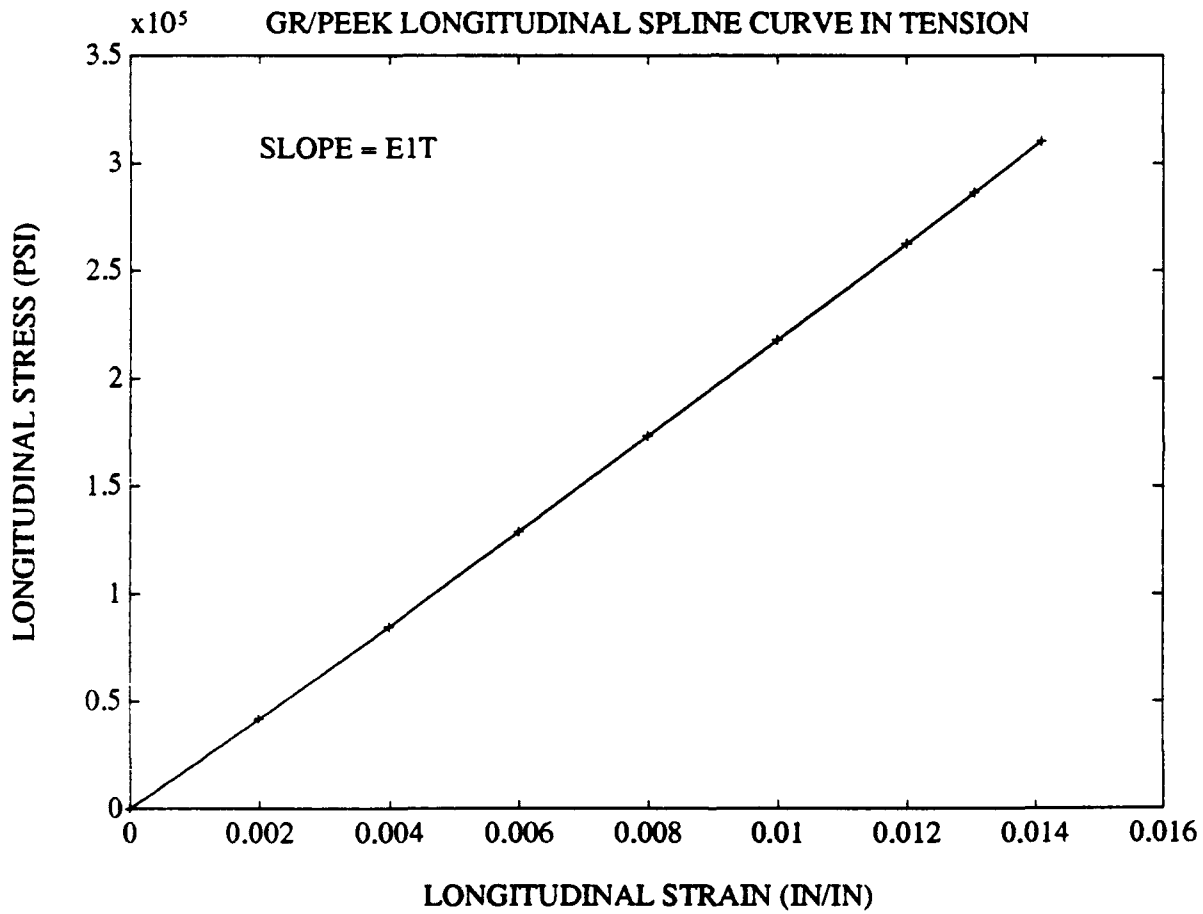


**Figure C-1 Gr/PEEK  $\sigma_1$  (ksi) versus  $\epsilon_1$  (in/in) (tension)**

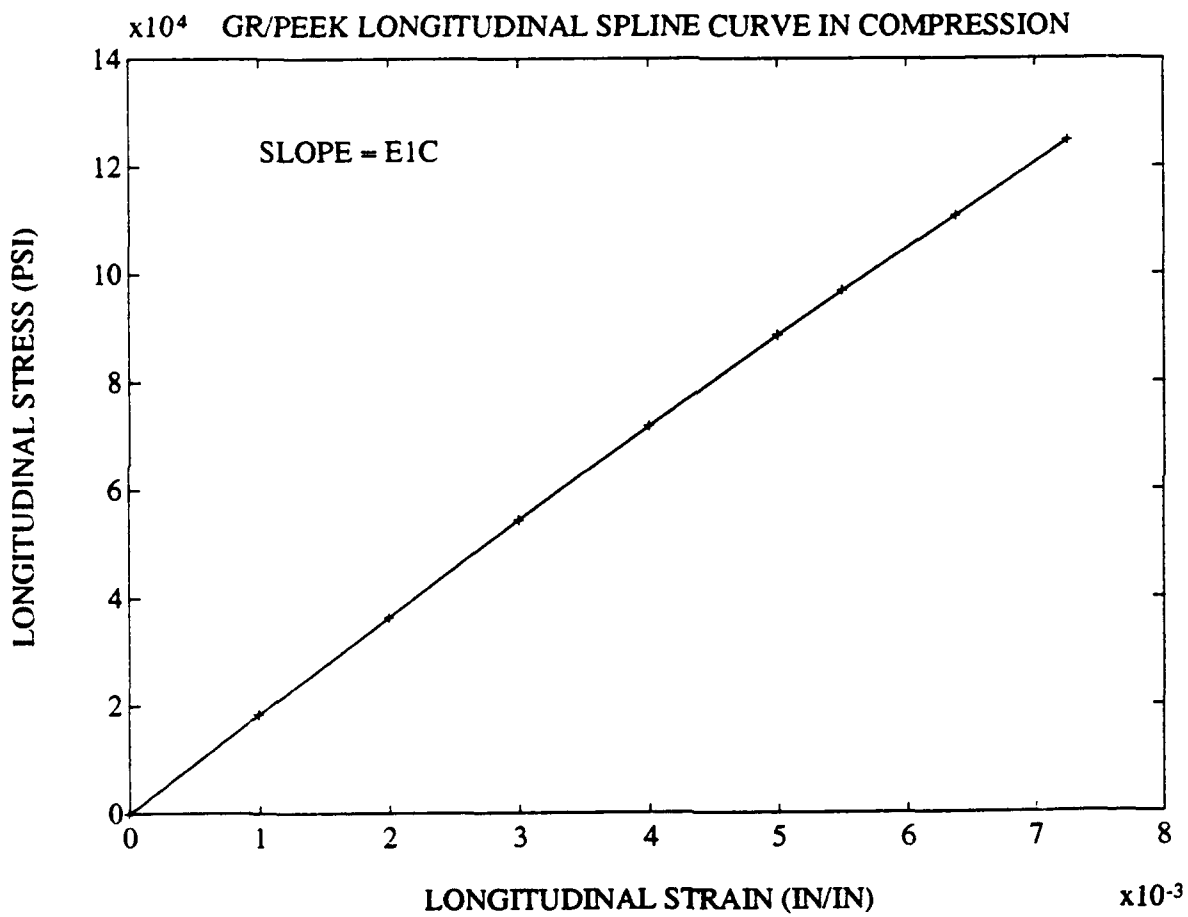


**Figure C-2 Gr/PEEK  $\sigma_1$  (ksi) versus  $\epsilon_1$  (in/in) (compression)**



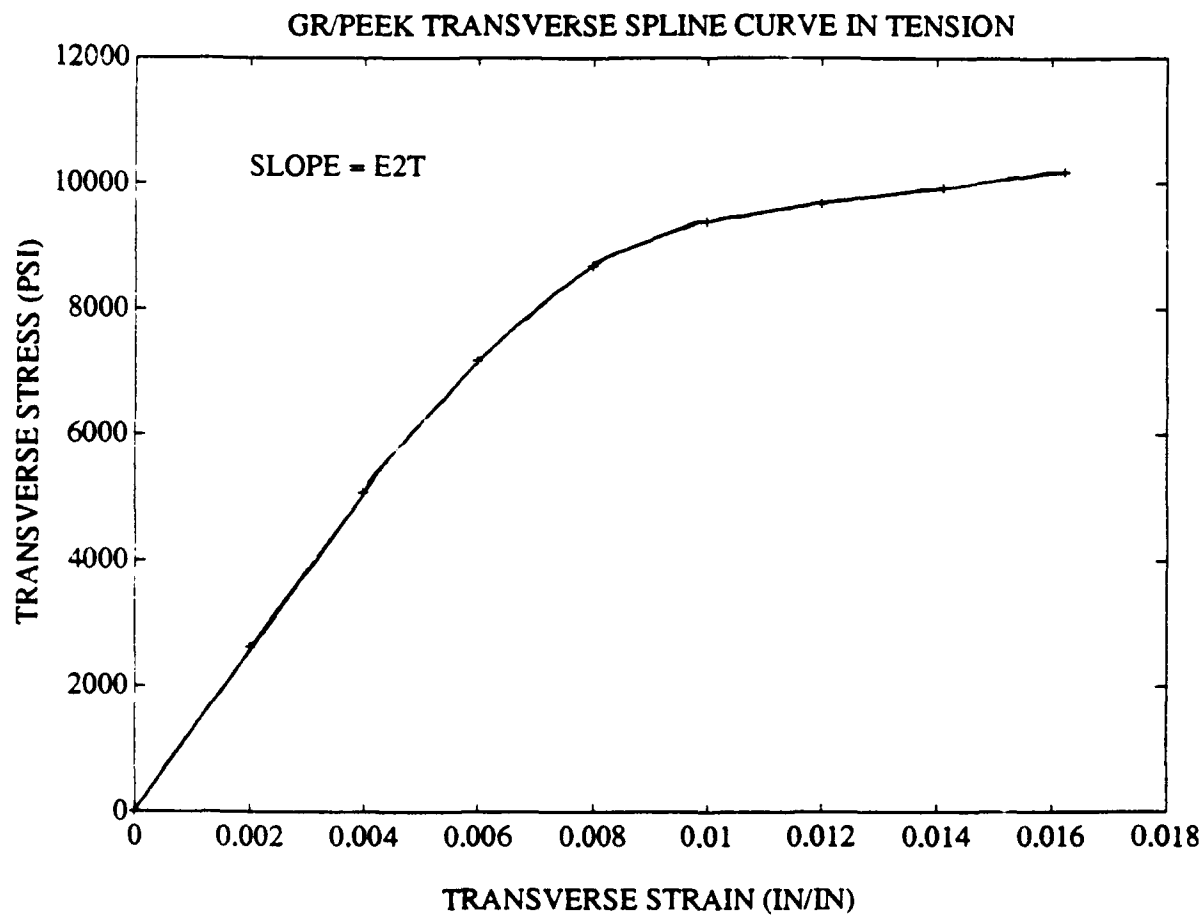


**Figure C-3 Gr/PEEK  $\sigma_2$  (ksi) versus  $\epsilon_2$  (in/in) (tension)**

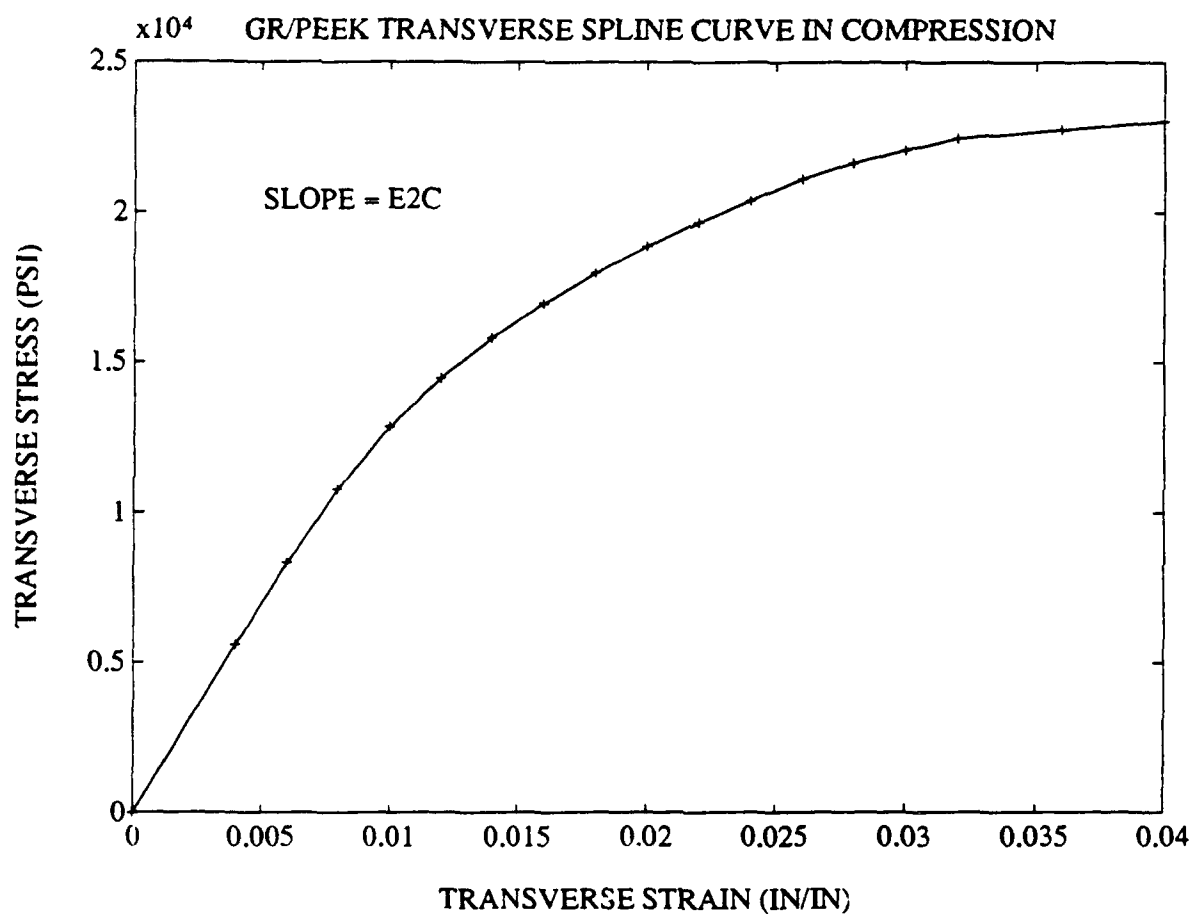


Figure C-4 Gr/PEEK  $\sigma_2$  (ksi) versus  $\epsilon_2$  (in/in) (compression)

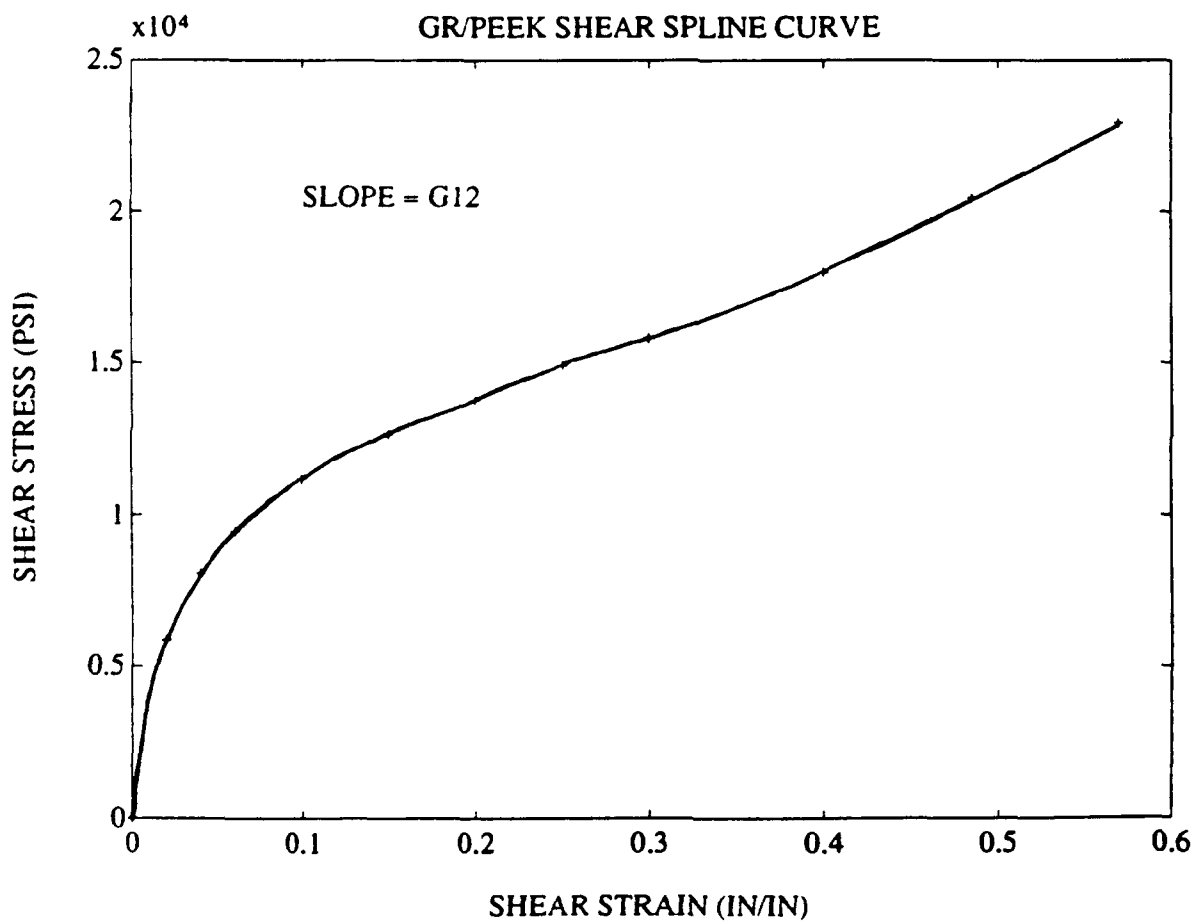
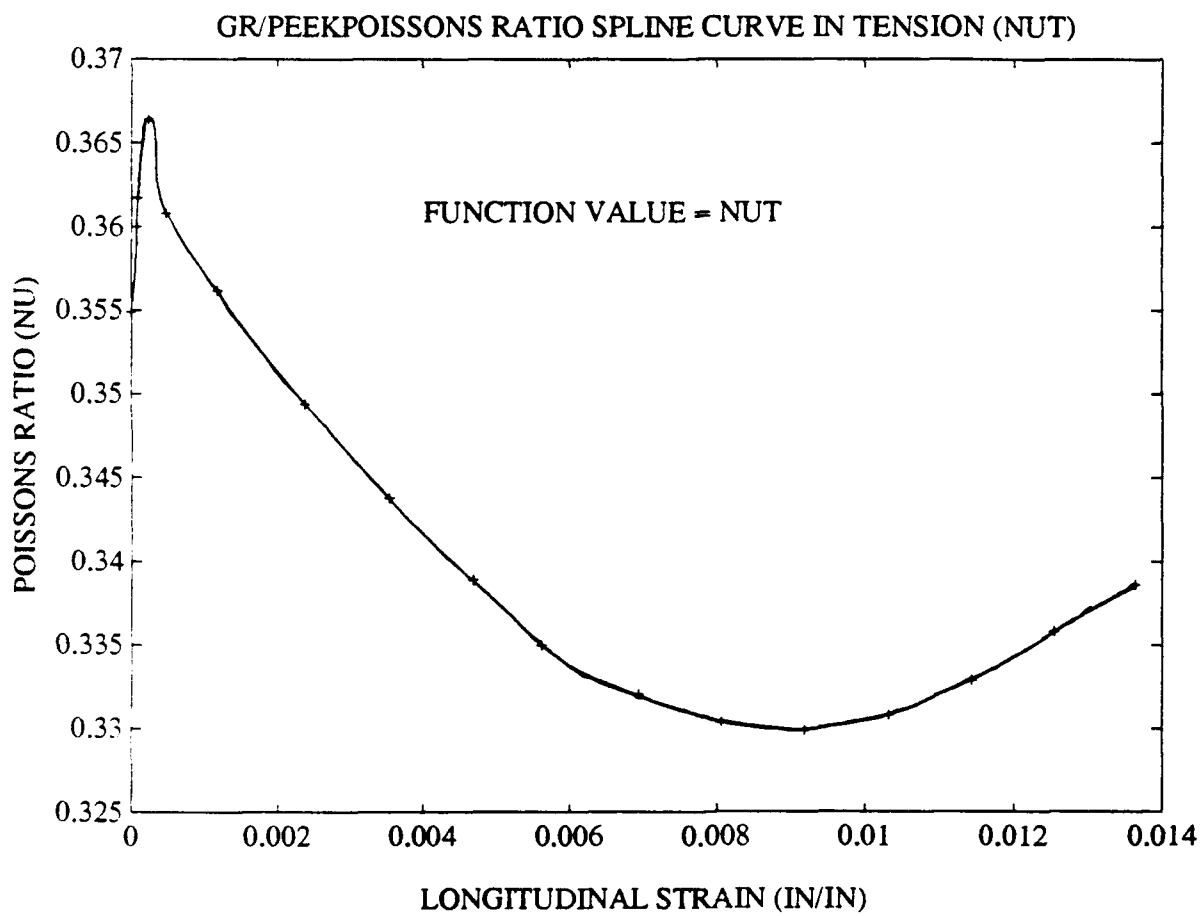
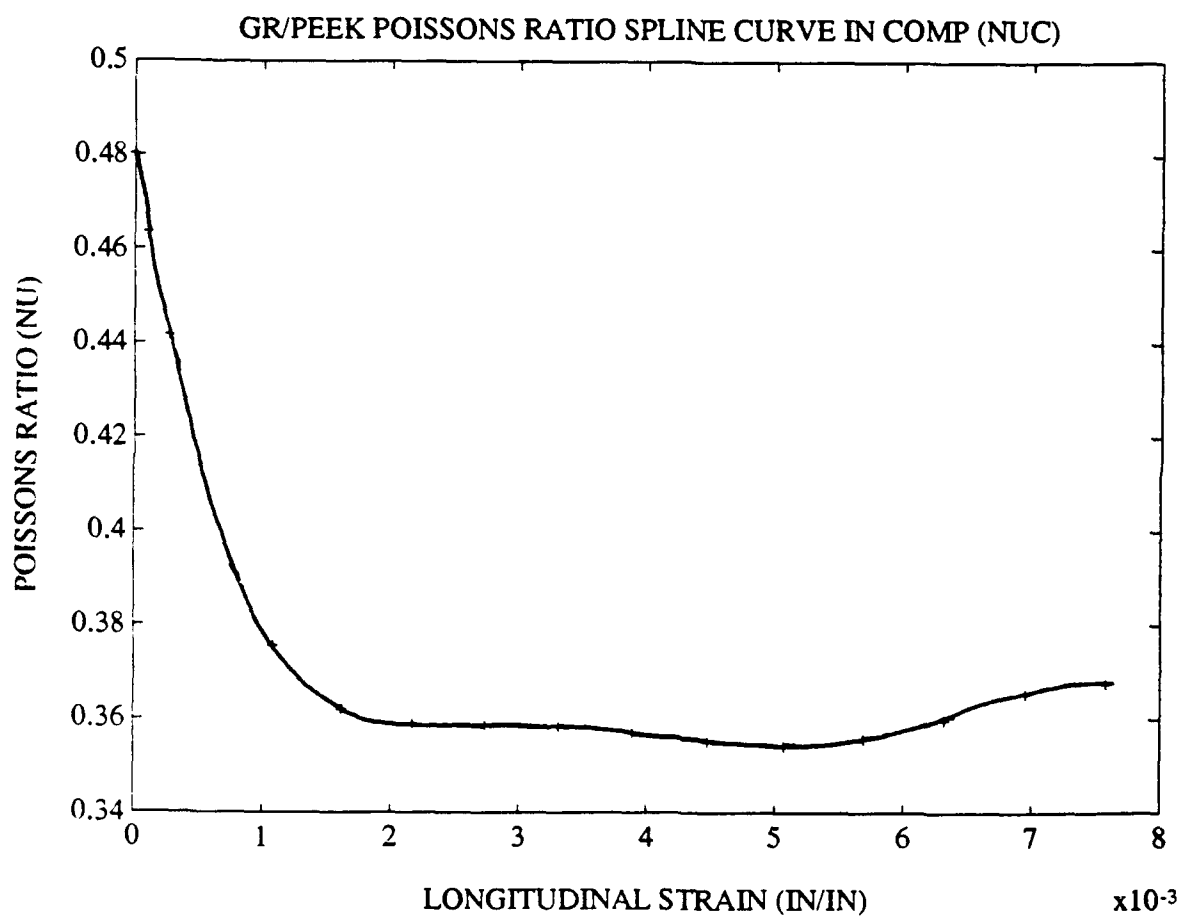


Figure C-5 Gr/PEEK  $\tau_{12}$  (ksi) versus  $\gamma_{12}(\pm 45)$



*Figure C-6 Gr/PEEK  $\nu_{12}$  (ksi) versus  $\epsilon_1$  (tension)*



*Figure C-7 Gr/PEEK  $\nu_{12}$  (ksi) versus  $\epsilon_1$  (compression)*

## Bibliography

1. Agarwal, B.D. and Broutman, L.J. *Analysis and Performance of Fiber Composites*. New York: John Wiley & Sons, 1980.
2. Ahlberg, J.H. Nilson, E.N., and Walsh, J.L. *The Theory of Splines and Their Applications*. New York: Academic Press, 1967.
3. Bathe, K. *Finite Element Procedures in Engineering Analysis*. Englewood Cliffs, NJ: Prentice Hall, 1982, pp. 301-318.
4. Cole, B.W., and Pipes, R.B. *Filamentary Composite Laminates Subjected to Biaxial Stress Fields*. AFFDL- TR-73-115, AD 785362, 1973. Air Force Flight Dynamics Laboratory, Wright-Patterson Air Force Base OH.
5. Cook, R. D. *Concepts and Applications of Finite Element Analysis*. Third Ed. New York: John Wiley & Sons, 1989.
6. Daniels, J.A. *A Study of Failure Characteristics in Thermoplastic Composite Laminates Due to an Eccentric Circular Discontinuity*. MS Thesis. AFTT/GAE/ENY/89D- 06. School of Engineering, Air Force Institutes of Technology (AU), Wright-Patterson Air Force Base OH, December 1989.
7. Finger, S., and Dixon, J. R. "A Review of Research in Mechanical Engineering Design. Part 1: Descriptive, Prescriptive, and Computer-Based Models of Design Processes". *Research in Engineering Design*, 1, 1989, pp. 51-67.
8. -----."A Review of Research in Mechanical Engineering Desing. Part 2: Representations, Analysis, and Design for the Life Cycle". *Research in Engineering Design*, 1, 1989, pp. 121-137.
9. Fisher, J. M. *A Study of Failure Chracteristics in a Thermoplastic Composite Material at High Temperature*. MS Thesis, AFTT/GAE/AA/88D-15. School of Engineering, Air Force Institute of Technology (AU), Wright- Patterson AFB OH, December 1988.
10. Hahn, H.T. "Nonlinear Behavior of Laminated Composites". *Journal of Composite Materials*, Vol. 7, April 1973, pp. 257-271.
11. Hahn, H.T. and Tsai, S.W., "Nonlinear Elastic Behavior of Unidirectional Composite Laminae," *Journal of Composite Materials*, Vol. 7, April 1973.
12. Hashin, Z., Bagchi, D., and Rosen, B.W. "Nonlinear Behavior of Fiber Composite Laminates," *NASA CR-2313*, 1973.
13. Herendeen, D.L., Hoesly, R.L., Johnson, E.H., and Venkayya, V.B. "ASTROS - An Advanced Software Environment for Automated Design," presented at the *AIAA/ASME/ASCE/AHS 27th Structures, Structural Dynamics and Materials Conference* AIAA-86-0856, San Antonio, TX, May 1986.

14. Johnson, E. H. and Venkayya, V.B. *Automated Structural Optimizaiton System (ASTROS)", Volume 1, Theoretical Manual*. Fight Dynamics Directorate, Wright Laboratory, AFSC, Wright-Patterson Air Force Base OH, March 1988.
15. Jones, R.M. *Mechanics of Composite Materials*. Washington, D.C.: Scripta book Comapany, 1975, p. 14.
16. Lifshitz, J.M. "Determination Nonlinear Shear Modulus of Fiber-Reinforced Lamina from the Axial Behavior of (45)s", *Journal of Composites Technology and Research*, Vol. 10, No. 4, Winter 1988, pp. 146-150.
17. Martin, J. *A Study of Failure Chracteristics in a Thermoplastic Composite Material at High Temperature*. MS Thesis, AFIT/GA/AA/88M-2. School of Engineering, Air Force Institute of Technology (AU), Wright- Patterson AFB OH, March 1988.
18. Neil, D.J., Johnson, E.H., and Canfield, R. *ASTROS - A Multidisciplinary Automated Structural Design Tool*. Northrop Corporations, Aircraft Division, Hawthorne, CA, 1986.
19. Peterson, R.E. *Stress Concentration Factors*. New York: John Wiley & Sons, 1974, p. 150.
20. Petit, P. H. and Waddoups, M. E. "A Method of Prediciting the Nonlinear Behavior of Laminated Composites," *Journal of Composite Materials*, Vol. 3, Jan. 1969, pp. 2-19.
21. Petit, P.H. "A Simplified Method of Determining the Inplane Shear Stress-Strain Response of Unidirectional Composites," *Composite Materials: Testing and Design*, STP 460, American Society for Testing and Materials, Philadelphia, 1969, pp. 83-93.
22. Ralston, A. and Wilf, H.S. *Mathematical Methods for Digital Computers*, Vol. II, J. Wiley, New York, pp. 156-168.
23. Rosen, B.W. "A Simplified Procedure for Experimental Determinations of the Longitudinal Shear Modulus of Unidirectional Composites," *Journal of Composite Materials*, Vol. 6, 1972, p. 552.
24. Saada, A.S. *Elasticity Theory and Applications*. Malabar, FL: Robert E. Krieger Publishing Company, 1989.
25. Sandhu, R.S. "Ultimate Strength Analysis of Symmetric Laminates," AFFDL-TR-73-137, AD 77927, 1973, Air Force Flight Dynamics Laboratory, Wright-Patterson Air Force Base OH.
26. Sandhu, R. S. "Nonlinear Behavior of Unidirecitional and Angle Ply Laminates", *Journal of Aircraft*, 13, No. 2 (February 1976), pp 104-111.
27. Tan, S. C. "Tensile and Compressive Notched Strength of PEEK Matrix Compoxite Laminates," *Journal of Reinforced Plactics and Composites*. Vol. 6 (July 1987), pp. 253-267.
28. Tsai, S.W., "Structural Behavior of composite Materials," NASA CR-71, July 1964.
29. -----, "Strength Characteristics of Composite Mateirals," NASA CR-224, April 1965.

30. Tsai, S.W., Adams, D.F., and Doner D.R., "Analysis of Composite Structures," NASA CR-620, November 1965.
31. Turino, J. *Managing Concurrent Engineering*, New York: Van Nostrand Reinhold, 1992.
32. Venkayya, V.R. and Tischler, V.A. *Analysis of Aerospace Structures with Membrane Elements (ANALYZE)*. Air Force Flight Dynamics Laboratory, Director of Science and Technology, Air Force Systems Command, Wright-Patterson AFB OH, August 1978.
33. Venkayya, V. B. Dr. Lecture ASTROS Training Workshop. Edwards AFB, CA, March 30, 1992.



## Vita

Captain Bob Bolha was born and raised in Greensburg, Pennsylvania as the youngest of six. After high school, he entered the USAF Academy. Graduating four years later with a B.S. in Astronautical Engineering, Second Lieutenant Bolha was initially stationed at AFCC's Standard System Center at Gunter AFB in Montgomery, Alabama. He began in the Test Division and left as Executive Officer for the Deputate for Acquisition. After AFTT, he looks forward to continuing on at Wright-Patterson AFB.

Permanent address:

232 Mitinger Avenue  
Greensburg, PA 15601